British Geological Survey

NATURAL ENVIRONMENT RESEARCH COUNCIL

Revised chronostratigraphy of the Faroe Islands Basalt Group and the British Palaeogene Igneous Province: implications for Selandian-Thanetian palynofloral assemblages and correlation with the Faroe-Shetland Basin

Energy Systems and Basin Analysis Programme

Commissioned Report CR/18/031

BRITISH GEOLOGICAL SURVEY

Revised chronostratigraphy of the Faroe Islands Basalt Group and the British Palaeogene Igneous Province: implications for Selandian-Thanetian palynofloral assemblages and correlation with the Faroe-Shetland Basin

Uni Árting, Dan Condon, James B. Riding and Morten S. Riishuus

Front cover

Keyworth, Nottingham　British Geological Survey　2018

BRITISH GEOLOGICAL SURVEY

The full range of our publications is available from BGS shops at Nottingham, Edinburgh, London and Cardiff (Welsh publications only) see contact details below or shop online at www.geologyshop.com

The London Information Office also maintains a reference collection of BGS publications, including maps, for consultation.

We publish an annual catalogue of our maps and other publications; this catalogue is available online or from any of the BGS shops.

The British Geological Survey carries out the geological survey of Great Britain and Northern Ireland (the latter as an agency service for the government of Northern Ireland), and of the surrounding continental shelf, as well as basic research projects. It also undertakes programmes of technical aid in geology in developing countries.

The British Geological Survey is a component body of the Natural Environment Research Council.

British Geological Survey offices

BGS Central Enquiries Desk

Tel 0115 936 3143   Fax 0115 936 3276

email enquiries@bgs.ac.uk

Environmental Science Centre, Keyworth, Nottingham NG12 5GG

Tel 0115 936 3241   Fax 0115 936 3488

email sales@bgs.ac.uk

The Lyell Centre, Research Avenue South, Edinburgh EH14 4AP

Tel 0131 667 1000   Fax 0131 668 2683

email scotsales@bgs.ac.uk

Natural History Museum, Cromwell Road, London SW7 5BD

Tel 020 7589 4090   Fax 020 7584 8270

Tel 020 7942 5344/45   email bgslondon@bgs.ac.uk

Columbus House, Greenmeadow Springs, Tongwynlais, Cardiff CF15 7NE

Tel 029 2052 1962   Fax 029 2052 1963

Maclean Building, Crowmarsh Gifford, Wallingford OX10 8BB

Tel 01491 838800   Fax 01491 692345

Geological Survey of Northern Ireland, Department of Enterprise, Trade & Investment, Dundonald House, Upper Newtownards Road, Ballymiscaw, Belfast, BT4 3SB

Tel 028 9038 8462   Fax 028 9038 8461

www.bgs.ac.uk/gsni/

Parent Body

Natural Environment Research Council, Polaris House, North Star Avenue, Swindon SN2 1EU

Tel 01793 411500   Fax 01793 411501
www.nerc.ac.uk

Website www.bgs.ac.uk
Shop online at www.geologyshop.com

Contents

Figures

Tables

Foreword

This report is the culmination of an investigation by the British Geological Survey (BGS) and Jarðfeingi (the Faroese Geological Survey) on behalf of the Faroe-Shetland Consortium (FSC). The principal thrust of this study is to determine the absolute age of the Faroe Islands Basalt Group (FIBG) in and around the Faroe Islands, and the correlative volcanic units in the Inner Hebrides, northwest Scotland and in Northern Ireland. This was achieved by radioisotope dating and the palynological analysis of some of the interbedded sedimentary rocks. Some stable isotope analyses were also carried out. The spatial and temporal relationships of these basalt-dominated formations, which were erupted as part of the North Atlantic Igneous Province (NAIP), are important in the hydrocarbon prospectivity of the Faroe-Shetland Basin. This work draws upon the results of previous FSC projects, especially Smith et al. (2013).

Acknowledgements

Summary

The chronostratigraphy of the Faroe Islands Basalt Group, and thereby the entire North Atlantic Igneous Province, presents a long-standing controversy among government, industry and academic stakeholders with activities in the Faroe-Shetland region. The application of biostratigraphy, magnetostratigraphy, radio-isotopic dating and seismic analysis have all failed to agree on the absolute age span of the volcanic province. The lack of an externally consistent chronostratigraphic framework pose a risk to the hydrocarbon prospectivity in the economically important Faroe-Shetland Basin.

This report provides a review of the onshore geology of the Faroe Islands Basalt Group and the British Palaeogene Igneous Province, and the contrasting age models for the emplacement of the North Atlantic Igneous Province are described in detail. New high-precision U/Pb zircon age determinations and palynological analyses of key stratigraphic sections from the Faroe Islands, Inner Hebrides and Northern Ireland are given. Available magnetostratigraphic, biostratigraphic and radio-isotopic age-constraining data from the literature and this study are assessed. It is demonstrated in detail how previous biostratigraphic interpretations, that constrain the collective pre- to syn-breakup eruptive products of the NAIP to the late Thanetian – early Ypresian (T40-T45), are fundamentally flawed. These interpretations have strongly influenced chronostratigraphic correlations between volcanically-saturated onshore basins and volcanically-starved offshore basins, and the portrayal of interaction between sedimentary and volcanic depositional processes in the Faroe-Shetland region. A consistent multidisciplinary age model for the protracted emplacement of the NAIP is presented, including absolute numerical age constraints and assessment of palynofloral assemblages from two key onshore occurrences of the Staffa Flora. The report also highlight the identification of remaining outstanding problems regarding the absolute chronostratigraphy for Palaeocene to early Eocene formations and sequences of the Faroe-Shetland Basin.

1 Introduction

The Faroe Islands are located in the North Atlantic Ocean, southeast of Iceland and northwest of the Shetland Islands (*Figure 1*). The islands are dominated by the the subaerially exposed part of an extensive succession of Palaeogene basalt formations known as the Faroe Islands Basalt Group (FIBG) (*Figure 2*; Rasmussen and Noe-Nygaard 1969, 1970; Passey and Jolley 2009). The FIBG erupted as part of the North Atlantic Igneous Province (NAIP) that formed during the opening of the North Atlantic Ocean (*Figure 3* and *Figure 4*; Saunders et al. 1997, Jolley and Bell 2002, Storey et al. 2007). The highly resistant basalts of the FIBG influence the highly distinctive rugged landscape in this remarkable archipelago of elongate islands, which are mainly oriented NNW-SSE (*Figure 2* and *Figure 5*).
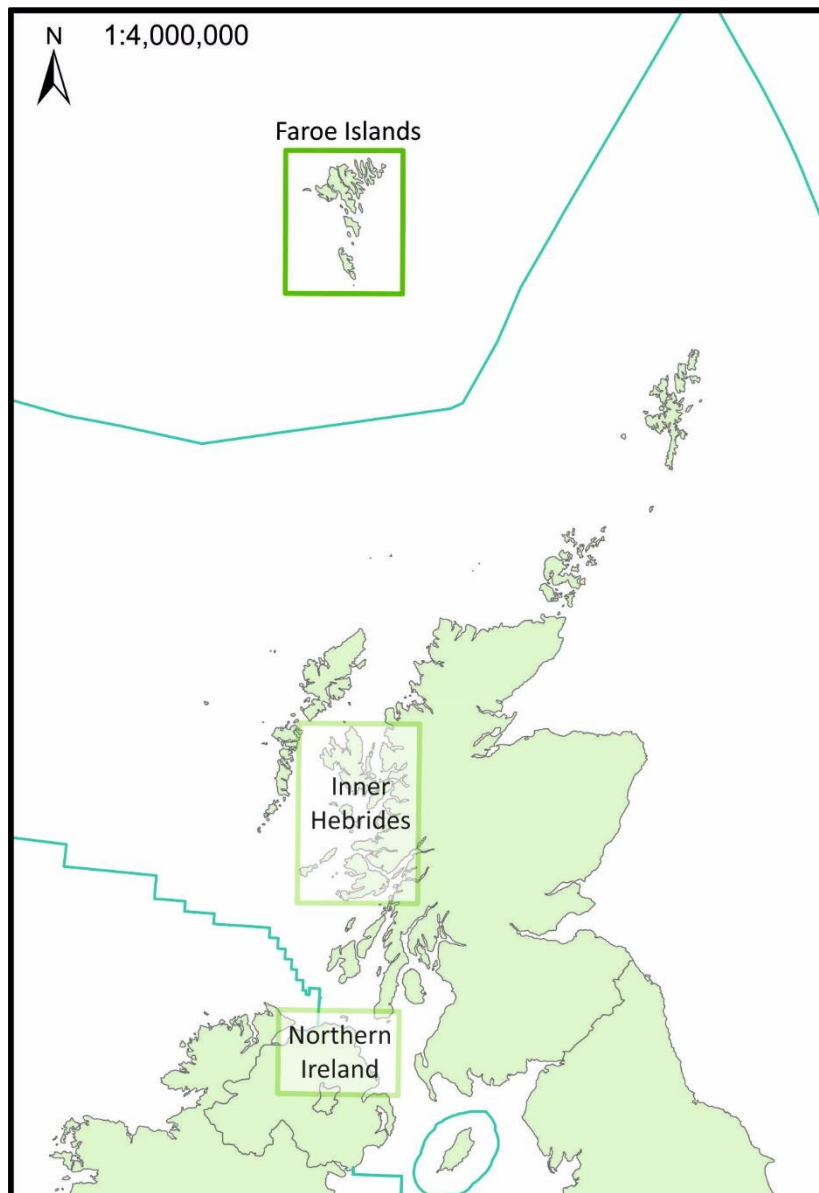
Figure 1 A geographical map, including territorial boundaries, of the Northeast Atlantic to the north of the UK and Ireland illustrating the location of the three areas that were studied herein, i.e. the Faroe Islands, the Inner Hebrides and Northern Ireland.
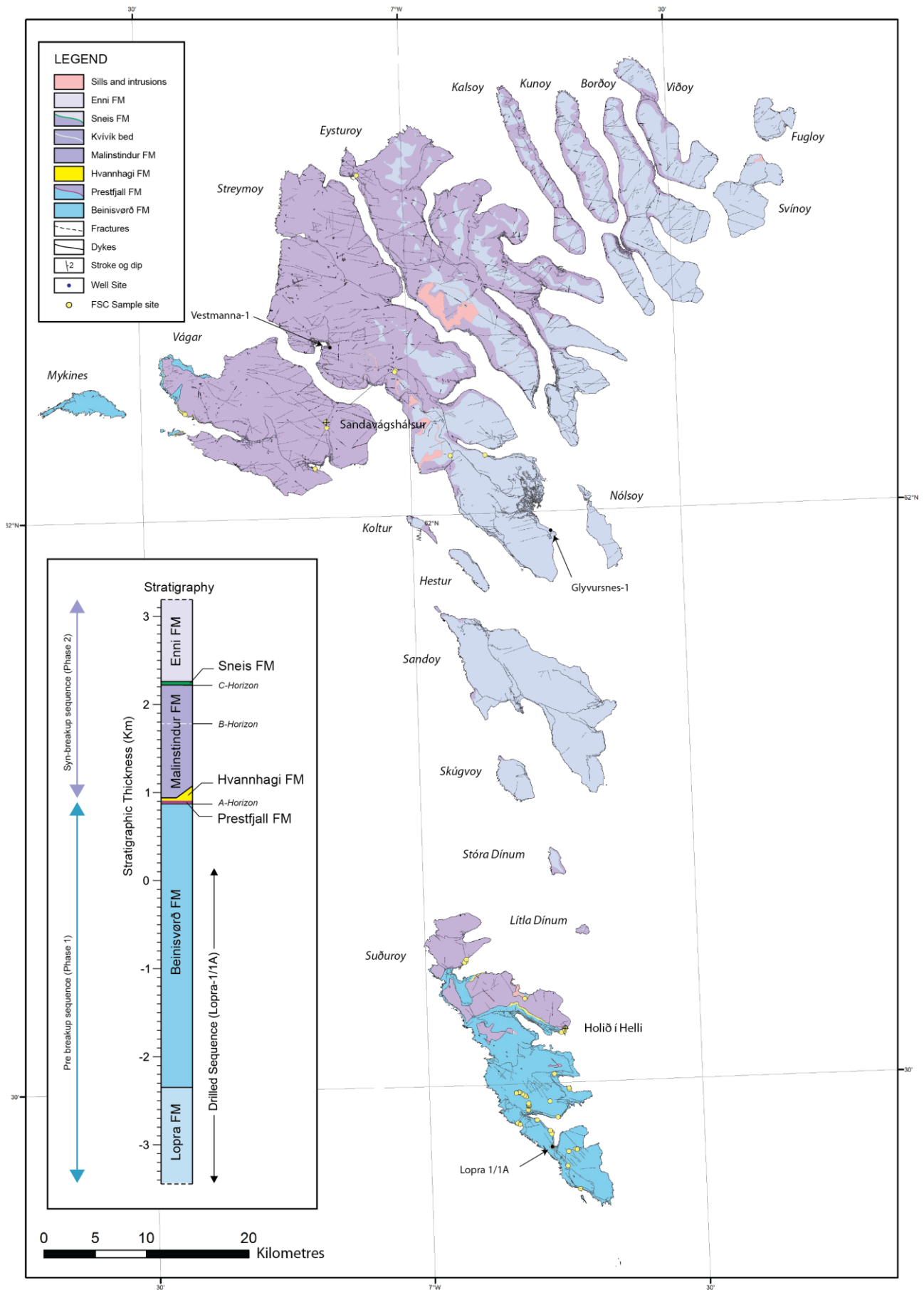
Figure 2 A geological map of the Faroe Islands modified after Rasmussen and Noe-Nygaard (1969, 1970) and Passey and Jolley (2009). The outcrops of the Beinisvørð to Enni formations of the Faroe Islands Basalt Group are illustrated (Table 1)

The FIBG is known from dredge samples, offshore and onshore boreholes, and outcrops (Waagstein 1988). It covers a very wide area (>120 000 km^2), and extends into the Faroe-Shetland Basin over 200 km to the E and SE of the Faroe Islands (Fig. 3). This volcanic group normally dips to the SE, and is ca. 6.6 km thick. This assessment of thickness is derived from a composite measured section of ca. 3.2 km, plus ca. 3.4 km proved by the Lopra-1/1A onshore borehole on Suðuroy (*Figure 2*; Chalmers and Waagstein 2006). This important unit was deservedly formalised as a group by Passey and Jolley (2009, *Figure 3*, *Table 1*), who subdivided their FIBG into seven formations (*Table 1*). Prior to Passey and Jolley (2009), the FIBG was subdivided into four, five and six informal lithostratigraphical units by Rasmussen et al. (1956), Rasmussen and Noe-Nygaard (1970), Waagstein (1988) and Ellis et al. (2002).

1 Anton Dohrn	11 Erlend	21 Mentone	31 Sula Sgeir
2 Blackstones	12 Faroe Bank	22 Owlsgard	32 Swithin
3 Brendan (Shetland)	13 Faroe Bank Channel Knoll	23 Regin Smidur	33 West Erlend
4 Brendan (Ireland)	14 Fraenir	24 Rockall	34 West George Bligh
5 Darwin	15 Geikie	25 Rohan	
6 Donn	16 Gondor	26 Rosemary Bank	
7 Drekaegya	17 Hebrides Terrace	27 St Kilda	
8 Drol	18 Lundy	28 Sandarro	
9 East George Bligh	19 Lyonesse	29 Sandastre	
10 Eriador	20 Mammal	30 Sigmundur	

Figure 3 The North Atlantic Igneous Province (NAIP) illustrating the geographical extent of offshore and onshore igneous and volcanic activity (from Emeleus and Bell 2005, fig. 2).

The age, architecture and spatial relationships of the FIBG have major implications for the hydrocarbon prospectivity and the regional petroleum geology of the Faroe-Shetland region and surrounding areas (e.g. Ellis and Stoker 2014, Hamilton and Minshell 2018). More specifically, the absolute age of the FIBG (Storey et al. 2007, Wilkinson et al. 2017), when considered in a regional context, has major consequences for the regional tectono-stratigraphical evolution of the Northeast Atlantic, in particular between the Faroe Islands and northwest Scotland. This, in turn, clearly substantially impinges on the hydrocarbon prospectivity of the earlier and contemporaneous sedimentary successions that underlie the FIBG.

Faroe Islands Basalt Group	
	Enni Formation
	Sneis Formation
	Malinstindur Formation
	Hvannhagi Formation
	Prestfjall Formation
	Beinisvørð Formation
	Lopra Formation

Table 1 The seven formations of the Faroe Islands Basalt Group as defined by Passey and Jolley (2009). The major three formations are in bold font.
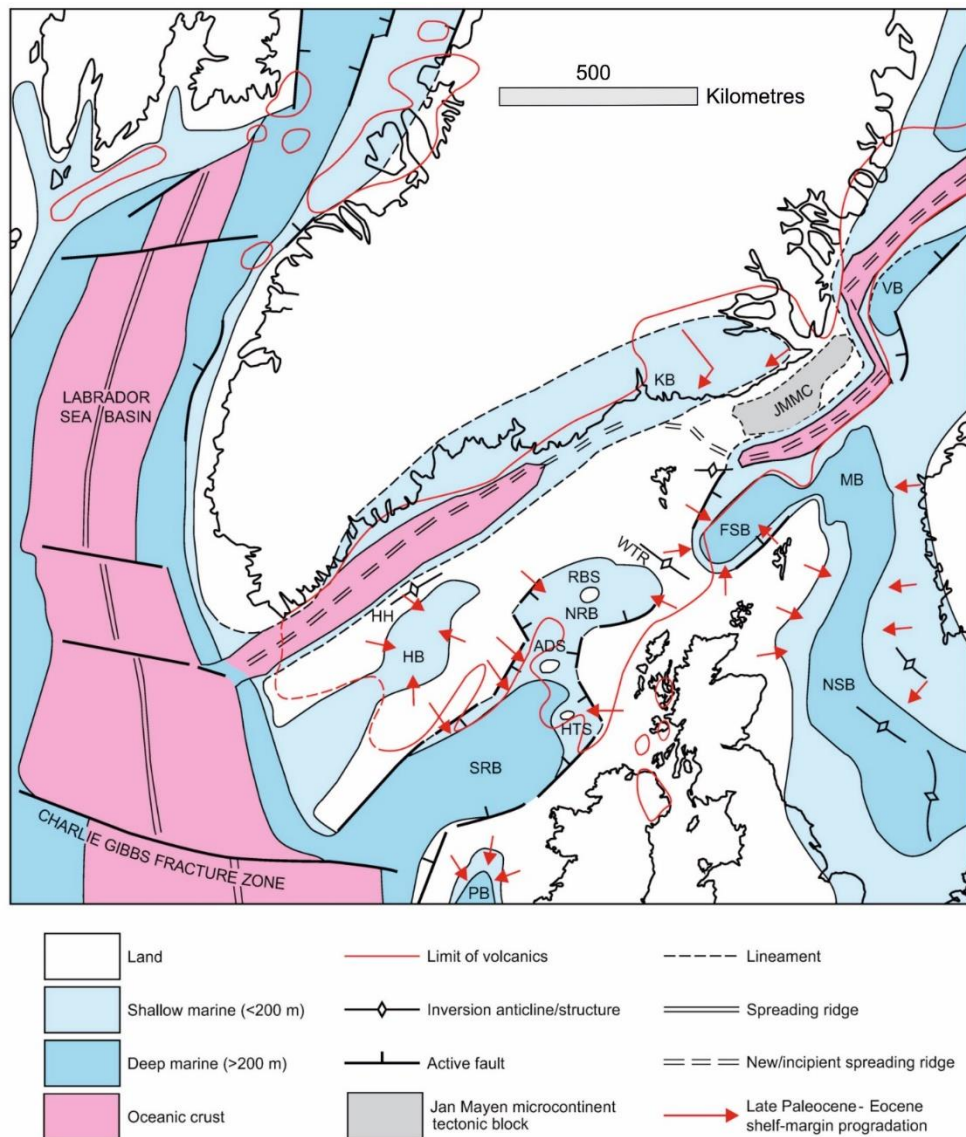
Figure 4 A generalised palinspastic map of the northeast Atlantic for the Late Palaeocene to Early Eocene interval modified from Stoker & Varming (2011). Acronyms: ADS - Anton Dohrn Seamount; KB - Kangerlussuaq Basin; MB - Møre Basin; NRB - North Rockall Basin; NSB - North Sea Basin; PB - Porcupine Basin; RBS - Rosemary Bank Seamount; SRB - South Rockall Basin; VB - Vøring Basin; WTR - Wyville Thompson Ridge.

At present, the chronostratigraphy of the FIBG is controversial. In summary, Schofield and Jolley (2013) attributed the Lopra, Beinisvørð, Malinstindur and Enni formations all to the early Ypresian (~56.0–54.8 Ma) interval. This conflicts markedly with the Selandian to Ypresian (~?61–54.8 Ma) age assessment of this succession by Storey et al. (2007) and Mudge (2015). This substantial chronostratigraphical conflict was recently discussed by Stoker et al. (2018, *Figure 3*), is summarised in *Figure 6* and is discussed in detail later in this report.

Figure 5 A montage of four photographs of typical Faroe Island landscapes to illustrate the glacially-eroded landscapes of the FIBG. A) The View from Hvannafelli on Suðuroy. B) Múlafossur in Gásadalur on the Island of Vágoy. C) The islet of Tindhólmur. D) The larger fjord is called Hovsvík and is on Suðuroy, the small islet/holm is called Hovshólmur.
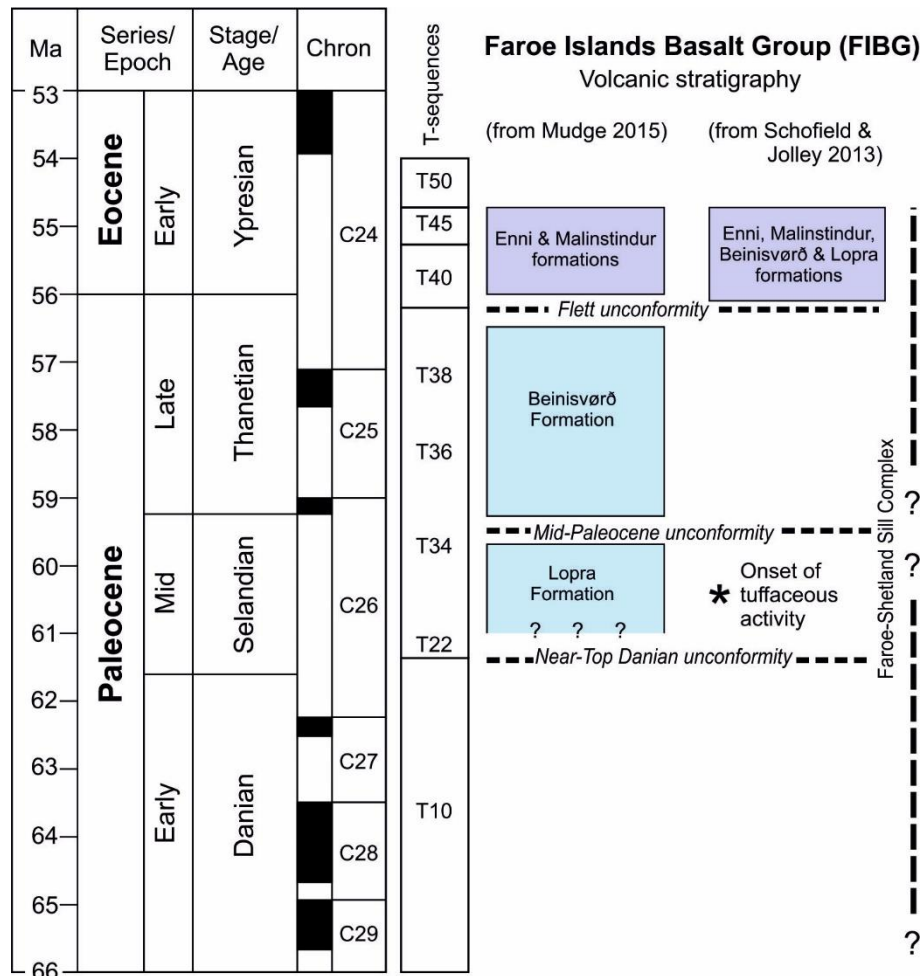
Figure 6 A stratigraphical chart to illustrate the substantially differing age models for the Faroe Islands Basalt Group, after Schofield & Jolley (2013), Mudge (2015) and Stoker et al. (2018). The information on the Faroe–Shetland Sill Complex and the onset of tuffaceous activity, which are both highly relevant to the volcanic activity, is taken from Mudge (2015), Schofield et al. (2017) and Watson et al. (2017). The timescale is based on Gradstein et al. (2012) and the T-sequences are from Mudge (2015).

Therefore, biostratigraphy, magnetostratigraphy, radio-isotopic dating and seismic analysis have hitherto failed to provide a consensus as to the age of this important major unit (Smith et al. 2013; Kimbell 2014). Following critical review of both the radio-isotopic and palynological data it was considered that considered uncertainty remained, due to interpretation of both the $^{40}Ar/^{39}Ar$ and palynological data, such that the data could not be used to discriminate between either 'Model 1' or 'Model 2' (*Figure 6*). The present study aims to place the FIBG into an accurate and reliable chronostratigraphical framework using radio-isotopic dating and palynology. The radio-isotopic method to be used is U-Pb zircon, and not $^{40}Ar/^{39}Ar$ whole rock analyses. The U-Pb zircon strategy uses an indirect approach to dating the basalts via analyses of zircon crystals in the inter-trappean sediments, an approach that is proving increasingly useful in other large igneous /flood basalt provinces.

This report summarises the data, interpretation and synthesis of that have arisen from the project. Following on from Phase 2 efforts, and the various SINDRI supported studies that attempted to address the issues outlined above (e.g., Sherlock et al., 2010) we proposed to take a more regional approach to the problem – rather than focussing just on dating the basalts themselves, which is challenging from a radio-isotopic dating perspective, could we step back and develop a regional chronostratigraphic framework using a set of robust constraints that directly and indirectly constrain the geology of interest.

The original project tasks are as follows:

- Radio-isotopic dating of ~10 key samples from a wider sample set (~30 samples). These would be from both the FIBG and the BPIP.
- Palynological investigations of a key reference section in the Faroe Islands, selected offshore wells in the Faroes area, and selected onshore sections from the Inner Hebrides (Scotland) and Antrim (Northern Ireland) in order to help interpret the biostratigraphy. (~190 samples)
- Compilation of published magnetostratigraphical data relevant to the localities used for the biostratigraphical, radio-isotopic dating and stable isotope analyses.
- The analysis of ~100 samples of sedimentary rocks for $\delta^{13}Corg$ in order to attempt to locate the Palaeocene–Eocene thermal maximum (PETM, ~56 Ma)
- Development of an integrated age model for the FIBG through integrated palynology-based biostratigraphy, magnetostratigraphy, radio-isotopic dating and stable isotope analysis.

All task have been complete and the programme of work was in fact expanded during the project to include additional study areas (i.e., dating of tuff from the Faroe-Shetland Basin) and the number of analyses undertaken has exceeded the amount planned. This report contains the background, methods, results, data interpretation and synthesis of the project.

2 Overall Background

The NAIP is a large igneous province centered on Iceland (*Figure 3*, Saunders et al. 1997). During the Paleogene, massive volumes of basalt lava were erupted. This formed the Thulean Plateau, which is $>1.3\times10^6$ km^2 in extent, and has a volume of ~6.6×10^6 km^3. (Eldholm and Grue 1994). The Thulean Plateau was fragmented during the opening of the North Atlantic. This breakup resulted in large fragments in the Faroe Islands, Greenland Iceland, the Inner Hebrides, northwest Scotland, Northern Ireland and Norway. The NAIP has also been termed the Brito-Arctic province, and the fragments around the British Isles are collectively known as the British Paleogene Igneous Province (Emeleus and Gyopari 1992; Emeleus and Bell 2005).

The magmatism across the NAIP was due to the Iceland Mantle Plume which was initiated during the latest Cretaceous (Schilling 1973). Magmatic activity continues today on Iceland and along the Mid-Atlantic Ridge. However contemporary activity is substantially less vigorous than during the Palaeogene when up to 6 km of extrusive igneous rocks were erupted during the primary rifting and the initiation of sea floor spreading. Much of the lava pile was subaerial due to the thermal doming caused by the plume.

In this section, the issues surrounding the chronostratigraphy of the FIBG, the central thrust of this report, are briefly discussed. The motivation behind this endeavour is that the age and the spatial relationships of the FIBG have major implications for the hydrocarbon prospectivity and the regional petroleum geology of the Faroe-Shetland region and surrounding areas.

At present, the chronostratigraphy of the FIBG is somewhat controversial among the research and industry communities that have activities in the FSB and bordering terranes. Biostratigraphy, magnetostratigraphy, radio-isotopic dating and seismic analysis have all failed to provide a consensus as to the age span of this important major volcanic group and its correlatives (*Figure 6*; Smith et al. 2013; Kimbell 2014). There are several contributory factors to this. Firstly, obtaining reliable age determinations from basalts is frequently very challenging. Basalts are low-potassium rocks which have normally been subjected to low-temperature alteration, argon loss, excess argon, and lack of zircon saturation. Moreover, the interpretation of their field relations can be difficult to precisely determine. Secondly, radio-isotopic age data from the literature is often subjective in terms of its interpretation. Finally, accurate magnetostratigraphy depends on absolute age constraints.

As set out in Section 1, Professor David W. Jolley and collaborators contend that the FIBG is chronostratigraphically constrained to the late Thanetian to early Ypresian (57–54.8 Ma) or the early Ypresian (~56.0–54.8 Ma) (e.g. Passey and Jolley 2009, fig. 18; Schofield and Jolley 2013, *Figure 3*). This view has been promulgated in several publications (Ellis et al. 2002, Jolley and Whitham 2004), and was justified by this group as largely being supported on the basis of pollen biostratigraphy. However, the palynological basis for the late Thanetian–early Ypresian age model has been challenged (e.g. Riisager et al. 2002, Storey et al. 2007, Larsen et al. 2014). Radio-isotopic data for the FIBG and correlatives in the Inner Hebrides and Scotland span the Danian to Priabonian interval (~62 to 34 Ma) as illustrated by Sherlock et al. (2010, fig. 19d) and Larsen et al. (2016, *Figure 11*). Similarly, for example, Mudge (2015) assigned the FIBG to the Selandian to Ypresian (~?61–54.8 Ma) age. This situation was recently discussed by Stoker et al. (2018, *Figure 3*) and the two conflicting hypotheses are summarised in *Figure 6*.

The lithostratigraphy of the Palaeogene succession west of Shetland, the Sullom Formation to the Balder Formation, is well-established (Ritchie et al. 2011). These five formations have been subdivided into a sequence stratigraphical framework based on biostratigraphy, heavy mineral analysis, lithofacies and sedimentology (Ebdon et al. 1995, Lamers and Carmichael 1999). The Sullom Formation to the Balder Formation succession is assigned to sequences T10 to T50 of Danian to Ypresian age (Ebdon et al. 1995, *Figure 4*; Passey and Jolley 2009, *Figure 18*).

3 Geological Background

In this section, the geological background for northwest UK and the Faroe Islands is outlined in three sections. Regionally, during the Palaeocene, the continental crust between Greenland and Europe was influenced by a syn-magmatic extensional tectonic regime associated with an early attempt to open the North Atlantic Ocean. The crust was extended, thickened and uplifted by the doming effects of the Iceland Mantle Plume. Seafloor spreading was then initiated at the mid-Atlantic Ridge in the latest Palaeocene to early Eocene (e.g. Pitman and Talwani 1972, Schilling 1973; Ito et al. 1996).

3.1   THE FAROE ISLANDS

The FIBG is an important constituent of the NAIP (*Figure 2* and *Figure 3*). It comprises an extensive and thick (~6.6 km) Paleogene basalt lava-dominated succession in the Faroe-Shetland Basin, which is one of the several rift basins on the margin of the northeast Atlantic Ocean. This important unit is part of an extensive continental flood basalt province. The FIBG is dominated by extrusive and intrusive igneous rocks, and was first studied by Rasmussen and Noe-Nygaard (1969, 1970). However, most of the succession comprises subaerial basalt lava flows. More recent research has centred on the geochemistry, geochronology and magnetostratigraphy of the basalts (e.g. Hald and Waagstein 1983, Waagstein 1988, Riisager et al. 2002). More recently, Passey and Jolley (2009) presented a new and revised formal lithostratigraphic division of the FIBG, including the volcanic section penetrated by the Lopra-1 and 1A well (Fig. 2, and Table 1).

The FIBG comprises three main periods of basalt lava eruption; these events produced the Beinisvørð, Malinstindur and Enni formations. The Lopra, Prestfjall, Hvannhagi and Sneis formations are distinctly subordinate by comparison (Passey and Jolley 2009, *Figure 17*). These three major units were erupted onto a subaerial setting that extended from East Greenland through the Faroe Islands and continuing south-east into the Faroe-Shetland Basin. The pre-breakup Beinisvørð Formation is ~3250 m thick and exhibits a classic tabular facies architecture, and comprises a succession of simple lava flows each of which comprises a single sheet lobe. Overlying the Beinisvørð Formation is the lithologically distinctive Malinstindur Formation, which exhibits compound-braided facies between ~1350 m and ~1250 m. The Enni Formation is the uppermost unit and comprises both compound and simple lava flows. This unit exhibits two architectures and facies, i.e. compound braided and classic tabular-classic. The nature of the sheet lobes of the Beinisvørð and Enni formations strongly suggests

emplacement via inflation. Lava supply and eruptive style probably influenced the morphology of the compound and simple flow successions of the FIBG (Passey and Jolley 2009). Both the Malinstindur and Enni Formations were erupted during the syn-breakup tectonic regime.

3.2   MULL AND SKYE, INNER HEBRIDES, NORTHWEST SCOTLAND

Material from the British Palaeogene Igneous Province (BPIP) of the NAIP was investigated herein. The BPIP lies along the west coast of Scotland, from Arran in the south to Skye and St Kilda in the north (*Figure 7*, Emeleus and Bell 2005, fig. 1; King 2016, fig. 187). It comprises large areas of the main islands in the Inner Hebrides and neighbouring areas and extends onto the adjacent mainland. The various units are of Danian/Selandian to early Ypresian age (*Figure 8*, King 2016, fig. 189).

Initially, fissure-fed flood basalts were erupted episodically, and these are separated by erosive surfaces and sedimentary units. The next phase was the development of centralised volcanic superstructures overlying intrusive plutonic centres (the central complexes) with NW–SE trending dyke swarms. The BPIP is one of the world's classic areas for central complexes. Here the central complex rocks crop out in restricted subcircular areas about 15 km wide and represent the eroded roots of major central volcanoes which were relatively short-lived (~1 Myr) (*Figure 8* and *Figure 9*). The basaltic lavas became more evolved as the BPIP developed (Emeleus and Bell 2005).
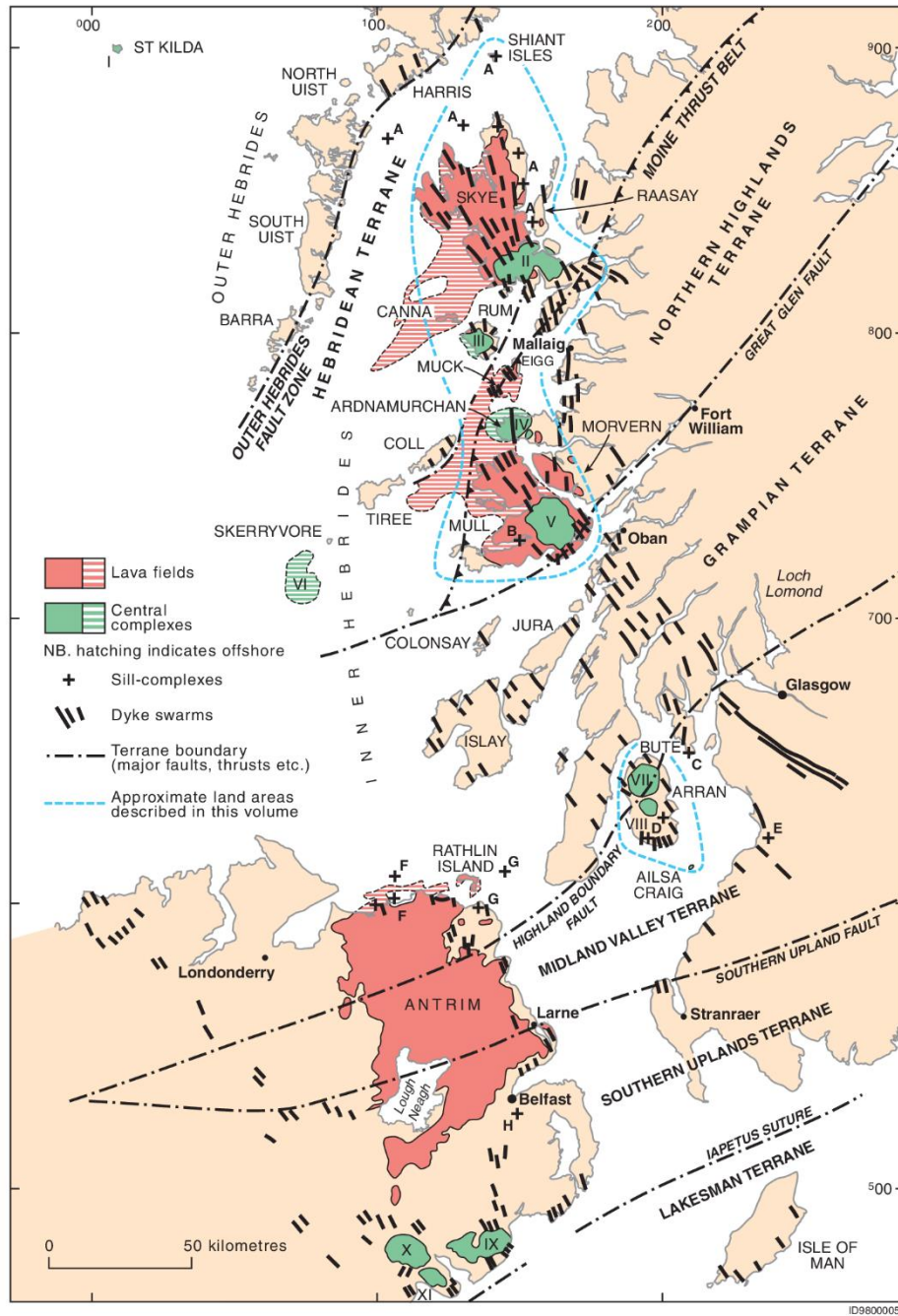
Figure 7 The British Paleogene Igneous Province (BPIP) of northwest Scotland and Northern Ireland. The map illustrates the central complexes (I–XI), dyke swarms (the thick bar ornament), lava fields (Antrim, Mull and Skye) and sill complexes (A–H) in the southeast part

17
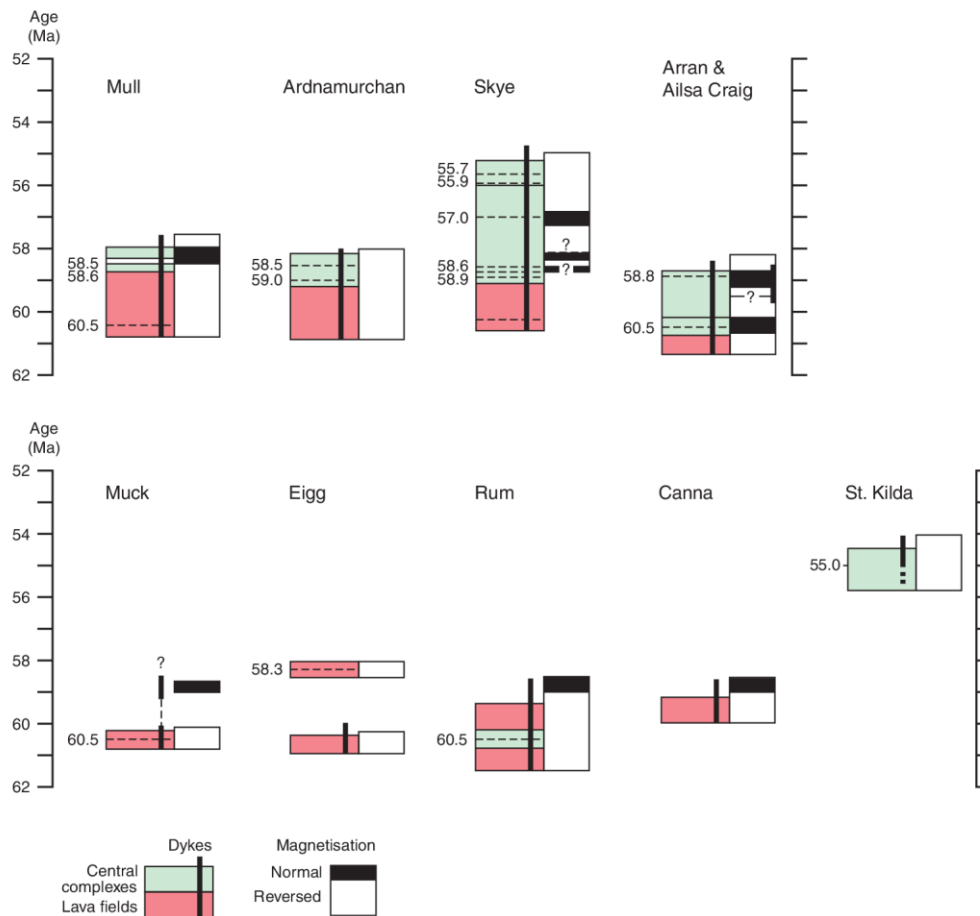
Figure 8 The age relationships of Paleogene igneous units in the British Palaeogene Igneous Province according to Mussett et al. (1988) with additional radio-isotope determinations (Emeleus and Bell 2005, table 8). The magnetochrons are 26N and 26R except for the Skye Central Complex which could extend to 24R (after Emeleus and Bell 2005, fig. 8).

3.2.1   Mull

The island of Mull lies close to the centre of the BPIP (*Figure 7* and *Figure 9*). The Palaeogene igneous succession follows the familiar pattern of extrusive basalts overlain by a central complex (*Figure 9*). The Mull Lava Group (MLG) is dominated by tholeiitic basalt and is around 1800 m thick. It comprises three basaltic formations, the Staffa Lava, Mull Plateau Lava and Mull Central Lava formations. The MLG crops out extensively throughout northern, western and coastal southern Mull in addition to several islands to the west and the mainland to the east as well as offshore (*Figure 9*). The flat-lying basalts produce well-developed trap topography including mountains such as Ben More.

The Gribun Mudstone Member of the Staffa Lava Formation is a thin sedimentary unit, and represents the lowermost subdivision of the MLG. This is overlain by several flows of columnar tholeiitic basalt and which include the Ardtun Conglomerate Member (see subsection 3.1.3). The overlying Mull Plateau Lava Formation comprises two units, the Ben More Main and the Ben More Pale members. The uppermost unit, the Mull Central Lava Formation is largely olivine-poor tholeiitic basalt and is largely present in and around the Mull Central Complex (Emeleus and Bell 2005, table 15).

Figure 9 The northern part of the British Palaeogene Province between Mull in the south and Skye in the north illustrating the central complexes, lava fields (with the five main units) and the Camasunary and Skerryvore faults (from Emeleus and Bell 2005, fig. 9)

3.2.2   The Ardtun Leaf Beds

The Staffa Lava Formation was defined by Williamson and Bell (2012) and was assigned to the early Selandian (chron 26r) by King 2016 (fig. 189). It is the oldest major unit in the post-Cretaceous succession on Mull, and comprises seven units of tholeiitic columnar basalt lava flows (A1 to A7) with seven thin sedimentary units interbedded between them (*Figure 10*; Williamson and Bell 2012, fig. 2). Radio-isotopic (^{40}Ar/^{39}Ar) dating of the associated basalts has been undertaken by Evans (1969), Mussett et al. (1972), Curry et al. (1978), Mussett (1986), Chambers and Pringle (2001) and Ganerød et al. (2010). The lowermost basalts were dated at 60 ± 0.5 Ma by Mussett (1986); this was

recalculated to 60.88 ± 1.16 Ma by Ganerød et al. (2010). Chambers and Pringle (2001) obtained an age of 60.5 ± 0.5 Ma. Hence the consensus of the published radio-isotopic ages is that the earliest lavas in the Staffa Lava Formation are late Selandian in age based on the time scale of Gradstein et al. (2012).

The relatively thin intertrappean sedimentary successions below volcanic units A2 and A7 are collectively termed the Ardtun Conglomerate Member, first reported by Campbell (1851). The Ardtun Conglomerate Member is between 4 and 17 m thick, and is dominated by flint-bearing conglomerates and sandstones. It represents alluvial fan, fluvial channel/overbank and shallow lacustrine depositional settings (Brown et al. 2009). Overall, this sedimentary succession was deposited in a shallow, temporary lake that was partially surrounded by marshy areas. Clastic material and plant debris were swept into the lake by local drainage systems, and lava occasionally flowed into the lake, producing pillow structures. The energy levels of fluvial input to the lake varied profoundly, the three separate leaf beds represent relatively quiet intervals characterised by low sedimentation rates. The unit was comprehensively described and illustrated by Williamson and Bell (2012, p. 32–38).
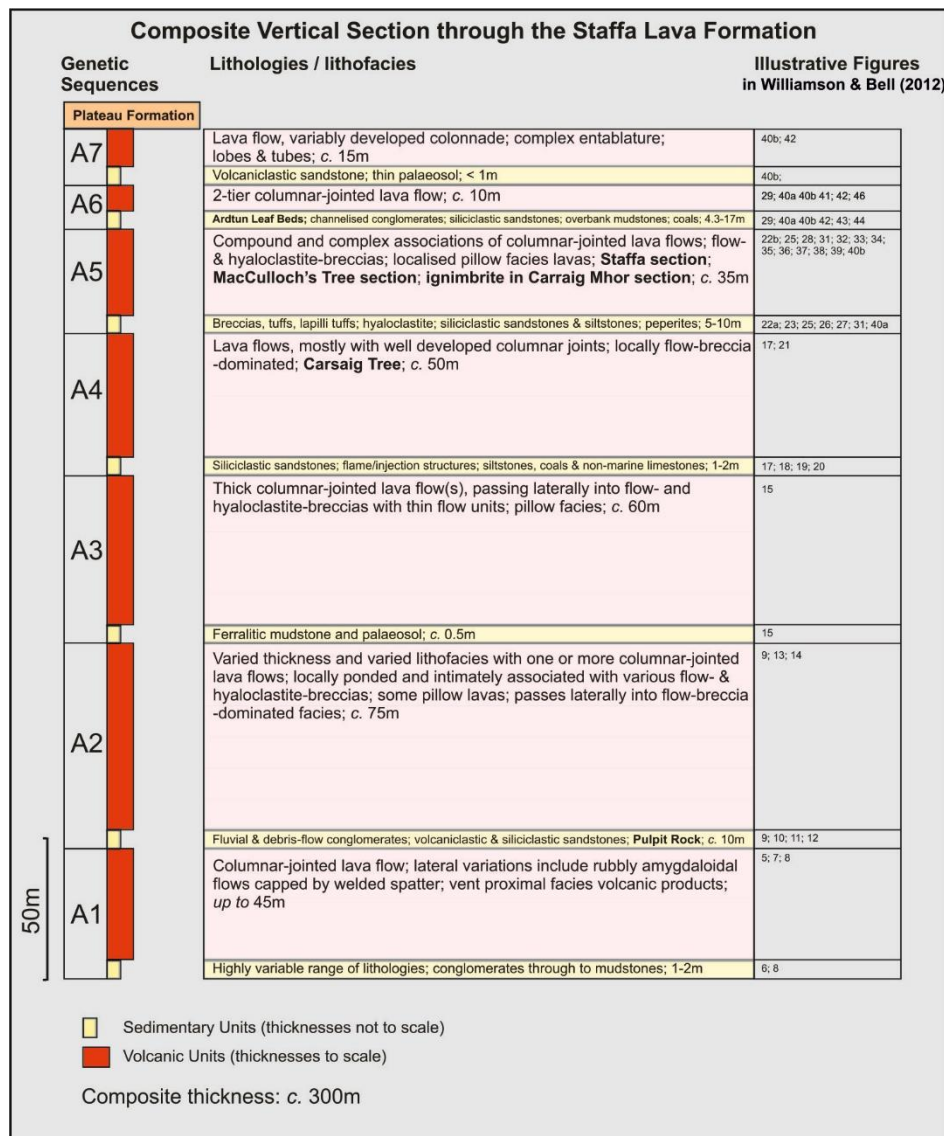
Figure 10 A summary of the lithostratigraphy of the Staffa Lava Formation in the Mull Lava Field (after Williamson and Bell 2012, fig. 2).

The Ardtun Leaf Beds are an informal lithostratigraphical unit within the Ardtun Conglomerate Member comprising three separate plant-fossil bearing beds intercalated between conglomerates and

sandstones (Williamson and Bell 2012, figs. 2, 40a), bracketed by units A5 and A6 in the upper part of the Staffa Lava Formation. Each of the three Leaf Beds is up to ~1 m thick consisting largely of mudstone and silty sandstone exposed in coastal cliffs and gullies on the Ardtun Peninsula, north of Bunessan and east of the Ross of Mull in southwest Mull (*Figure 11*). The lowermost Leaf Bed is underlain by a thin coal which passes down into a thin, pale palaeosol with roots, which is in turn underlain by volcanic unit A5 (Bailey et al. 1924).

It was quickly realised that the abundant angiosperm plant fossils in the Ardtun Leaf Beds may allow biostratigraphical dating of the sedimentary rocks and the associated basalts. Major publications on the Ardtun Leaf Beds and associated strata are Bailey et al. (1924) and Skelhorn (1969).
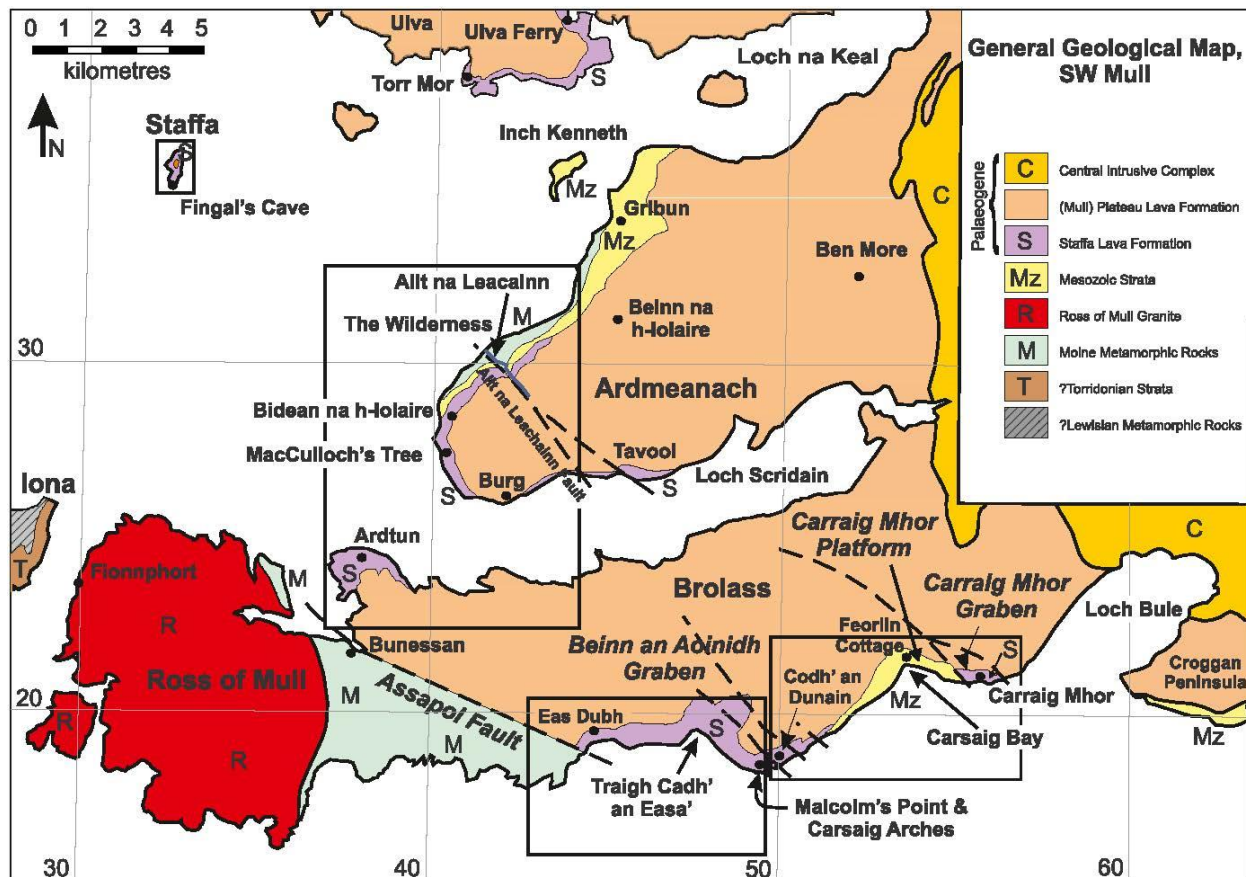
Figure 11 A simplified geological map of southwest Mull to illustrate the location of the Ardtun Leaf Beds on the Ardtun Peninsula, north of Bunessan and Carraig Mhor, Malcolm's Point and the Pulpit Rock (after Williamson and Bell 2012, fig. 4a). The Pulpit Rock lies centrally between Malcolm's Point and Carsaig Bay.

The Ardtun Leaf Beds contain angiospermous plant fossils, mainly fruits, leaves, pollen and seeds. The macrofossils can be relatively common and extremely well-preserved (Campbell 1851, Boulter & Kvacek 1989). Leaves are especially prominent and has been termed 'one of the "classic" leaf floras from the Palaeocene-Eocene transitional interval' by Cleal et al; (2001). This assemblage represents a temperate palaeoclimate based on the plants, which are dominantly trees, and include *Corylus* (hazel), *Ginkgo* (maidenhair tree), *Platanus* (plane) and *Quercus* (oak) (see Skelhorn 1969). Other fossils include arthropods and molluscs (Gardner 1887, Edwards 1922, Zeuner 1941, 1944, Cooper 1979, Jarzembowski et al. 2010).

The biostratigraphy of the plants and pollen of the Ardtun Leaf Beds has been widely discussed in the literature. The macrofossils were originally assigned a probable Eocene age by Seward and Holttum in Bailey et al. (1924). Research on the pollen assemblages has provided a variety of conclusions. The first interpretation was Miocene or Early Pliocene (Simpson 1961). This was revised to latest Cretaceous (Maastrichtian) by Srivastava (1975). Both the previous studies were correctly deemed to be inaccurate by Boulter in Curry et al. (1978), who invoked a Paleocene age.

Bell and Jolley (1997) and Jolley (1997) placed the Ardtun Leaf Beds in the earliest Ypresian (~55 Ma) using an interpreted correlation to some well-constrained assemblages in the Faroe-Shetland Basin. However, this age assessment has proved controversial. Kerr et al. (1998, 1999) stated that Bell and Jolley (1997) had made the assumption that the initiation of Paleogene volcanic activity on Mull also at ~55 Ma (early Ypresian). This is clearly substantially (~5 My) younger than the reliable radio-isotopic (^{40}Ar/^{39}Ar) ages of the basalt lavas published by Mussett (1986) and Chambers and Pringle (2001), which was ~60 Ma. Assuming that the lowermost basalt lavas in the Staffa Lava Formation are not significantly older than the Ardtun Conglomerate Member, the latter is probably ~59 Ma (i.e. early Thanetian). Furthermore, King (2016, p. 570) detailed five specific apparent problems with the pollen-based biostratigraphical age assessment of earliest Ypresian for the Ardtun Leaf Beds. These are largely the over-interpretation of certain taxa, for example the presence of common *Monocolpopollenites tranquillus* was used to justify the earliest Ypresian age interpretation. However this species is also present in significant proportions in the late Selandian and early Thanetian (Gruas-Cavagnetto 1972, Gruas-Cavagnetto 1976, Eldrett et al. 2014). *Monocolpopollenites tranquillus* has also been reported from the latest Cretaceous (Herngreen et al. 1986).

The pollen association from the Ardtun Leaf Beds was referred to as the 'Staffa-type palynoflora' by Jolley et al. (2002), and interpreted this assemblage as a hyperthermal biota which is characteristic of the relatively brief (~170 Ky at ~56 Ma) Paleocene–Eocene Thermal Maximum (PETM). The latter authors stated that 'The Staffa-type palynoflora recovered from Mull is typified by common *Caryapollenites veripites* and *Platycaryapollenites platycaryoides*…..' (Jolley et al. 2002, p. 7). However, Aubry et al. (2003) noted that these pollen species were not recorded from Mull by Jolley (1997). They are also not recorded in this study (section 4.1.4). Hence it appears that the Staffa-type palynoflora of Jolley et al. (2002), while being a valid marker for the PETM, is absent in the Ardtun Leaf Beds. Aubry et al. (2003) and Wei (2003) have heavily criticised the chronostratigraphical conclusions and the correlations proposed by Jolley et al. (2002). Indeed, the former authors stated 'We view Jolley et al.'s (2002) claims that a miscalibration by up to 5 Myr of currently adopted time scales to be without foundation, a result of selective use and misinterpretation of geochronologic data and undue reliance on imprecise and unsubstantiated palynologic evidence' Aubry et al. (2003, p. 468). The so-called recalibration proposed by Jolley et al. (2002) has not been accepted by researchers in this area, and was further substantially critiqued by King (2016, p. 80–81).

In conclusion, the age assessment of early Ypresian by Bell and Jolley (1997) and Jolley (1997) based on their pollen data is not supported herein. Using the records reported from the Faroe-Shetland Basin in Bell and Jolley (1997), it is clear that the Ardtun Leaf Beds are earliest Thanetian or older and this negates the 'miscalibration' of the palynological and radio-isotopic age dates documented in Jolley et al. (2002). King (2016, p. 570, fig. 22) stated that the absence of *Caryapollenites* and *Momipites* indicates a correlation with the Paleocene Palynoflora 1 Zone 1 (PP1).

3.2.3   Skye

Skye is at the northeast extremity of the HIC and the relevant succession comprises the Skye Lava Group which is Selandian in age and is overlain by four Thanetian to Ypresian central complex successions (King 2016, fig. 189). The Skye Lava Group belongs to the Skye Main Lava Series and is largely comprised of alkali basalts, hawaiites and mugearites (Cattell 1989). It forms the Skye Lava Field of north and west-central Skye (*Figure 12* and *Figure 13*). Much of its southern outcrop virtually surrounds the Cuillins Central Complex, and this unit extends south to several smaller islands such as Canna, northwest Rum and Sanday (*Figure 9*). It is thought to be middle Thanetian in age (Jolley 1997, Bell and Williamson 2002). However King (2016, fig. 189) placed this unit in the late Selandian.

Figure 12 An outlier of tholeiitic basalt lava belonging to the Talisker Formation of the Skye Lava Group at Preshal Beg, southwest Skye. The Talisker Formation is the youngest unit of the Skye Lava Group in west-central Skye and overlies the Preshal Beg Conglomerate, an intertrappean sedimentary unit which was sampled in this study (Emeleus and Bell 2005, table 9). The Skye Lava Group is also visible as Macleod's Tables in the distance on the left of the image. BGS photograph P580466.
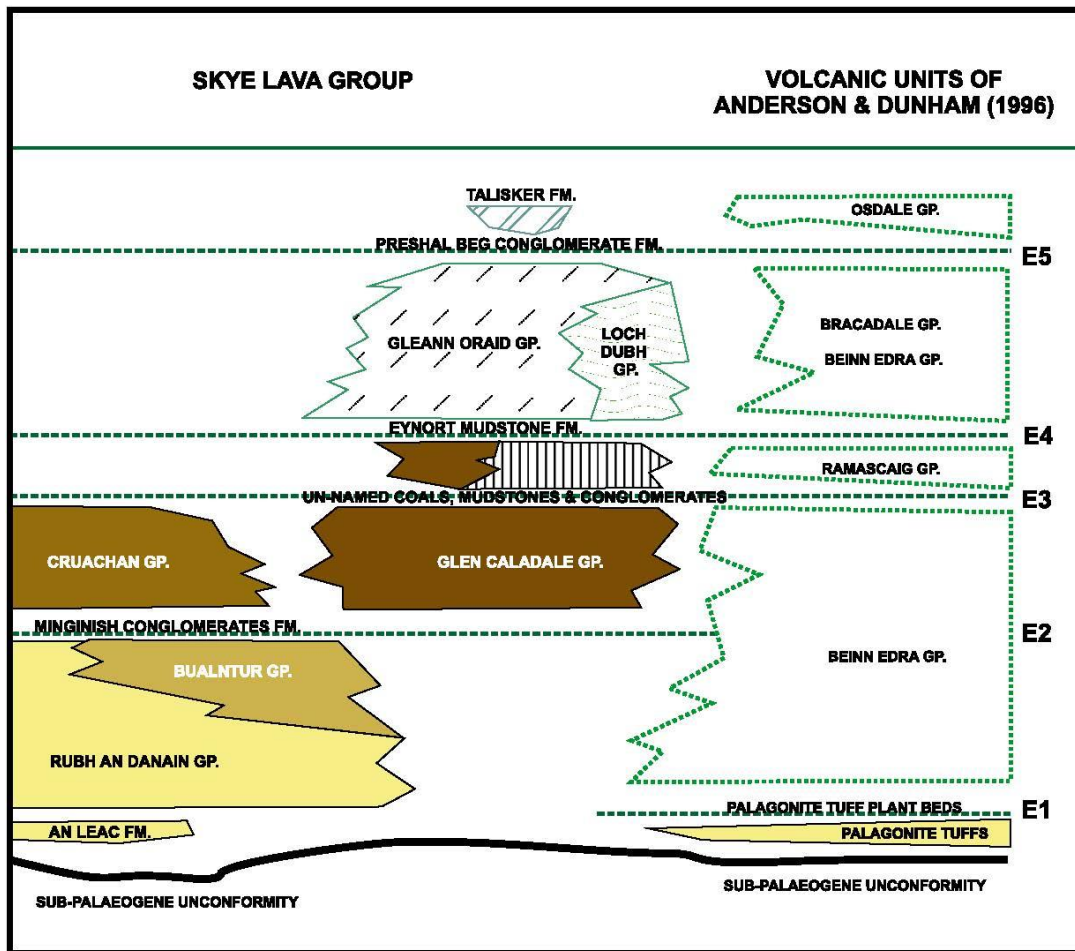
Figure 13 The units of the Skye Lava Group in west-central Skye and the five intrabasaltic palaeosurfaces (E1 to E5) of Jolley (1997). The five palaeosurfaces are also correlated with the equivalent units of Anderson and Dunham (1966). After Jolley (1997, fig. 2)

This major group is subdivided into several units (*Figure 13*; Jolley 1997, fig. 2; King 2016, fig. 188) ranked as groups and formations by Williamson and Bell (1994) but reclassified as formations and members respectively by British Geological Survey (2000) and Emeleus and Bell (2005, table 9). The Skye Lava Group of west-central Skye is difficult to correlate with this unit in northern Skye, however King (2016, fig. 188) gave a speculative summary.

Jolley (1997) designated five intertrappean sedimentary successions within the Skye Lava Group as palaeosurfaces E1 to E5 (*Figure 13*). These units are mainly documented in west-central Skye and represent intervals of erosion, non-marine sedimentation and pedogenesis. Therefore, as originally defined, they are sedimentary successions and not surfaces.

3.3   NORTHERN IRELAND

Northern Ireland lies to the south of the BPIP (*Figure 8*) and was also affected by the plume-related doming and volcanism. Here basaltic lavas were erupted and formed the geographically extensive Antrim Plateau and its offshore equivalents (*Figure 14*; Bell and Jolley 1997). These lavas are termed the Antrim Lava Group which overlies the earliest Palaeogene Danian) Clay-with-Flints unit. The Antrim Lava Group comprises The Lower Basalt, Interbasaltic and Upper Basalt formations, which have been dated as Seelandian to Thanetian (61–58 Ma) (*Figure 15*; Mitchell 2004, table 14.1). The Lower Basalt and Upper Basalt formations represent two cycles of fissure eruption of olivine tholeiite basalt lavas. Effects of fractional crystallisation of the parent magma in the uppermost part of the Lower Basalt Formation are evident. The Interbasaltic Formation comprises intensely weathered, lateritised basalt from the Lower Basalt Formation. The Interbasaltic Formation thus represents a relatively short interval of sub-tropical weathering. The detailed stratigraphy and geographical distributions of the three formations was described in detail by Mitchell (2004, p. 167–178).
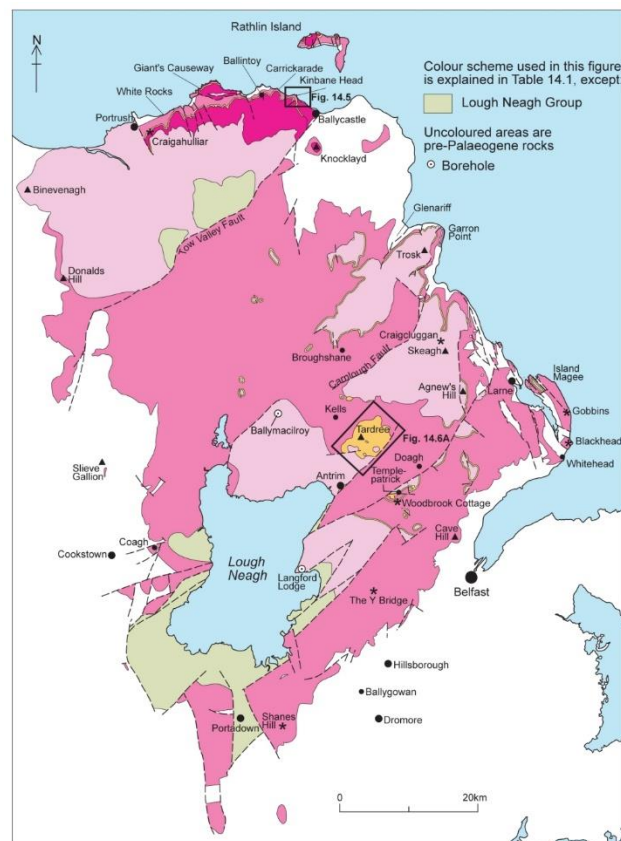
Figure 14 A sketch geological map of the Antrim Lava Group in Northern Ireland (from Mitchell 2004).
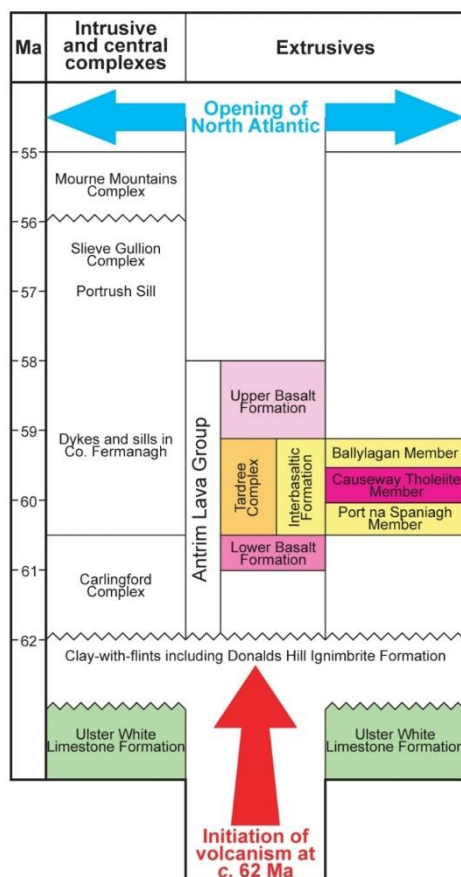
Figure 15 The geochronology and lithostratigraphy of the igneous rocks of Northern Ireland including the Antrim Lava Group (from Mitchell 2004).

4 Palynology

In this section, the palynology of material collected in the Inner Hebrides, Northern Ireland and the Faroe Islands is described below.

4.1   MULL, INNER HEBRIDES, NORTHWEST SCOTLAND

Four localities on the Brolass Peninsula of southwest Mull, Ardtun Head, Carraig Mhor, Malcolm's Point and the Pulpit Rock, were sampled (Figs. 10, 16). In total, 15 samples were collected from the four sedimentary units associated with units A2, A4, A5 and A6 of the Staffa Lava Formation (Williamson and Bell, 2012, fig. 2). In summary, only the Ardtun Leaf Beds at Ardtun Head (unit A6) yielded relatively common palynofloras which, taken in isolation, are indicative of a probable early Thanetian age (subsection 4.1.4). The samples from Carraig Mhor, Malcolm's Point and the Pulpit Rock produced barren or extremely sparse palynomorph associations, and detailed age assessments are not feasible.

4.1.1   The Pulpit Rock, Carsaig Bay, south Brolass, southwest Mull

Two samples of the Ardtun Conglomerate Member, MPA 68171 and MPA 68172, from a siliciclastic succession which overlies volcanic unit A1 were collected from the Pulpit Rock, west of Carsaig Bay, south Brolass, Mull (Williamson and Bell 2012, figs. 4d, 10–13) and studied for palynomorphs. This sedimentary unit is an intertrappean bed ~10 m thick between volcanic units A1 and A2 of the Staffa Lava Formation (Williamson and Bell 2012, fig. 2).
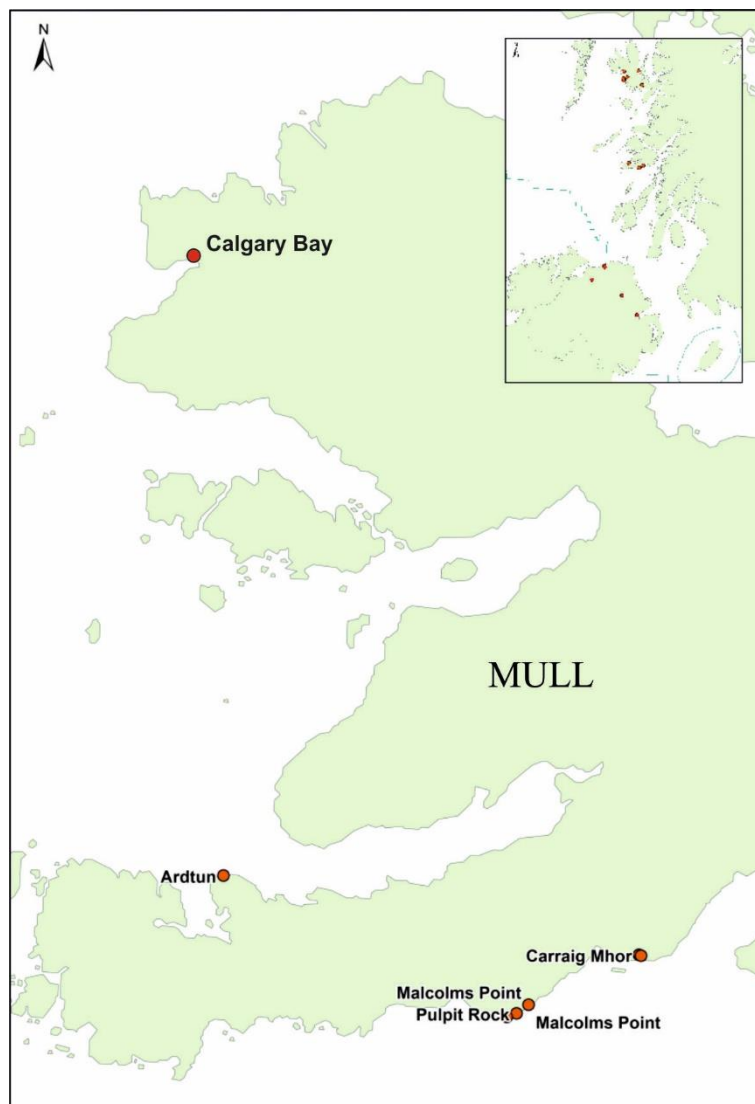
Figure 16. Sample localities on Mull.

Sample MPA 68171 is of a coarse-grained sandstone-conglomerate close to the contact with the basalt of volcanic unit A1, within sedimentary unit C1 of Williamson and Bell (2012, figs. 10–13). It yielded an extremely sparse palynoflora. Fungal material is present to common, and the only recognisable palynomorphs are very rare specimens of the pollen species *Inaperturopollenites hiatus* and undifferentiated smooth trilete fern spores. This assemblage lacks any key biostratigraphical markers. For example, *Inaperturopollenites hiatus* has its inception in the Cretaceous and is extant. An age determination is therefore not possible.

Sample MPA 68172 is from a dark grey/green sandstone close to the top of the lighter-coloured unit C2 of Williamson and Bell (2012, figs. 10–13) and proved entirely devoid of palynomorphs. An age determination is precluded.

4.1.2   Malcolm's Point, south Brolass, southwest Mull

Three samples from coals and a conglomerate at the base of unit A4 of Williamson and Bell (2012), immediately overlying unit A3 were collected from Malcolm's Point (Figs 10, 11, 16; Table A2). These all proved entirely devoid of palynomorphs, hence an age assessment is not possible.

4.1.3   Carraig Mhor, Carsaig Arches, southwest Mull

At this locality (*Figure 10*, *Figure 11*, *Figure 16*), five samples of sandstone and siltstones at the base of unit A5, overlying unit A4, were taken. All the horizons were barren of identifiable palynomorphs, hence a biostratigraphical age cannot be attributed on this basis.

26

4.1.4   The Ardtun Leaf Beds of Ardtun Head, north Brolass, southwest Mull

The Ardtun Leaf Beds, at the base of unit A6 of Williamson and Bell (2012) were sampled at Ardtun Head, north Brolass, southwest Mull (*Figure 10*, *Figure 11*, **Figure 16**, Table A2). Five samples were collected from this locality, which was previously sampled by Simpson (1961), Phillips (1974), Srivastava (1975) and Jolley (1997); all five of the horizons yielded palynomorphs (*Figure 17*). The palynofloras were relatively sparse, and the preservation was generally poor. Counts yielded between 35 to 92 specimens, and 21 taxa were recorded.

The dominant elements are long-ranging gymnospermous pollen grains; these are undifferentiated bisaccate pollen attributable to the Pinaceae (pine family) and *Inaperturopollenites hiatus* (*Glyptostrobus* or *Metasequoia*). The gymnosperm *Monocolpopollenites tranquillus* (=*Cycadopites shiabensis*) is also very common. This abundance is anomalous and probably reflects local environmental conditions because *Monocolpopollenites tranquillus* is stratigraphically long-ranging. The pollen floras also contain relatively rare members of the family Betulaceae (birch) (i.e. *Alnipollenites* spp., *Triatriopollenites* spp. and *Triporopollenites mullensis*), representatives of the family Juglandaceae (walnuts) (i.e. *Momipites* spp. and *Pterocaryapollenites stellatus*), and long-ranging tricolpate pollen. These are all stratigraphcally extensive genera which are typical of the British Palaeogene Igneous Province (BPIP). The fungal palynomorph ?*Pesavis tagluensis* is present; this is an Eocene marker in the Arctic, but has a Palaeocene first occurrence at lower latitudes. Reworking from the Carboniferous and Jurassic is also common.

The only important taxon that is absent from an otherwise typical high latitude Palaeocene floodplain deposit is the genus *Caryapollenites* spp. The lack of *Caryapollenites* spp. from these pollen floras is therefore somewhat surprising. This important form-genus was also not observed by Simpson (1961), Srivastava (1975) or Jolley (1997) from Mull. In the central North Sea, *Caryapollenites circulus* (=*Caryapollenites simplex*) and *Caryapollenites veripites* are important markers from the latest Thanetian to early Ypresian (Schröder 1992; Kender et al. 2012; Eldrett et al. 2014). The genus generally is indicative of the ?mid Thanetian to earliest Ypresian. However well 22/11-N1 in the Nelson Field of the Central North Sea has yielded low but consistent proportions of *Caryapollenites simplex*, *Caryapollenites triangulus* and *Caryapollenites veripites* in the middle Thanetian uppermost Andrews Formation and lowermost Lista Formation (Eldrett et al. 2014). The acme of *Caryapollenites* spp. approximates to the Paleocene–Eocene boundary (PETM). Hence the absence of *Caryapollenites* spp., and the dominance of gymnosperms, is inconsistent with the Palaeocene–Eocene transition. Moreover, the absence of *Caryapollenites,* together with the presence of typical elements of high-latitude floodplain floras, strongly suggests an older age.

The only taxa with any stratigraphical significance are the fungal species *Pesavis tagluensis* which has a single occurrence, and has also been recorded by Jolley (1997) from this locality, and *Labrapollis labraferiodes* that has two occurrences herein. The latter pollen species was observed by Simpson (1961) and Srivastava (1975) from Mull (as *Engelhardtioidites granulata* and *Engelhardtia granulatus*). *Pesavis tagluensis* is an important marker in Arctic Canada for the Eocene and has a range zone based around its common occurrence (e.g. Norris 1997). The age range in the UK is unknown and in North America is appears in the Middle Palaeocene in the lower high latitudes before appearing in the Eocene in higher Arctic latitudes (Rouse 1977, Lund 1989).

Labrapollis labraferiodes (=*Triporopollenites granulatus*) was also observed in the Artun Leaf Beds. This species first appears in North America in the Danian–Selandian (Leffingwell 1971), and is present consistently in the late Selandian–early Thanetian on the US Gulf Coast (Elsik and Crabaugh 2001) and in the late Thanetian in Wyoming (Pocknall and Nichols 1996). In the central North Sea it is an important marker for the Paleocene–Eocene boundary (e.g. Schröder 1992, Eldrett et al. 2014), and coincides with the presence of the dinoflagellate cyst species *Apectodinium augustum* (see Schröder 1992, Eldrett et al. 2014). Its total range in the North Sea is mid Thanetian to the earliest Ypresian. *Labrapollis labraferiodes* features in most palynomorph biozonations throughout the North Sea area. The only record of this pollen species outwith the Paleocene–Eocene Thermal Maximum (PETM) in the UK is that of Jolley and Morton (1992) from a lignite immediately underlying a tuff

in the uppermost Andrews Formation. This indicates its presence around the middle Thanetian in the North Sea region; the range base is unknown.

The pollen genus *Montanapollis* was recorded from the Ardtun Leaf Beds of Mull by Srivastava (1975) and the latest Paleocene (Thanetian) of the Faroes (Lund 1989). This taxon was not found in this study. This distinctive, large pollen is present in Arctic Canada as *Derviella* (see Rouse 1977; McIntyre 1991, 1994; Kalkreuth et al. 1996; Norris 1997; Harrington et al. 2012). In the Arctic, it is present from the early Ypresian from between the end of the PETM and prior to the Early Eocene Climatic Optimum (EECO) event (Harrington et al. 2012). The age range of *Montanapollis* in the UK is not known with certainty. It is rare in the North Sea, however, Jolley (1997) recorded the genus from the lower Sele Formation in the North Sea, which is of probable Thanetian age.

The most parsimonious interpretation for the age of the Ardtun Leaf Beds is that this unit is Thanetian in age. More specifically, the absence of *Caryapollenites* is significant because this form genus is normally ubiquitous in the fossil record following its inception in the mid Thanetian. *Labrapollis* can be older than earliest Ypresian, and the age range of *Montanapollis* (=*Derviella*) is not known in the UK. Otherwise, the pollen assemblage is consistent with late Paleocene floras from the Arctic (McIntyre 1989). The Ardtun Leaf Beds floras conform to the Brito-Arctic assemblage of Boulter and Kvaček (1989) and Boulter and Manum (1989). It is extremely unlikely that the floras are from the Paleocene–Eocene boundary as argued by Bell and Jolley (1997) and Jolley (1997). This is because the absence, or profound rarity, of gymnosperms is a key feature observed from the Arctic south to the middle latitudes and also from montane basins at this time (Wing and Currano 2013). The predominance of gymnosperms in Mull is therefore completely inconsistent with this phenomenon. Furthermore, *Caryapollenites circulus* (=*Caryapollenites simplex*) and *Caryapollenites veripites* are abundant and increase in proportion markedly in the Palaeocene–Eocene boundary interval. This is a well-established acme event (Schröder 1992; Kender et al. 2012; Eldrett et al. 2014). The absence of both these species of *Caryapollenites* strongly suggests that the Ardtun Leaf Beds are older than middle Thanetian, i.e. probably early Thanetian in age. However, radioisotopic dating of the Ardtun Leaf Bed in this study is indicative of a Selandian age, i.e. older than Thanetian (section 6.1.1). This absolute age dating has thus provided a calibration to the pollen biostratigraphy.

Reworking of dinoflagellate cysts, pollen and spores from the Jurassic was occasionally noted but this was not examined in detail; this phenomenon was previously recorded by Phillips (1974).

4.1.5   A biostratigraphical overview of the samples from Mull

The 10 samples taken from Carraig Mhor, Malcolm's Point and the Pulpit Rock could not be assigned a biostratigraphical age due to their sparsity. By contrast, the pollen assemblages from the Ardtun Leaf Bed strongly indicate that this unit is older than middle Thanetian, hence probably early Thanetian in age. However, radio-isotopic dates from this succession are indicative of the Selandian and this geochronological assessment provides a reliable calibration for the pollen biostratigraphy.
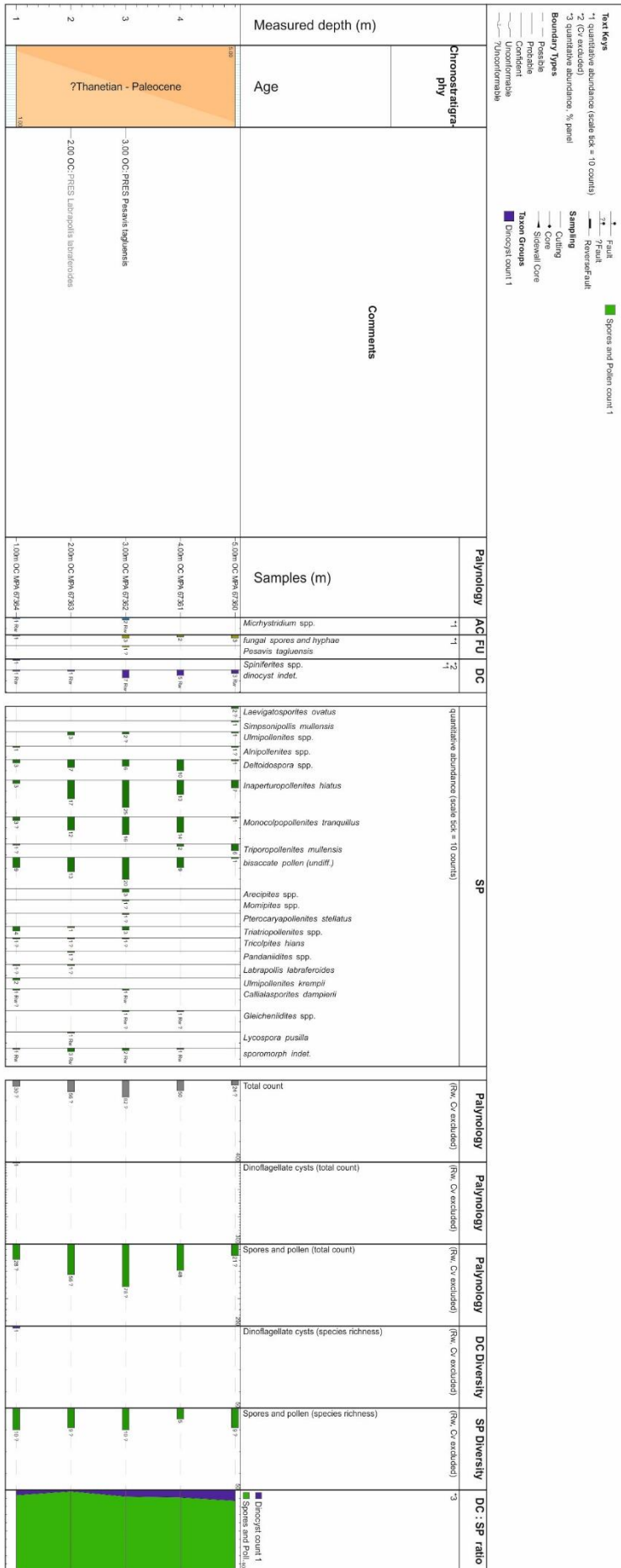
Figure 17 Palynology of the Ardtun Leaf Bed.

4.2   SKYE, INNER HEBRIDES, NORTHWEST SCOTLAND

Five localities with intertrappean sedimentary rocks developed within the Skye Lava Group on Skye were sampled. Four of the sites, Carbost Burn Waterfall, Dunn Beag, Preshal Beag and Preshal Mhor, are in the west-central Skye lava field between Loch Harport and Loch Eynort in the southwest of the island. However, Camas Tianavaig is in east-central Skye close to the Sound of Raasay (*Figure 9*, *Figure 18*). A total of 19 samples were collected from palaeosurfaces E1, E3, E4 and E5 of Jolley (1997) (Table A3).

Of the 19 samples collected, only nine produced palynoflaras. All the nine pollen-bearing horizons yielded sparse assemblages that are not age-diagnostic. The absence of key markers such as *Caryapollenites* and *Momipites* precludes age assessments of this material on palynological grounds (see subsection 4.2.5).
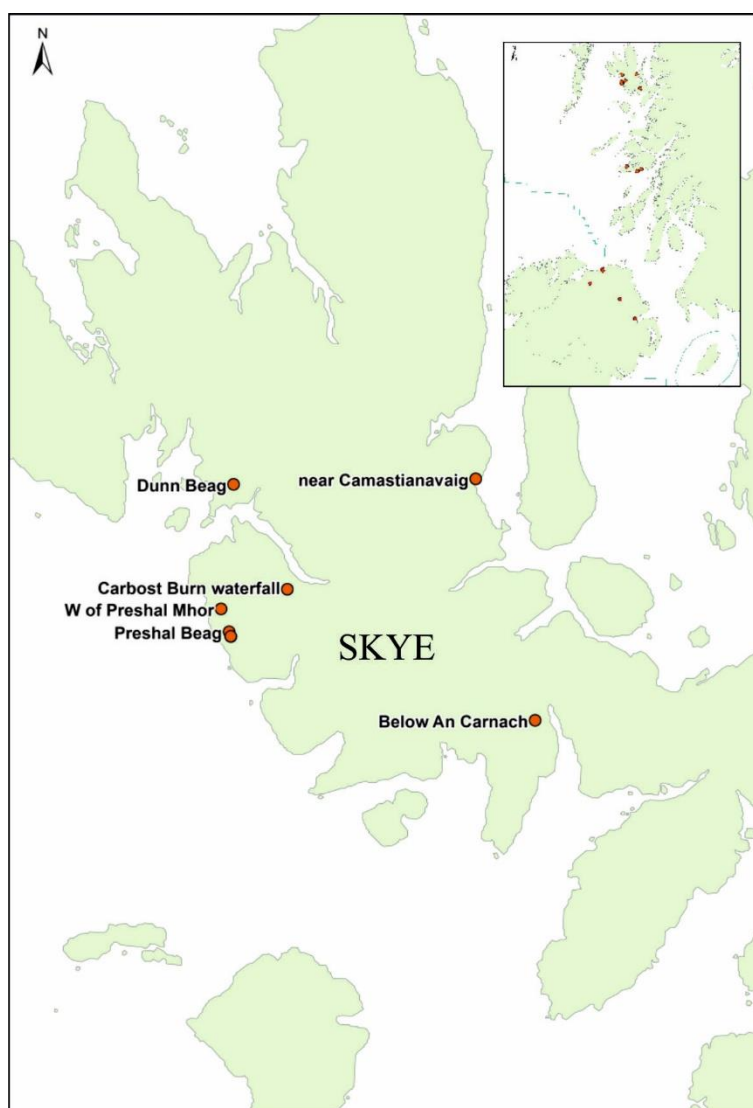
Figure 18 Sample localities on Skye.

4.2.1   Near Camas Tianavaig, Sound of Raasay, east central Skye

Two samples of sandstone from the Palagonite Tuff Plant Beds at this locality were collected (*Figure 18* Table A3). This is palaeosurface E1 of Jolley (1997). Only one of these, MPA 68200, yielded palynomorphs, however this was an extremely sparse assemblage. Fungal material is present, in addition to very low numbers of pollen grains. The latter are *Alnipollenites verus, Inaperturopollenites hiatus, Laevigatosporites haardtii, Triatriopollenites* spp. (undifferentiated),

Tricolpites hians and *Triporopollenites mullensis.* The sparsity of this assemblage, coupled with the long-ranging nature of these pollen taxa, means that a detailed age determination is not possible.

4.2.2   Carbost Burn Waterfall, Carbost, southwest of Loch Harport, west central Skye

Of the three samples collected from palaeosurface E3 of Jolley (1997), below the Fiskavaig Group at this locality, only one, MPA 68192 produced palynomorphs (*Figure 18*, Table A3). This shaly sandstone yielded an extremely sparse palynoflora. It contains fungal material and spores, together with small numbers of specimens of pollen attributable to *Laevigatosporites haardtii*. Another sparse element is potentially the pollen genus *Ericipites,* although these specimens may be modern contaminants of *Calluna vulgaris* (= common heather). Other contaminants were present. Furthermore, six specimens of indeterminate sporomorphs and a single specimen of an indeterminate dinoflagellate cyst were observed. The sparsity of this assemblage, and the long stratigraphical range of *Laevigatosporites haardtii* means that an age determination is not possible.

4.2.3   Dunn Beag, north of Loch Harport, west central Skye

Four of the five samples, largely siltstones, collected from the Eynort Formation at Dunn Beag, near Loch Harport, yielded extremely sparse palynomorph residues (*Figure 18*, Table A3). These samples are all from palaeosurface E4 of Jolley (1997). Only MPA 68197 proved barren. Samples MPA 68199, MPA 68198, MPA 68196 and MPA 68195 produced palynomorph associations similar in character to the sample from Carbost Burn Waterfall (subsection 4.2.2). The samples produced fungal material, together with low numbers of pollen grains. The latter are bisaccate pollen, indeterminate pollen, *Laevigatosporites haardtii, Triatriopollenites* spp., *Tricolpites hians* and *Triporopollenites mullensis.* Additionally possible specimens of *Ericipites* were noted, but these may be modern contaminants (*Calluna vulgaris* = common heather). Some other contaminants are noted, but these are not determinable. The long-ranging nature of the identifiable pollen means that an age assessment is impossible.

4.2.4   Preshal Beag and Preshal Mhor, Skye

Nine samples were collected from the Preshal Beag Conglomerate Formation from Preshal Beag and Preshal Mhor in west central Skye, WSW of Talisker Bay (*Figure 18*, Table A3). The Preshal Beag Conglomerate Formation is palaeosurface E5 of Jolley (1997). Eight of the samples are from Preshal Beag, but MPA 68190 was collected from west of Preshal Mhor. The latter proved palynologically barren. Three samples from the eight horizons collected at Preshal Beag yielded palynomorphs. These are MPA 68183, MPA 68184 and MPA 68189; the remainder were devoid of organic microfossils. The three productive samples contain extremely sparse assemblages which include some modern contamination. However, stratigraphically long-ranging indigenous taxa such as *Alnipollenites verus,* bisaccate pollen, *Deltoidospora* spp., *Inaperturopollenites hiatus* and *Pterocaryapollenites stellatus* are present in very low numbers. All these forms infer no biostratigraphical information.

4.2.5   A biostratigraphical overview of the samples from Skye

The pollen and spore flora in the nine productive samples from Skye contain a very sparse, low diversity *in-situ* palynoflora comprising stratigraphically long-ranging taxa. The most abundant elements of this palynoflora are gymnosperms such as undifferentiated bisaccate pollen (Pinaceae), and *Inaperturopollenites hiatus* (*Metasequoia, Glyptostrobus*). The remaining pollen are typical of the British Palaeogene Igneous Province (BPIP). These include include Betulaceae pollen (*Alnipollenites* spp., *Triatriopollenites* spp. and *Triporopollenites mullensis*), Juglandaceae pollen belonging to *Momipites* spp. and *Pterocaryapollenites stellatus* (Preshal Beag only), and long-ranging tricolpate pollen.

The important pollen taxa that are absent from an otherwise typical high latitude floodplain depositional setting here are *Caryapollenites* spp. and *Momipites* spp. Of these, *Caryapollenites* spp. is an important form-genus, and was not recorded by Simpson (1961), Srivastava (1975) and Jolley

(1997) from Mull. In the central North Sea, *Caryapollenites circulus* (= *Caryapollenites simplex* herein) and *Caryapollenites veripites* are important markers for the latest Thanetian to early Ypresian (Schröder 1992, Kender et al. 2012, Eldrett et al. 2014). However, well 22/11-N1 from the Nelson Field in the central North Sea clearly demonstrates that *Caryapollenites simplex, Caryapollenites triangulus* and *Caryapollenites veripites* are consistently present in low numbers in the middle Thanetian. This corresponds to the uppermost Andrews Formation–lowermost Lista Formation interval within Shell zone PT-15.2.5 (Eldrett et al. 2014). Despite this, the acme of *Caryapollenites* spp. approximates to the Paleocene–Eocene transition.

According to Naylor et al. (1999, fig. 4), the range top of *Momipites tenuipolus* is in the Middle Thanetian Lamba Formation with a second reappearance around the Thanetian–Selandian boundary in the Faroes-Shetland area. Jolley and Morton (1992) reported common *Momipites tenuipolus* from a questionably Lower Thanetian lignite which immediately overlies the Andrews Formation in Borehole 82/15. Eldrett et al. (2014) demonstrated that the range top of *Momipites tenuipolus* is latest Thanetian age (Shell zones PT-19.1.2 and 19.1.1) based on records from the lowermost Forties Sandstone Member of the Sele Formation.

The absence of samples with abundant and diverse palynofloras which include key markers means that no age determinations can be assigned to any of the nine productive samples from Skye. The lack of key markers which are used in the Brito-Arctic region such as *Caryapollenites, Labrapollis* and *Montanapollis* may be due to poor preservation or age-related factors. These factors could also apply to the absence of *Momipites tenuipolus*.

4.3   NORTHERN IRELAND

Eleven samples were collected from the Antrim Lava Group and the immediately underlying Clay-with-Flints from five localities in Northern Ireland in July 2017 by Mark R. Cooper and Robert J. Raine of the Geological Survey of Northern Ireland (GSNI) (Table A4). Upon standard palynological preparation, all the samples proved relatively organically sparse. The residues largely comprise black and brown wood fragments, and resistant mineral grains. Sample 5 from Belfast Zoo produced significant levels of brown amorphous organic material. The dark nature of the non-palynomorph organic materials, and the lack of palynomorphs, is indicative of high levels of thermal maturation due to the proximity of the basalts. The high levels of heat flow appear to have destroyed any indigenous palynomorphs.

Samples 1, 4–9 and 11 proved entirely barren of palynomorphs. Samples 2, 3 and 10 each yielded only a few pollen grains. These were generally poorly-preserved and largely unidentifiable, even to genus level. Two specimens of the long-ranging (Cretaceous to modern) pollen species *Inaperturopollenites hiatus* were encountered in sample 10 from the Upper Basalt Formation at Donald's Hill.
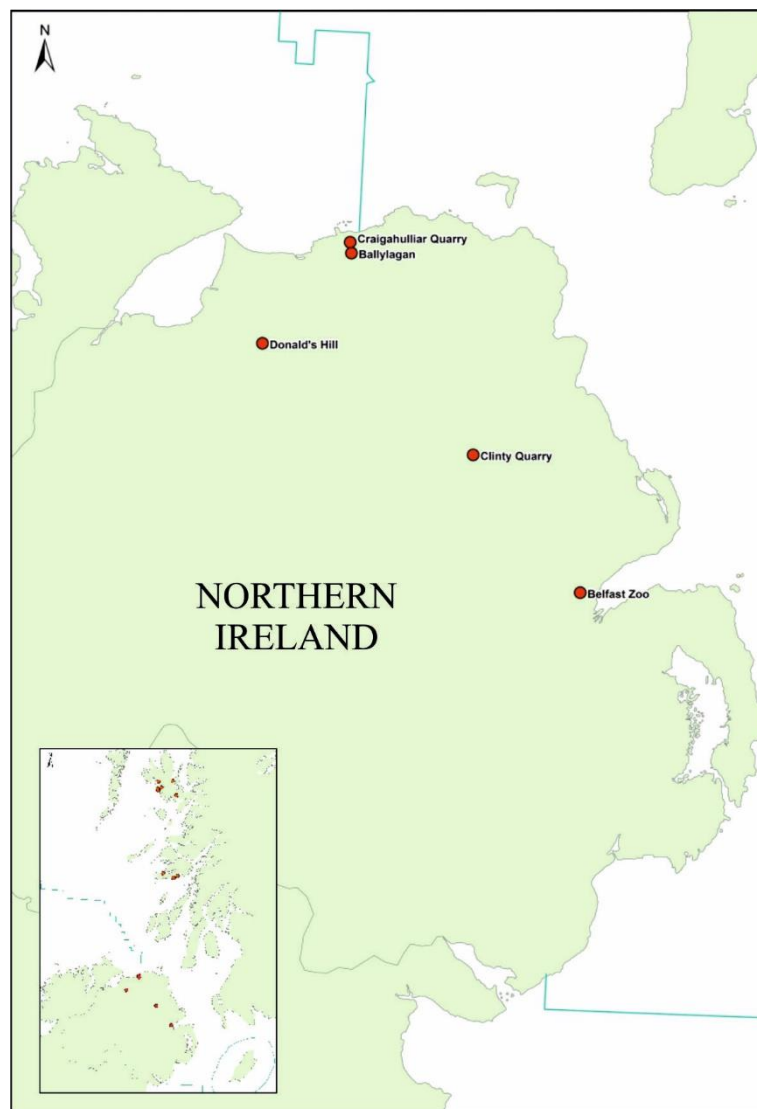
Figure 19 Sample localities in Northern Ireland.

4.4   FAROE ISLANDS

From the onshore parts off the FIBG 207 samples were collected for palynological studies and radiometric dating. The main focus was the transition from the pre-breakup sequence of the Beinisvørð Formation and Prestfjall Formation through to the syn-breakup sequences of the Hvannhagi Formation, and Malinstindur Formation. The complete sample list is given in Appendix A5 and the sample localities are shown in *Figure 24*. The stratigraphic range of the sample series is shown in *Figure 25* (strat log with all samples). In addition to the onshore sample localities, the Vestmanna-1 Well was also sampled. This cored well penetrates the base of Malinstindur Formation and through the Prestfjall Formation into the Beinisvørð Formation.

Detailed sections were also logged at the Holið í Helli locality (Section 4.4.1) and a mountain traverse/profile matching Major Profile number x from Rasmussen and Noe-Nygaard (1969).

Below are descriptions from each of these main localities that did show palynological data.

4.4.1   Vágóy, Eysturoy and Streymoy

Interlava lithologies are found throughout the sequence, but become more common towards the top of the formation. Although the Malinstindur Formation is sparse in fine grained thick sedimentary horizons, suitable for palynological studies, some isolated beds were selected for this study. Below are some of the localities from the Malinstindur Fm. intra lava sedimentary units from Vágóy, Streymoy and Eysturoy described. These samples are from the upper parts of the Malinstindur Fm.
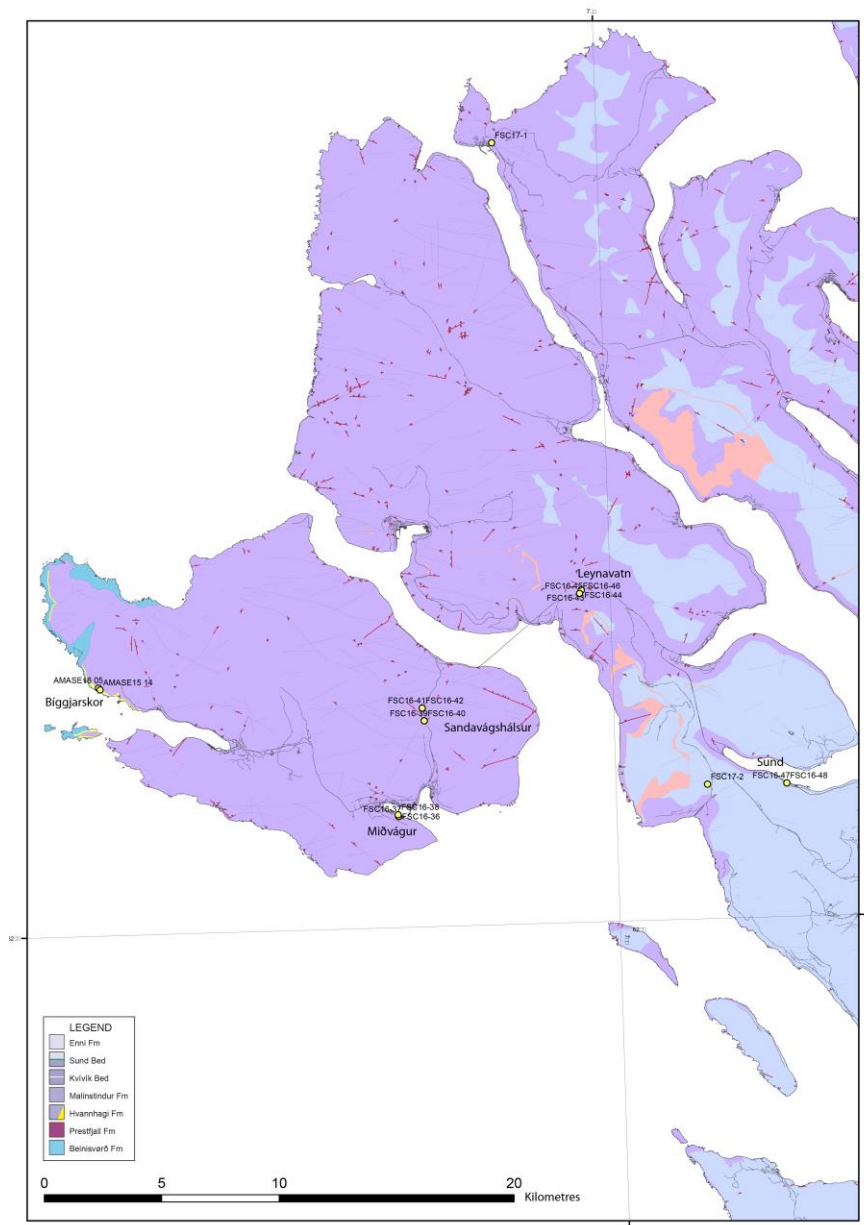
Figure 20 Map showing the sample localities from Vágoy, Eysturoy and Streymoy on the Faroe Islands.

4.4.1.1 MIÐVÁGUR QUARRY

In the Malinstindur Formation at the quarry in Miðvágur (*Figure 21*) intra-lava volcaniclastic sedimentary beds are seen. The beds are relatively coarse, bur grading into fine-grained top. These samples were selected for both zircon separation (coarse units) and palynological studies (fine units). The samples collected at this locality proved to be barren of palynomorphs.

Figure 21 A 15-20 cm think volcaniclastic bed, Coarse grained at the base and grading into fine grained top. Two separate samples were taken at this locality. Location of the volcaniclastic bed is shown as the white dotted line on left photo.

4.4.1.2 SANDAVÁGSHÁLSUR (ONSHORE)

At the Sandavágshálsur locality (*Figure 22*) two intra-lava sedimentary units were sampled. These fine grained volcanclastic sandstones are some 20 cm thick and show two sequences of coarse to fine gradational bands. The stratigraphical height of these samples correlates roughly to the Kvívík Beds from Passey and Jolley (2009).

Figure 22 A 15 cm thick sedimentary bed in the Malinstindur Formation at Sandavágshálsur. Note the varying grain sizes.

Two samples, MPA 68209 and MPA 68207, were analysed from Sandavágshálsur. They both proved virtually devoid of palynomorphs. Two specimens of the long-ranging smooth spore *Cyathidites* were encountered in MPA 68209 and one indeterminate dinoflagellate cyst was recognised in MPA 68207. There were two other palynomorph specimens in both samples, but these are not identifiable. No age assessment is possible.

4.4.1.3 VESTMANNA-1 WELL (ONSHORE SCIENTIFIC WELL)

From the Vestmanna-1 Well, 25 samples (FSC16-103 1-25) were taken. The stratigraphical range of these samples spans from the top most parts of the Beinisvørð Formation through the Prestfjall Formation and up through the lowest most 500 m of the Malinstindur Formation. The intra-lava lithologies from the Beinisvørð Formation comprise dark brown mud- and siltstones, while the lithologies become slightly coarser from siltstones to sandstones in the Malinstindur Formation. The samples collected at this locality proved to be barren of palynomorphs.

4.4.1.4 KLIVARNAR, LEYNAVATN

In the Malinstindur Fornmation at Klivarnar on Streymoy, an erosional fluvial system/channel with cross bedded volcaniclastic sandstones is seen (*Figure 23*). The sandstone is ca 1 m thick at the centre of the channel and the thickness rapidly decreases away from the central parts. The sandstone is poorly sorted, coarse with lithic fragments (IGC field guide, Passey 2008) in the central parts. Samples both for zircon separation and palynological studies were taken at this locality. The samples collected at this locality proved to be barren of palynomorphs.

Figure 23 Central part of the fluvial volcaniclastic channel at Klivarnar Locality, Streymoy. Samples MPA 68211 and MPA 68214 were collected here.

4.4.1.5 SUND QUARRY

At Sund Quarry the Sund Bed is exposed. The basal Sund Bed is part of the Sneis Formation (Passey and Jolley, 2009) and is ca. 1m thick. The bed is crudely graded as well as finely laminated in places. The volcaniclastic sandstone is generally medium grained and poorly sorted. The unit is dominated by sub-rounded to rounded clasts of reworked palagonitised basaltic glass, although larger clasts still preserve vesicles and cuspate margins. A characteristic feature of the Sund Bed and which is clearly evident at this locality is the preservation of creamish, charcoalified wood fragments (branches) that have a classic 'boxwork' structure. These fragments are typically found in a layer approximately two-thirds above the base of the bed. This surface is well exposed on fallen blocks where wood fragments up to 4 m in length can be seen. The Sund Bed is overlain by a volcaniclastic conglomerate sequence that has been intruded by a thick basaltic sill which forms the quarry face. Thin 'pockets' of the conglomerate can been seen directly overlying the Sund Bed in the quarry but the conglomerate is more clearly seen above the sill in sections above the main road to the north of this location. The Sund Bed and the overlying volcaniclastic conglomerate are interpreted to have been deposited from hyperconcentrated and debris flow regimes, respectively (Passey, S.R, 2008. IGC Excursion No.6, Field Guide). The samples collected at this locality proved to be barren of palynomorphs.

4.4.2   Suðuroy

The Island of Suðuroy is comprised of the Beinisvørð Formation lavas through to the basal parts of the Malinstindur Formation (*Figure 21*).The Beinisvørð Formation was strategically sampled from the lower most intra-lava sediments at Sumba through to the upper most part of the formation at Holið í Helli. Furthermore samples from the basal parts of the Malinstindur Formation were sampled on Suðuroy (Figure of Suðuroy_Uni).

The total number of 150 samples taken from Suðuroy are, of these 37 were processed (*Table 1*).

A series of intra-lava sedimentary sections were sampled (Samples MPA 68319 to MPA 68375 in *Table 1*). These comprise coal seams (MPA 68319, Ádalsmøl), clay-, sand- and siltstones from the Hvannfelli profile (MPA 68327, MPA 683335 and MPA 68340), black mudstones and grey claystones from Áin Mikla (MPA 68365, MPA 68366) and brown mudstone from Hov (MPA 68375).

In addition to these samples the Beinisvørð Formation was sampled in the Vestmanna-1 Well.
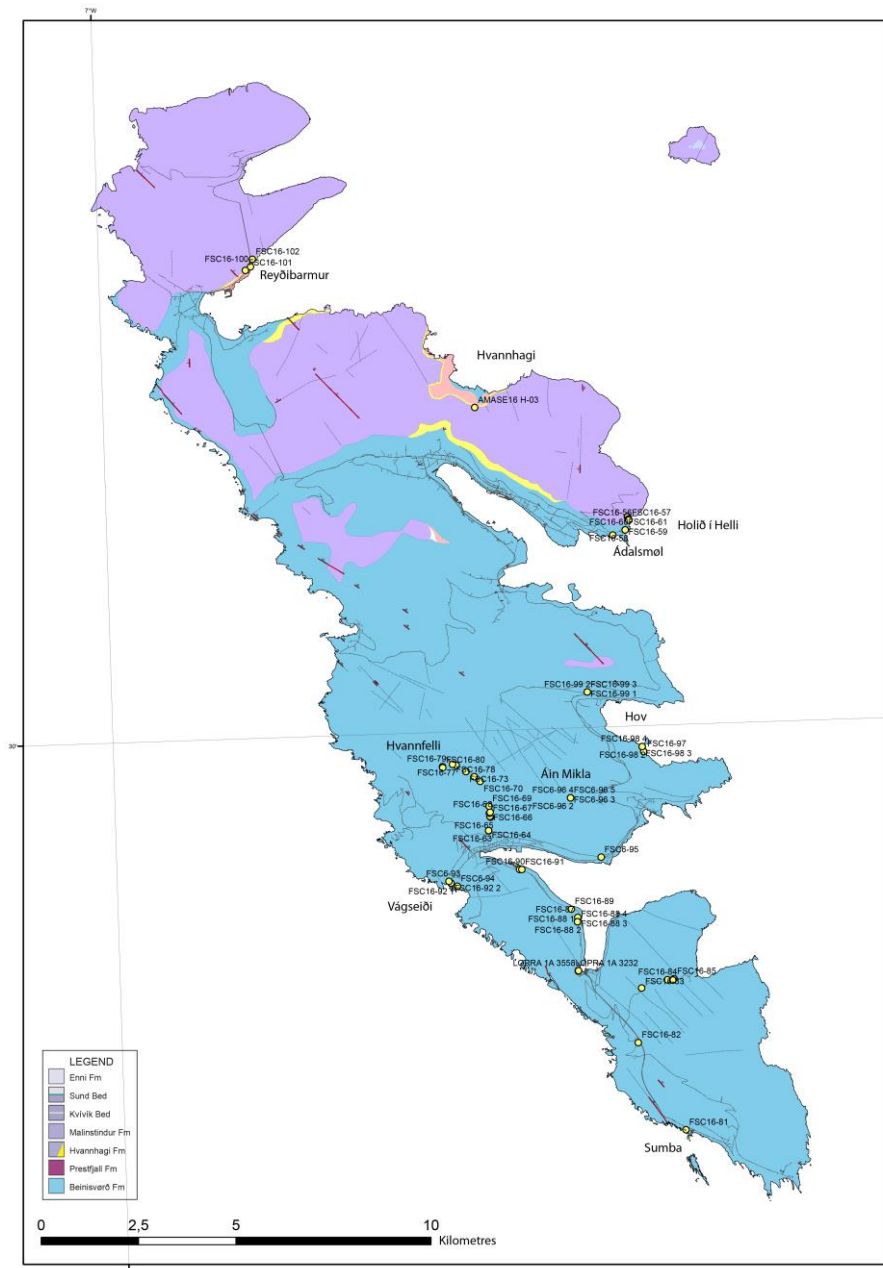
Figure 24 Geological map of Suðuroy, showing all the sample localities from the FSC field work.

4.4.2.1 HOLIÐ Í HELLI, SUÐUROY (ONSHORE FAROE ISLANDS)

The Holið í Helli section comprises a completely exposed sequence through the sediment dominated Prestfjall and Hvannhagi Formations (*Figure 25*). They are intercalated between the heavily weathered uppermost simple lava flow of the Beinisvørð Formation below and the lowermost compound lava flow of the Malinstindur Formation above. Neither the Prestfjall nor Hvannhagi formations are typical at this location.
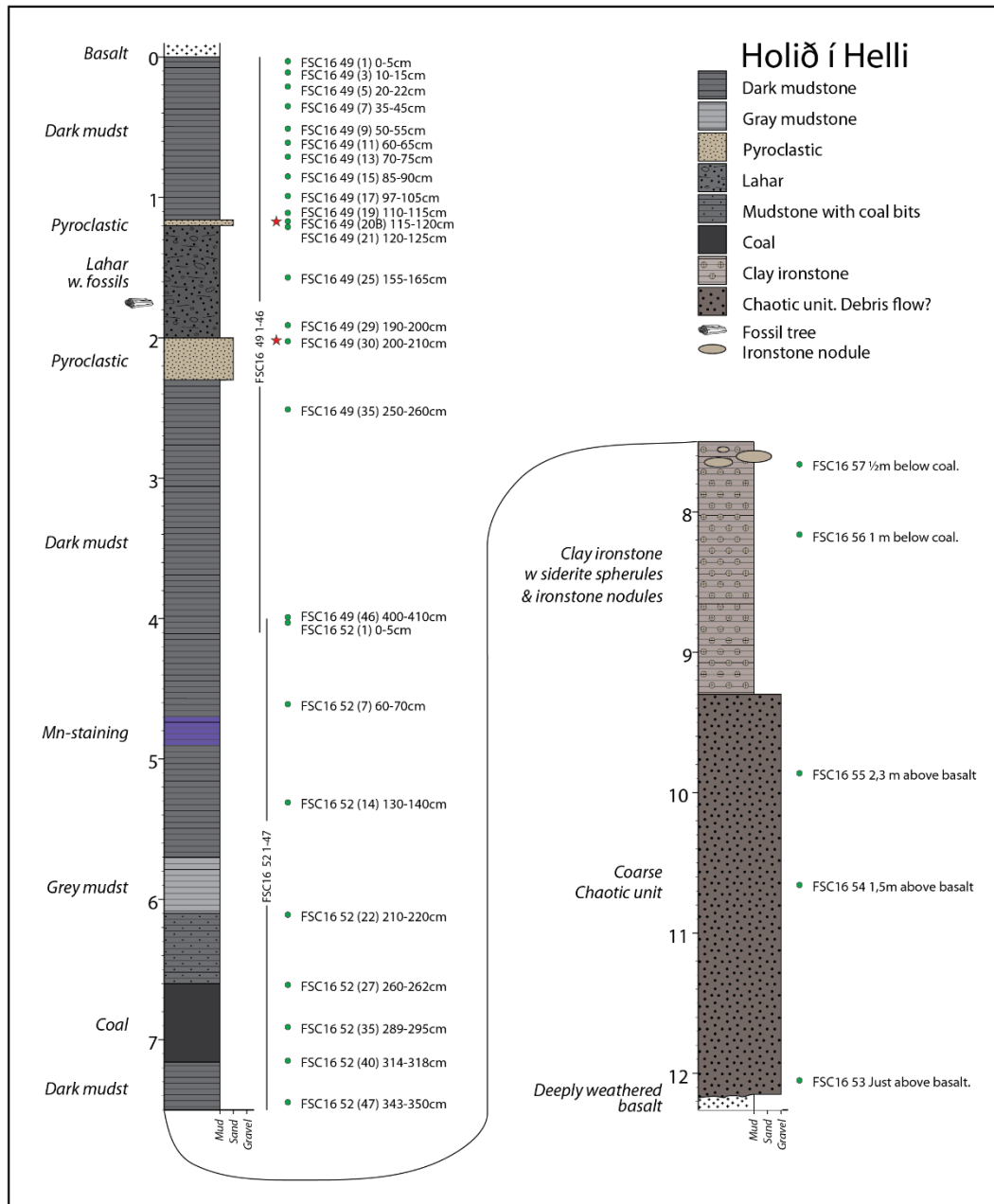
Figure 25 Detailed logs from the Holið í Helli section on Suðuroy.

The section is ca 12 m thick. The uppermost clay dominated 7.5 m have been intensively sampled, whereas only a few specimens have been sampled from the lowermost ca 5 m of coarser sediments. Here only a short description is presented. For a more detailed description refer to, for example, Passey (2014).

The lowermost unit is a ca 3 m thick dark yellowish brown coarse chaotic sediment, that is matrix supported with up to gravel sized clasts, that could possibly represent a debris flow. The overlying unit is ca 2 m thick yellowish brown clay ironstone with siderite spherules. Towards the top of this unit are abundant up to 15 cm wide ironstone nodules. On top of this is ca 30 cm of claystone followed by a 55 cm thick coal band that in turn is overlain by ca 50 cm of dark claystone with mm-sized fragments of coal. Ca 3.5 m of grey and dark organic rich mudstone with occasional Manganese staining are deposited on top the coal bearing mudstone. This is followed by two 30 and 5 cm thick bands of coarser pyroclastic material separated by a 80 cm thick lahar deposit with abundant silicified fossil tree fragments. The uppermost unit is a ca 1 m thick dark mudstone.
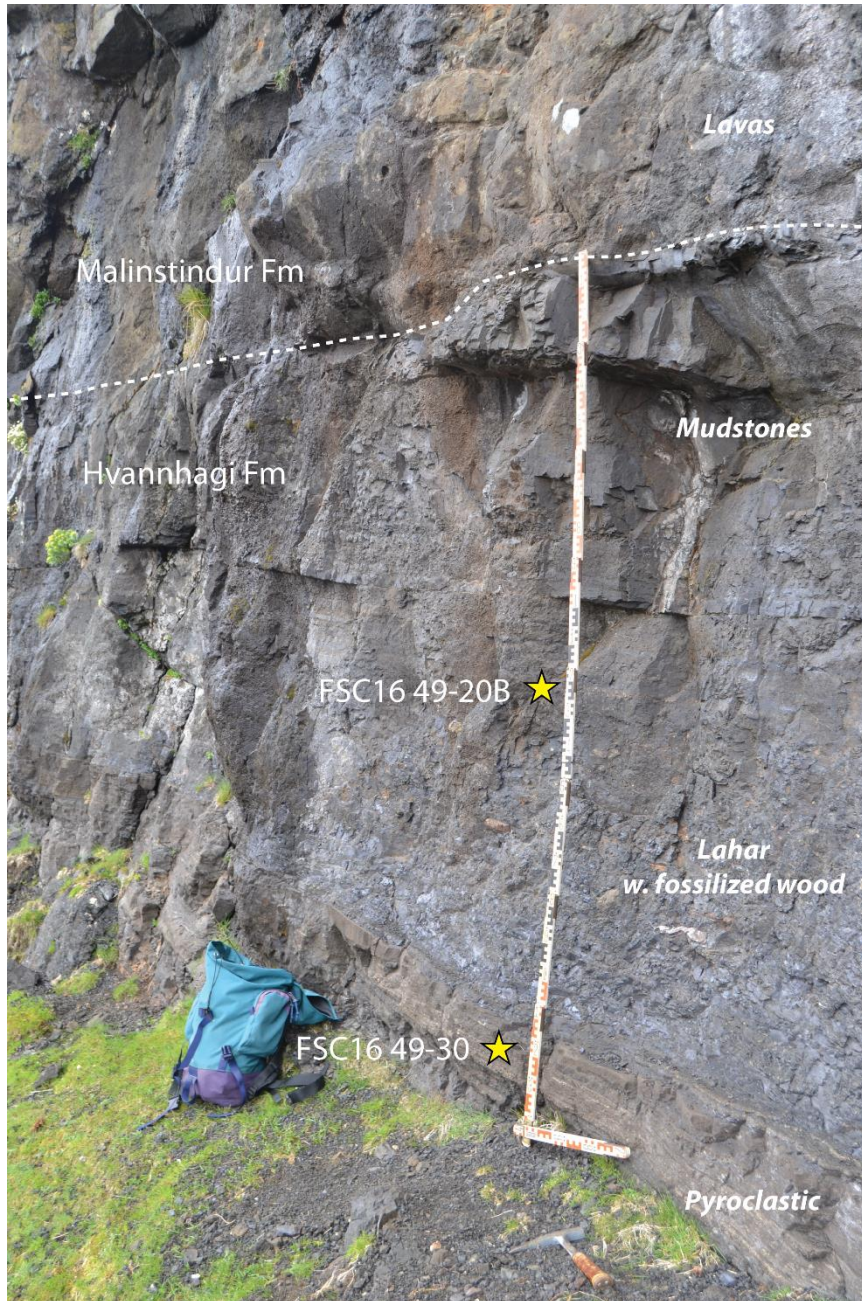
Figure 26 Transition from the Hvannhagi Fm volcaniclastic/pyroclastic rocks to the Malinstindur Fm lavas. Sample sites for the U/Pb ages also indicated on the figure.

Twenty-one samples from a measured section at Holið í Helli, east central Suðuroy (*Figure 25*), were studied for palynology (Appendix 1). The yields of palynomorphs are relatively poor in the uppermost samples, but are significantly more productive at the base of the succession (*Figure 25*). The productive palynofloras entirely comprise pollen and spores typical of the Brito-Arctic Igneous Province Flora of Boulter and Manum (1989); no marine indices such as dinoflagellate cysts were recovered.
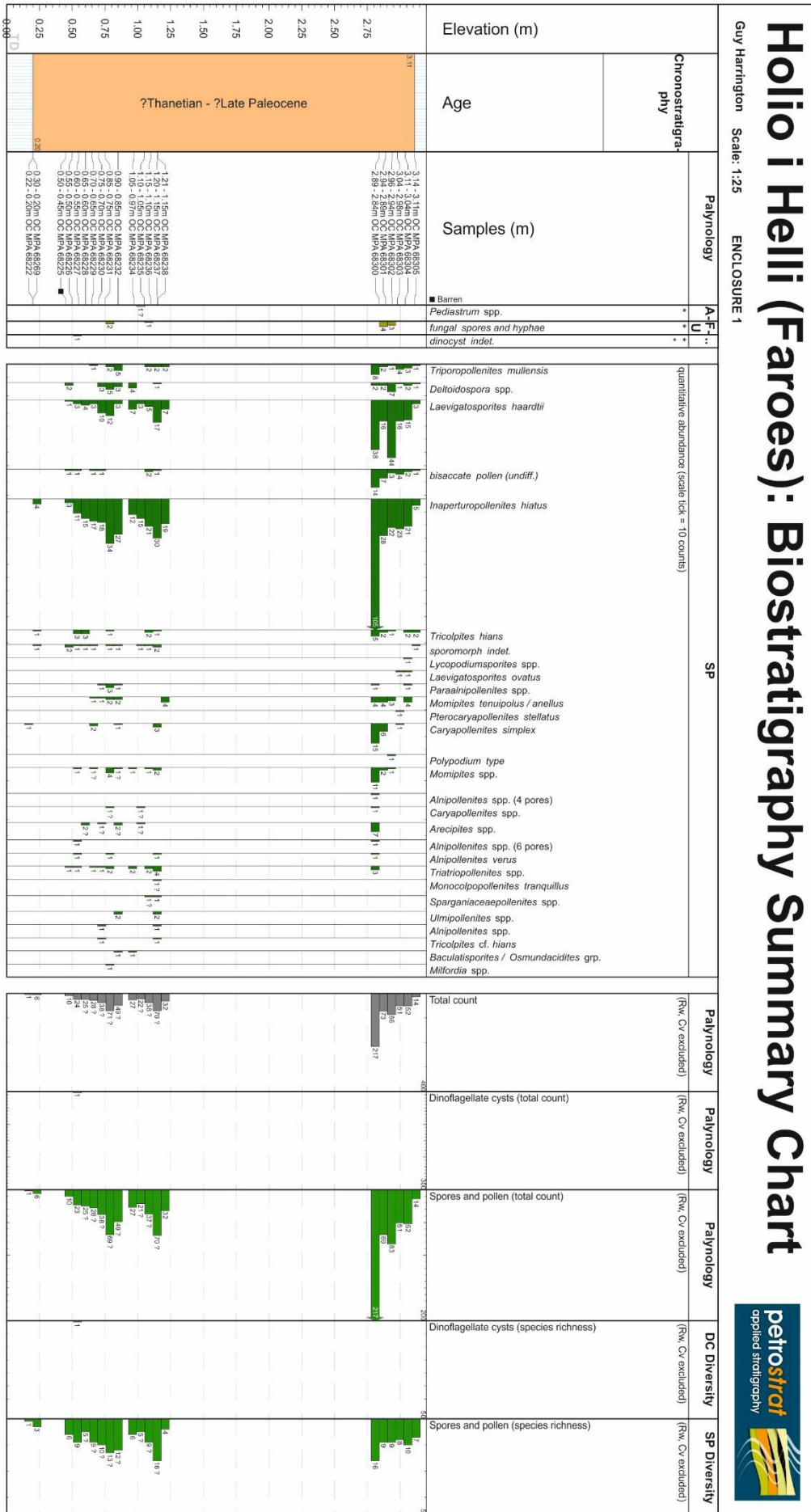
Figure 27 Palynology of Holið í Helli.

Inaperturopollenites hiatus is relatively abundant, and other taxa which are abundant/common are Betulaceae type pollen (e.g. *Triatriopollenites* spp. and *Triporopollenites mullensis*) and *Momipites anellus/tenuipolus. Labrapollis* is absent. *Caryapollenites* spp. are also present and *Caryapollenites simplex* is common, especially in the uppermost, more organic-rich (coaly), part of the section. Abundant levels of *Caryapollenites* is characteristic of the Sele and Balder formations (Ypresian) in the North Sea. *Caryapollenites veripites* was not encountered; this species is also present in the Sele Formation. It is also present in the Canadian Arctic (Lund 1989; McIntyre 1991, 1994; Kalkreuth et al. 1996; Harrington et al. 2012). It is present in Shell Zone PT15.2.5 from the central North Sea; this is middle to late Thanetian (Eldrett et al. 2014)

Lund (1989) and Boulter and Manum (1989) contended that the age of the Faroe Islands intrabasaltic sediments is probably late Thanetian–early Ypresian. The composition of the palynofloras observed herein is inconsistent with this conclusion due to the absence of *Caryapollenites veripites,* which has an acme at the PETM (Schröder 1992; Kender et al. 2012; Eldrett et al. 2014). Furthermore the relative lack of the probable palm pollen *Arecipites* (it is only common in one sample) and the abundant gymnosperm pollen are contradictory with the PETM. This is characterised by a decrease in, or an absence of, the gymnosperm *Inaperturopollenites hiatus* and bisaccate pollen (McInerney and Wing 2011; Kender et al. 2012; Wing and Currano 2013; Eldrett et al. 2014; Sluijs et al. 2014). It is considered that the changes in abundance of the different pollen taxa throughout the Holið í Helli section reflects the changes in lithofacies between the different beds, for example the uppermost samples are more organic rich.

Based on the presence of common *Caryapollenites simplex* and *Momipites tenuipolus/anellus,* an age of late Thanetian is suggested herein since these two taxa co-occur in the section. However, early Ypresian (post-PETM and pre-Early Eocene Climatic Optimum [EECO]) cannot be excluded because the range top of *Momipites tenuipolus* is not known. If the last occurrence of this taxon is at the base of the PETM (Eldrett et al. 2014), a latest Thanetian age may be possible.

4.4.3 The Longan Well (OCS 6005/15-1), offshore Faroe Islands

The pollen and spores in five productive samples from the Longan well (*Figure 28*) between 3512.39 m and 3508.39 m are typical of the Paleocene, and contain many stratigraphically long-ranging taxa typical of the Brito-Arctic flora. The palynoflora is dominated by gymnospermous pollen such as bisaccate grains (Pinaceae) and *Inaperturopollenites hiatus* (*Glyptostrobus, Metasequoia*). Other elements typical of the Brito-Arctic Igneous Province Flora of Boulter and Manum (1989) include *Alnipollenites* spp. with >5 pores, representatives of the Juglandaceae (i.e. *Momipites* spp. including *M. tenuipolus*) and *Pterocaryapollenites stellatus*. There is one specimen of possible *Caryapollenites* spp. but this identification is not certain. In the central North Sea, *Caryapollenites circulus* (=*C. simplex* herein) and *Caryapollenites veripites* are important markers for the latest Thanetian to early Ypresian (Schröder 1992; Kender et al. 2012; Eldrett et al. 2014). *Caryapollenites simplex, Caryapollenites triangulus* and *Caryapollenites veripites* are rare but consistent in Shell zone PT-15.2.5 that corresponds with the uppermost Andrew and lowermost Lista formations (Eldrett et al. 2014) in the middle Thanetian. According to Naylor et al. (1999, fig. 4), the range top of *Momipites tenuipolus* is in the middle Thanetian Lamba Formation in the Faroes-Shetland area, with a second reappearance close to the Thanetian–Selandian transition. Jolley and Morton (1992) reported common *Momipites tenuipolus* from three lignite samples immediately above the Andrew Formation in Borehole 82/15 that is ?early Thanetian. Eldrett et al. (2014) reported the range top of *Momipites tenuipolus* in the lowermost Forties Sandstone Member of the Sele Formation. This datum is of latest Thanetian age and it occurs in Shell zones PT-19.1.2 and 19.1.1.
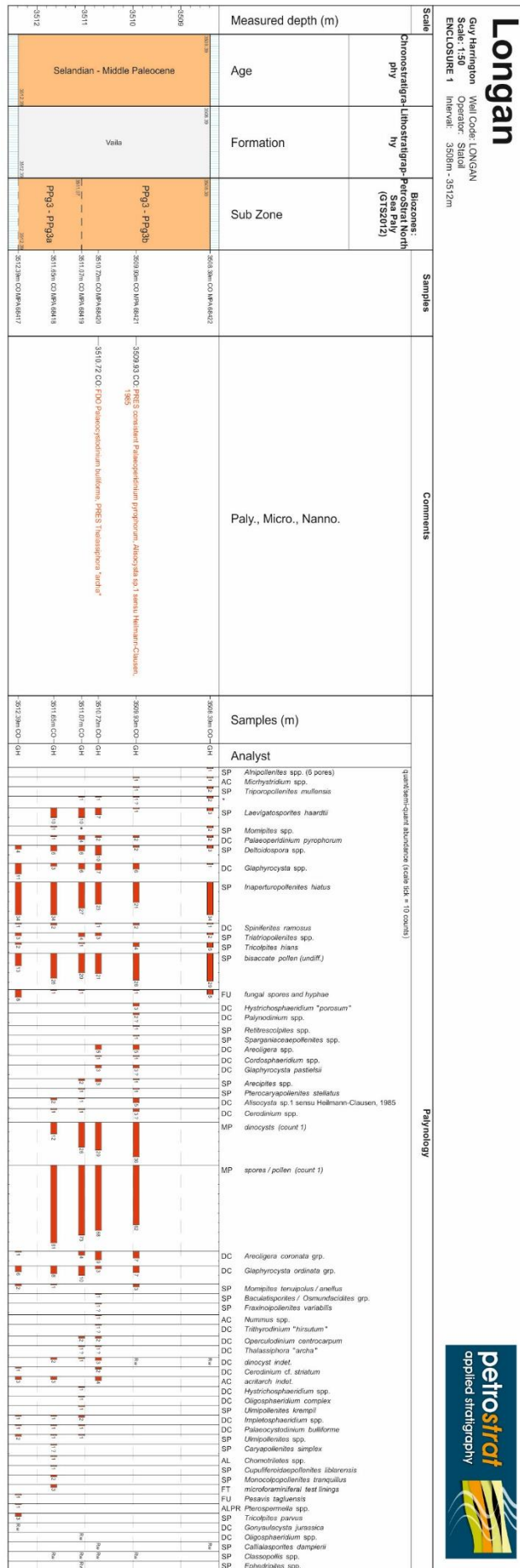
Figure 28 The palynology of the Longan Well.

This study has lowered the stratigraphical range of *Momipites tenuipolus* into the middle part of the early Selandian because these samples contain age-diagnostic dinoflagellate cysts. Both *Impagidinium* sp. 1 of Heilmann-Clausen (1985) and *Palaeoperidinium pyrophorum* indicate an age older than Thanetian. The middle Selandian and older is indicated by the consistent presence of *Alisocysta* sp. 1 of Heilmann-Clausen (1985) and *Thalassiphora "archa"* (informal taxon). The range top of *Palaeocystadinium bulliforme* marks PetroStrat zone PPg3a, and is indicative of the earliest Selandian. This is why the range base of *Momipites tenuipolus* is extended to the early Selandian.

In summary, dinoflagellate cyst evidence indicates an early Selandian age for the succession examined in the Longan Well.

4.4.3   The Marjun Well (OCS 6004/16-1Z), offshore Faroe Islands

Two samples at 3456.67 m and 3450.70 m were examined from the Marjum Well (*Figure 29*). Both produced relatively sparse indigenous marine and terrestrially-derived palynomorphs, thereby indicating a marine depositional setting. The presence of the dinoflagellate cyst *Impagidinium* sp. 1 of Heilmann-Clausen (1985) strongly suggests an age older than Thanetian. Furthermore, the genus *Hystrichosphaeridium*, including the species *Hystrichosphaeridium tubiferum*, is relatively common, which is consistent with a Selandian age. Therefore, an age assignment of Selandian is suggested. The pollen associations exclusively comprise stratigraphically long-ranging taxa and these cannot confirm or refine the Selandian age determination.

4.4.4   The Svinoy Well (OCS 6004/12-1), offshore Faroe Islands

Five core samples were collected from the Svinoy Well (*Figure 30*) between 3604.65 m and 3582.21 m. A marine depositional setting is invoked due to the presence of both indigenous marine and terrestrially-derived palynomorphs. Unfortunately, the palynomorphs recognised are not particularly age diagnostic. The dinoflagellate cyst *Cerodinium striatum* is common and consistent in the Selandian of Denmark (Heilmann-Clausen 1985). Hence the section studied may possibly be Selandian to early Thanetian in age. *Caryapollenites simplex* and *Caryapollenites* spp. are present in the uppermost sample at 3582.21 m. This horizon appears to represent a different unit, or lithofacies, from the underlying four samples. The most significant pollen in the lower lithofacies is *Momipites tenuipolus* that, in the absence of *Caryapollenites* spp., implies a probable Selandian age. Therefore a Selandian age is tentatively invoked for the entire interval.

Figure 29 The palynology of the Marjun Well.

Svinoy

Guy Harrington
Well Code: SVINOY
Scale: 1:500　　Operator: BP
ENCLOSURE 2　　Interval: 3580m - 3607m

Scale		Chronostratigra-Lithostratigrap-hy		Samples		Palynology

Measured depth (m)

Period/Epoch — Paleocene

Formation — Vaila

Samples (m)

Analyst

quant/semi-quant abundance (scale tick = 10 counts)

- SP Alnipollenites spp.
- DC Areoligera coronata grp.
- SP Caryapollenites simplex
- SP Caryapollenites spp.
- SP Cupuliferoipollenites pusillus
- SP Milfordia spp.
- SP Nyssapollenites kruschii
- FU Pesavis tagluensis
- SP Platycarya platycaryoides
- SP sporomorph indet.
- SP Granulatisporites spp.
- DC Spiniferites ramosus
- SP Triatriopollenites spp.
- MP dinocysts (count 1)
- MP spores / pollen (count 1)
- DC Areoligera spp.
- DC Cerodinium cf. striatum
- SP Deltoidospora spp.
- SP Inaperturopollenites hiatus
- SP Laevigatosporites haardtii
- SP Momipites spp.
- SP Momipites tenuipolus / anellus
- SP Paraalnipollenites spp.
- SP Sparganiaceaepollenites spp.
- SP Tricolpites hians
- SP Ulmipollenites krempii
- SP bisaccate pollen (undiff.)
- FU fungal spores and hyphae
- DC Adnatosphaeridium spp.
- DC Areoligera cf. senonensis
- DC Cordosphaeridium spp.
- DC Impletosphaeridium spp.
- DC Oligosphaeridium complex
- DC Spiniferites pseudofurcatus
- FT microforaminiferal test linings
- DC Glaphyrocysta ordinata grp.
- SP Alnipollenites verus
- SP Lycopodiumsporites spp.
- AL Tetraporina spp.
- SP Baculatisporites / Osmundacidites grp.
- SP Pterocaryapollenites stellatus
- DC Lingulodinium machaerophorum
- AC Nummus spp.
- ALPR Pterospermella spp.
- SP Triporopollenites mullensis
- DC Isabelidinium spp.
- SP Tricolpites cf. hians
- DC Cribroperidinium spp.
- DC Gonyaulacysta jurassica
- DC Odontochitina spp.
- DC Oligosphaeridium spp.
- DC Systematophora spp.
- DC dinocyst indet.
- SP Callialasporites dampierii
- SP Classopollis spp.

petro*strat*
applied stratigraphy

Figure 30 The palynology of the Svinoy Well.

5 Stable Isotope analysis

Some of the onshore successions on the Faroe Islands which were sampled for palynology and radio-isotopic dating were thought to include the Paleocene–Eocene Thermal Maximum (PETM). This relatively short-lived hyperthermal event is characterised by a negative carbon isotope excursion (CIE) between -2 and -7% in marine and terrestrial sediments (Schouten et al., 2007). Consequently, 43 samples from these PETM candidate successions were analysed for $\delta^{13}C$ (Table A1). All 43 samples proved to contain very low levels of organic matter (<0.1%), which is below detection limits for $\delta^{13}C$ analysis in the BGS laboratories.

6 Radio-isotopic dating

A major objective of this project was to establish an absolute chronology for key portions of the NAIP that inform the chronology of the Faroe-Shetland basin. These regions are (1) the UK Inner Hebrides in order to test data that underpin the Jolley/Sherlock post-PETM emplacement age model for the FIBG; (2) the FIBG in order to establish independent constraints for the timing of volcanism, and (3) the key volcanic units (e.g., Kettla Tuff) from the Faroe-Shetland Basin in order to establish independent constraints for the timing of volcanism as well as sedimentary sequences in the basin. In this section we describe the data acquired in each area, sample by sample, provide age interpretation and discuss how these data constrain the geology of interest.

In this study we have employed a combined U-Pb (zircon) geochronology approach using both microbeam and high-precision methods. Laser ablation inductively coupled plasma mass spectrometry (LA-ICP-MS) was employed for effective screening of zircon populations in samples where a single age population was not apparent based upon mineral morphology (i.e., detrital zircon samples), these data were then used to select grains of interest for high-precision analyses. High-precision U-Pb determinations were made using established isotope dilution thermal ionisation mass spectrometry (ID-TIMS) methods. These data employed methods and calibrations that are those used to generate the U-Pb data that underpins the calibration of the numerical timescale (i.e., GTS 2016). All U-Pb methods are outlined in detail in [Appendix 2](#) and all U-Pb data are reported in Appendix 3 (ID-TIMS) and Appendix 4 (LA-ICP-MS).

Region	Sample ID	Sample Short Description	Stratigraphic Context	$^{238}U/^{206}Pb$ age (Ma)[1]	± X (Myr)[2]	± Y (Myr)[2]	± Z (Myr)[2]	Interpretation	Reference
FIBG	FSC16-4930	Coarse grained tuff	Hvannhagi Formation	**56.38**	0.09	0.10	0.11	Extrusion/eruption	this study
	FSC16-100	Reydibarmur tuff	Hvannhagi Formation	**56.84**	0.42	0.42	0.43	Extrusion/eruption	this study
	AMASE16	Pyroclastic/tuff	Hvannhagi Fm	**97.19**	0.16	0.17	0.20	Youngest detrital zircon, maximum age	this study
Faroe-Shetland Basin	SSK76525	sampled @9635", volcaniclastic sandstone	205/01-1 ('Middle Rosebank')	58.78	0.31	0.32	0.32	Youngest detrital zircon, maximum age	this study
	SVÍNOY3126	samples @3117+m, tuff/volcaniclastic sed.	6004 12/1 (Lamba Fm, Kettla Tuff Mb)	**57.75**	0.23	0.23	0.24	Youngest detrital zircon, maximum age, approximates sedimentation age	this study
	SSK76523	sampled @3611m, volcaniclastic sandstone	205/09-1 ('Kettla Tuffite')	**53.33**	0.10	0.11	0.12	Youngest detrital zircon but age too young based upon geological inference	this study
	SSK76527	sampled @1936.65m, volcaniclastic sandstone	204/19-3A ('Kettla Tuffite')	58.75	0.05	0.06	0.09	Youngest detrital zircon, maximum age	this study
	SSK76330	sampled @2036.55m, volcaniclastic sandstone	204/19-3A ('Kettla Tuffite')	61.21	0.16	0.16	0.18	Youngest detrital zircon, maximum age	this study
	SSK76532	sampled @2091.71m, volcaniclastic sandstone	204/19-3A ('Kettla Tuffite')	64.02	0.45	0.45	0.46	Youngest detrital zircon, maximum age	this study
	SSK76537	sampled @9664'0", volcaniclastic sandstone	213/27- 2 ('Kettla Tuffite')	**57.53**	0.21	0.21	0.22	Youngest detrital zircon, maximum age, approximates sedimentation age	this study
Skye Lava Group and Skye Central Complex	SD-MOL-01	Ignimbrite, Moll, east Skye	Skye Lava Group	**57.32**	0.11	0.11	0.13	Extrusion/eruption	Unpublished, NIGL data
	SD-BS-01	Dyke cutting Durness limestone, Ben Suardal	Skye Central Complex	**56.45**	0.15	0.15	0.16	Intrusion	Unpublished, NIGL data
	SD-AMS-01	Ignimbrite, Allt nan Suidheachan, near Kilchrist	Skye Lava Group	**56.14**	0.20	0.20	0.21	Extrusion/eruption	Unpublished, NIGL data
	SG16-00	Loch Ainort Grantie	Skye Central Complex	**57.10**	0.04	0.05	0.08	Intrusion	this study
	FSC-16-26	Loch Ainort Grantie	Skye Central Complex	**56.99**	0.08	0.08	0.10	Intrusion	this study
	Hugh-1	granophyre is from near another Fionna Choire	Subvolcanic intrusion	**58.97**	0.06	0.07	0.10	Extrusion/eruption	this study
	SC1/2	*Cullins Gabbro*	*Skye Central Complex*	*58.91*	*0.07*	*0.09*	*0.11*	*Intrusion*	*Hamilton et al., 1998*
	SD-FC-01	Ignimbrite, Fionn Choire, NW Cuillins	Skye Central Complex	**60.13**	0.05	0.06	0.09	Extrusion/eruption	Unpublished, NIGL data
Small Isles Volca	EP1-98	Eigg Pitchstone	Sgurr of Eigg Pitchstone Formation	**60.12**	0.38	0.38	0.39	Extrusion/eruption	this study

Region	Sample ID	Sample Short Description	Stratigraphic Context	$^{238}U/^{206}Pb$ age (Ma)[1]	± X (Myr)[2]	± Y (Myr)[2]	± Z (Myr)[2]	Interpretation	Reference
	ET1-100	Eigg Tuff	Eigg Lava Formation	**61.61**	0.07	0.07	0.10	Extrusion/eruption	this study
	MT2	Muck Tuff	Eigg Lava Formation	**61.64**	0.17	0.17	0.19	Extrusion/eruption	this study
Mull Lava Group and Central Complex	LB1	Loch Ba Ring Dyke	Mull central Complex	**58.94**	0.07	0.08	0.10	Intrusion	this study
	FSC15-7	Calgary Bay Tuff	Mull Plateau Lava Formation	**61.10**	0.09	0.10	0.12	Extrusion/eruption	this study
	FSC15-2	Ardtun Leaf Bed	Staffa Lava Formation	61.65	0.13	0.13	0.15	Youngest detrital zircon, maximum age, approximates sedimentation age	this study
	FSC15-6	Ardtun Leaf Bed	Staffa Lava Formation	61.55	0.15	0.16	0.17	Youngest detrital zircon, maximum age, approximates sedimentation age	this study
	FSC16-11	Carsaig Bay Ignimbrite	Staffa Lava Formation	**61.74**	0.14	0.14	0.16	Extrusion/eruption	this study
N. Ireland	Tardree	Tardree Ignimbrite	Intra-basalt volcanic	**60.89**	0.18	0.18	0.19	Extrusion/eruption	this study
	CWF	Clay With Flints, sub-basaltic volcanics	earliest Paleogene volcanism, Northern Ireland	**61.57**	0.04	0.05	0.08	Extrusion/eruption	this study

1. Ages in black bold - Interpreted as ages of the rocks analysed (i.e., timing of eruption or intrusion); ages not in bold, maximum depositional ages based upon youngest U-Pb zircon dates, ages in bold grey are considered to reflect Pb-loss and are younger than the inferred stratigraphic age
2. Age uncertainties are reported at three levels: X - analytical uncertainty only; Y - Analytical plus U/Pb tracer calibration uncertainty; and Z - Analytical plus U/Pb tracer calibration plus 238U decay constant uncertainty.

Table 2 Summary of the U-Pb (zircon) U-Pb ages, their uncertainties, with comment on age interpretation, for the samples studied for this project.

6.1   BRITISH PALEOGENE IGNEOUS PROVINCE

6.1.1   Mull and the Small Isles, Inner Hebrides, Northwest Scotland

Background - The Paleogene rocks of the Island of Mull and the adjacent Small Isles (Muck and Eigg) were a target due to their playing a critical role in prior studies undertaken as part of the SINDRI Group (Chambers et al., 2005, Sherlock et al., 2010). In these studies the rocks of the Staffa Lava Formation, Mull, were used as a test bed to explore $^{40}Ar/^{39}Ar$ dating of Paleogene basalts, data complexity and interpretive frameworks. A number of lavas were subsampled and analysed for $^{40}Ar/^{39}Ar$ geochronology and each lava yielded complex age spectra with single flows returning model ages that range from ca. 55 to ca. 60 Ma. A general trend was observed, where the base of the flow gave the of youngest $^{40}Ar/^{39}Ar$ date, with ages getting older higher up or towards the core of a flow. In their report Sherlock et al (2010) assign an age of 54.0 to 55.5 Ma age based upon palynological data (Jolley, 1997) and subsequently interpret the ca. 55 Ma dates from the bases of the flows as being the most accurate in terms of the eruptive age. This interpretative model is then applied to $^{40}Ar/^{39}Ar$ data from basalts sampled within the FIBG.

In this section we go through the U-Pb data obtained on each sample and at the end synthesise these data and compare against prior studies, specifically the Sherlock et al. (2010) study.

Figure 31 Samples from Carsaig Bay, Mull. A. Weathered matrix-supported conglomerate / sandstone between two lava flows, Malcolm's Point; B. 1.5m thick igimbrite between basalt lava flows, Carraig Mhor.

FSC16-11 is a sample of the Carraig Mhor Ignimbrite from the base of the Staff Lava Formation, east Carsaig Bay, Island of Mull (Figure 24). LA-ICPMS analyses of zircon from this sample yield a range in U-Pb dates, dominated by Archaean and Proterozoic populations, together with a population of 'Caledonian' (c. 445 Ma) age (Fig. 32). Zircons with ca. 60 Ma ages make up ca. 5% of the grains present. Analyses of the youngest zircons from FSC16-11 yield (^{230}Th corrected) $^{238}U/^{206}Pb$ dates that range between 61.81 and 61.66 Ma (n = 5) with 2σ uncertainties on the order of 0.2 to 0.5 Myr). These dates are statistically indistinguishable from one another, and given their uniform morphology, we interpret that the zircons represent a single age population with an interpreted geological (weighted mean) age of 61.74 ± 0.14 (MSWD = 0.108, n = 5; *Figure 33*). This sample from the Carraig Mhor ignimbrite, constrains the age of the base of the Staffa Lava Formation.

A sample of conglomerate (FSC-16-4) within the volcanic succession at Malcolm's Point, west Carsaig Bay (*Figure 24*), shows a similar distribution of detrital zircon ages; only one ca. 60 Ma grain was detected in this sample (*Figure 32*).
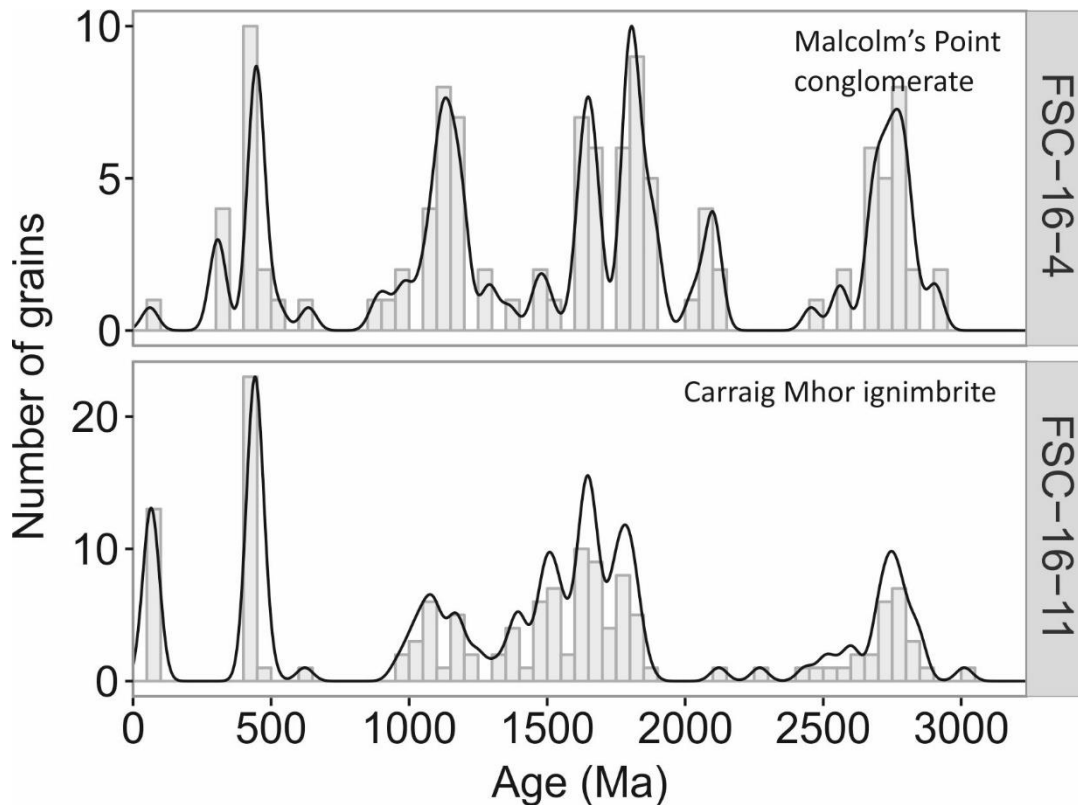
Figure 32 Kernel Density Estimator (KDE) plots and histograms showing the distribution of LA-ICPMS zircon dates from the Malcolm's Point conglomerate and Carraig Mhor ignimbrite, Carsaig Bay, Mull.

FSC15-2 and FSC15-6 were two sediment samples collected for detrital zircon analyses from the Ardtun Leaf bed interval (Fig. 34) in order to explore the potential for intra-basalt sediments to yield zircons from weathered broadly contemporaneous volcanism, the dates of which will approximate the timing of sedimentation. LA-ICP-MS analyses of detrital zircon from both samples yield a range of U-Pb dates dominated by Archaean and Proterozoic populations. Both samples contain a Permo-Carboniferous zircon population, and sparse (5-10%) grains with ages of ca. 60 Ma (*Figure 32*). Zircons with youngest U-Pb LA-ICP-MS dates were selected for ID-TIMS analyses and yield (^{230}Th corrected) ^{238}U/^{206}Pb dates that range between 61.99 and 61.55 Ma (n = 3) with 2σ uncertainties on the order of 0.13 to 0.8 Myr. These dates are statistically indistinguishable from one another, and given their uniform morphology, we interpret that the zircon represent a single age population with an interpreted geological (weighted mean) age of 61.74 ± 0.14 (MSWD = 0.108, n = 3; *Figure 33*). These zircons are detrital, so cannot be used to directly establish the age of the Ardtun Leaf Bed. However, the age of the youngest population can be used to define a maximum depositional age for the unit. This sample, from the Ardtun Leaf Beds, constrains a maximum age of the Staffa Lava Formation at this level, and is indistinguishable from the U-Pb age of the underlying Carraig Mhor Ignimbrite from Carsaig Bay.

FSC15-7 is a sample of the Calgary Bay Tuff, which is a trachytic tuff that occurs within the Mull Plateau Lava Formation (*Figure 10*). Analyses of zircon from FSC15-7 yield (^{230}Th corrected) ^{238}U/^{206}Pb dates that range between 61.17 and 60.43 Ma (n = 6) with 2σ uncertainties on the order of 0.14 to 0.36 Myr. These dates are statistically indistinguishable from one another, except for the youngest date (z6, 60.43 Ma) which is an outlier. Given their uniform morphology and the fact that this youngest date is a single outlier (i.e., not reproduced), we interpret that the remaining five zircon represent a single age population with an interpreted geological (weighted mean) age of 61.098 ± 0.09 (MSWD = 0.49, n = 5). This sample, from within the Mull Plateau Lava Formation provides a constraint on volcanism at this level, and a minimum age for the top of the Staffa Lava Formation.
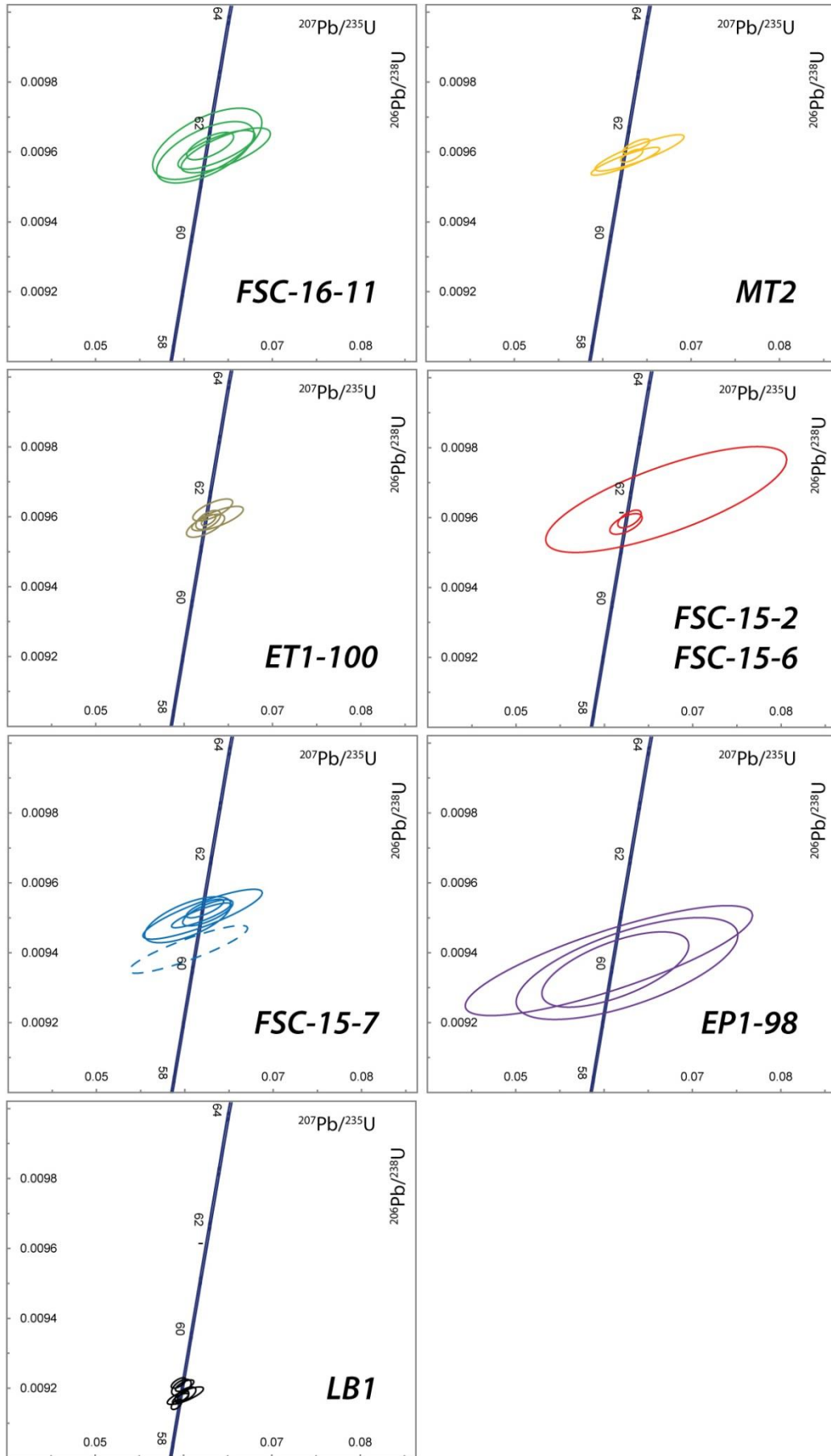
Figure 33 U-Pb (Whetherill) Concordia plots displaying the CA-ID-TIMS U-Pb results for zircon recovered from samples from the Palaeogene volcanic and intrusive rocks from Mull.

Figure 34 Location of samples collected from within the Ardtun Leaf Bed, Mull.
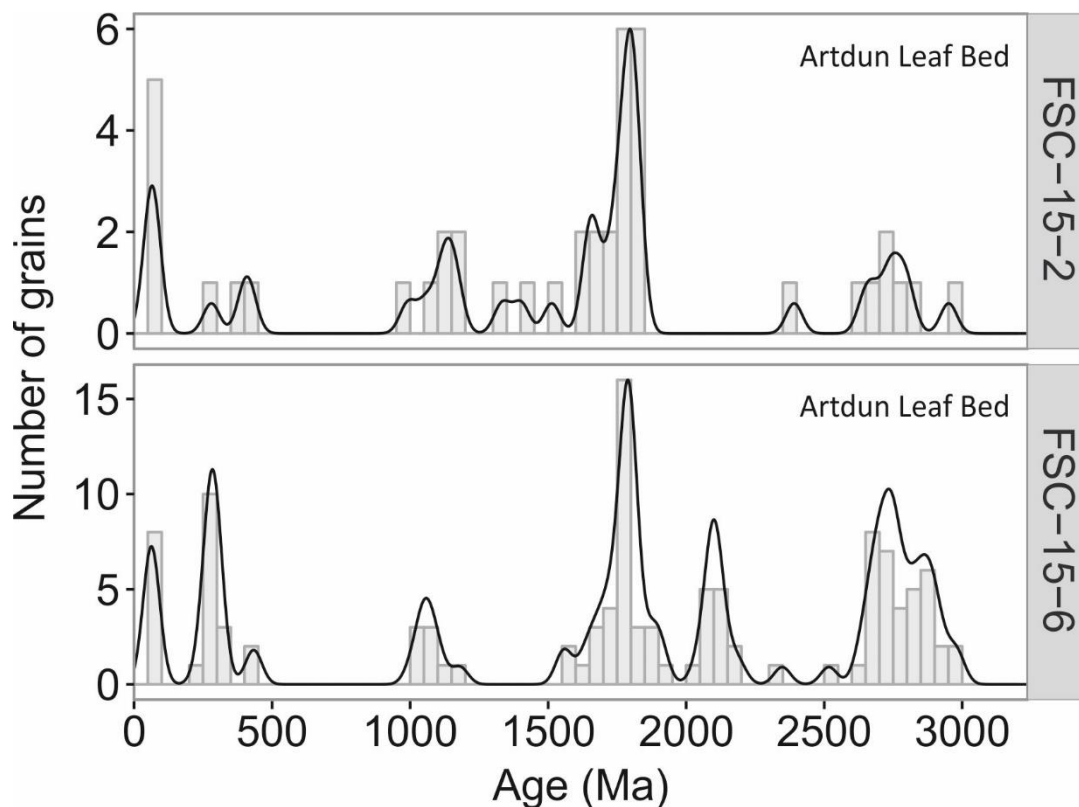
Figure 35 KDE plots and histograms showing the distribution of LA-ICPMS zircon dates from the Ardtun Leaf Bed, Mull.

LB1 is a sample of the Loch Ba Felsite. The Loch Ba Felsite is from a ring dyke that is part of Centre 3 of the Mull Central Complex (Figure 9) which intrudes into the Mull Lava Group Formation. The ring dike therefore provides a minimum age constraint on the eruption of the Mull Lava Group. Analyses of zircon from LB1 yield (^{230}Th corrected) ^{238}U/^{206}Pb dates that range between 59.22 and 58.83 Ma (n = 9) with 2σ uncertainties on the order of 0.08 to 0.13 Myr. These dates display variation outside of what is expected for a single population reflecting zircon crystallisation over a ~400 kyr interval. Based upon the understanding of protracted zircon crystallisation in magmas we interpret

the youngest coherent age population to best approximate the emplacement of the Loch Ba Felsite. This youngest coherent population yields an interpreted geological (weighted mean) age of 58.936 ± 0.072 Ma (MSWD = 2.4, n = 6; *Figure 33*). This sample, from within the Mull Plateau Lava Formation provides a constraint on volcanism at this level, and a minimum age for the top of the Staffa Lava Formation.

MT-2 is a sample of the Muck Tuff which occurs close to the base of the Eigg Lava Formation (Figure 8) and is from the same sample utilised in Chambers et al (2005). Analyses of zircon from MT-2 yield (^{230}Th corrected) ^{238}U/^{206}Pb dates that range between 64.66 and 61.50 Ma (n = 5) with 2σ uncertainties on the order of 0.08 to 0.3 Myr. Excluding the oldest date (z4, 64.66 Ma) the remaining four dates are statistically indistinguishable from one another, and given their uniform morphology, we interpret that the zircon represent a single age population with an interpreted geological (weighted mean) age of 61.64 ± 0.17 (MSWD = 2.7, n = 4; *Figure 33*). This is statistically older than the previously published U/Pb zircon date of 61.15 ± 0.17 Ma however we consider our new, older date, to be more accurate as it is based upon data calibrated using improved experiments compared to the ca. 2005 data, benefits from the chemical abrasion pre-treatment method performed on single zircon crystals and with laboratory blank levels nearly two ordered of magnitude lower. This sample, from the base of the Eigg Lava Formation provides a constraint on volcanism at this level.

ET1-100 is a sample of a tuff from within the Eigg Lava Formation, Eigg (Figure 8). Analyses of zircon from ET1-100 yield (^{230}Th corrected) ^{238}U/^{206}Pb dates that range between 61.77 and 61.50 Ma (n = 5) with 2σ uncertainties on the order of 0.08 to 0.17 Myr. These dates are statistically indistinguishable from one another, and given their uniform morphology, we interpret that the zircon represent a single age population with an interpreted geological (weighted mean) age of 61.613 ± 0.058 (MSWD = 1.4, n = 5; *Figure 33*). This sample, from the base of the Eigg Lava Formation, provides a constraint on volcanism at this level.

EP1-98 is a sample of the Sgurr of Eigg Pitchstone lava that unconformably overlies the Eigg Lava Formation, Eigg (Figure 8). Analyses of zircon from EP1-98 yield (^{230}Th corrected) ^{238}U/^{206}Pb dates that range between 60.2 and 60.1 Ma (n = 5) with 2σ uncertainties on the order of 0.6 to 1.6 Myr reflecting the low uranium content of the zircon and resultant low level of radiogenic Pb for analyses (0.3 to 0.9 pg). These dates are statistically indistinguishable from one another, and given their uniform morphology, we interpret that the zircon represent a single age population with an interpreted geological (weighted mean) age of 60.12 ± 0.38 (MSWD = 0.051, n = 4; *Figure 33*). This date is older than the previously determined ^{40}Ar/^{39}Ar date of 58.72 ± 0.07 Ma (Chambers and Pringle, 2001), however, this was determined relative to Fish Canyon sanidine at 27.64 Ma, and using a more accurate estimate for Fish Canyon sanidine will increase the ^{40}Ar/^{39}Ar date to ~59.9 Ma, concordant with the U-Pb zircon date. This sample, from the Sgurr of Eigg Pitchstone Formation provides a constraint on volcanism at this level.

Summary - Combined, these U-Pb (zircon) ages for key lithologies from the Paleogene of Mull and the adjacent Small Isles constrain the timing of key volcanic intervals that have been central to the debate concerning the age of the NAIP and associated palynomorphs. These new U-Pb zircon dates provide an internally consistent chronology; the base of the Staff Lava Formation is now dated at 61.74 ± 0.14 Ma and is similar in age to the base of the Eigg Lava Formation (61.64 ± 0.17 Ma). The Ardtun Leaf Bed is constrained as being younger than 61.65 ± 0.13 Ma (the age of reworked zircons in the Ardtun Leaf Bed sediments), and a tuff from the overlying Mull Plateau Lava Formation (dated at 61.098 ± 0.090 Ma) provide a minimum age on the Staffa Lava Formation. The Sgurr of Eigg Pitchstone Formation, dated at 60.12 ± 0.38 Ma, is broadly coeval with Mull Plateau Lava Formation. A final constraint is provided by the age of the Loch Ba Felsite that is dated at 58.936 ± 0.072 and intrudes the Mull Plateau Lava Formation, hence providing firm constraint on the minimum age.

Critically, it is units within Staffa Lava Formation that were used in the SINDRI ^{40}Ar/^{39}Ar study (Sherlock et al 2010) that concluded that the Staffa Lava Formation is ca. 55 Ma based upon an interpretation of complex ^{40}Ar/^{39}Ar data and an inferred palynological age. We conclude that this ca.

55 Ma age assignment is not correct and we present a coherent data set of U-Pb (zircon) age determinations that constrain the age of the Staffa Lava Formation between 61.7 and 61.1 Ma.

6.1.2   Isle of Skye, Inner Hebrides, Northwest Scotland

Background - The volcanic and intrusive rocks of the Isle of Skye were an auxiliary target in order to further develop a chronostratigraphic understanding of the broader region. A number of levels within the Skye Lava Group were targeted for palynology (see section 4), however, the lack of age diagnostic material made Skye a lower priority compared to Mull, the FIBG and the Faroe Shetland Basin. In addition we have non-published data from Skye which is included in Table Y.
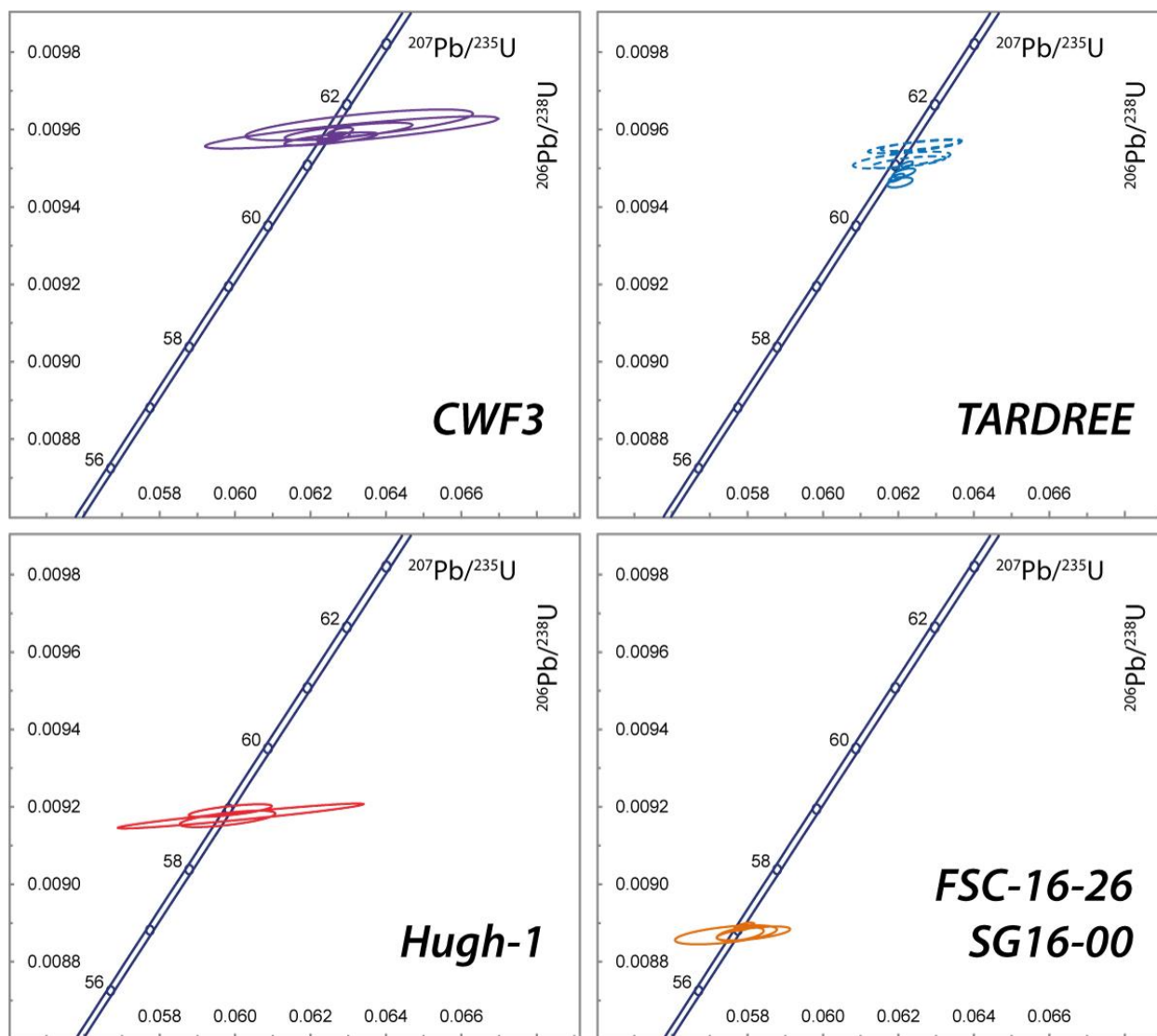
Figure 36 U-Pb (Wetherill) Concordia plots displaying the CA-ID-TIMS U-Pb results for zircon recovered from samples from the Palaeogene volcanic rocks of Northern Ireland and intrusive rocks from Skye.

Hugh-1 is a sample of a subvolcanic granophyre from the Skye Central Complex (Figure X). Analyses of zircon from Hugh-1 yield (^{230}Th corrected) ^{238}U/^{206}Pb dates that range between 59.03 to 58.87 Ma (n = 3) with 2σ uncertainties on the order of 0.09 to 0.17 Myr. These dates are statistically indistinguishable from one another, and given their uniform morphology, we interpret that the zircon represent a single age population with an interpreted geological (weighted mean) age of 58.97 ± 0.06 (MSWD = 2.4, n = 3; *Figure 36*). This sample, from within the Skye Central Complex provides a constraint on magmatism within this complex and is consistent with an U-Pb zircon date of 58.91 ± 0.07 Ma obtained from a gabbro also within the Skye Central Complex (Hamilton et al., 1998).

SG16-00 is a sample of the Loch Ainort Granite, the same sample used in the Chambers and Pringle (2001). Analyses of zircon from SG16-00 yield an interpreted geological (weighted mean) (^{230}Th corrected) ^{238}U/^{206}Pb age of 57.10 ± 0.04 (MSWD = 2.7, n = 3). FSC-16-26 is another sample of the Loch Ainort Granite and analyses of zircon from this sample yield (^{230}Th corrected) ^{238}U/^{206}Pb an interpreted geological (weighted mean) age of 56.99 ± 0.08 (MSWD = 0.25, n = 2; *Figure 36*). This sample, from within the Skye Central Complex and provides a constraint on volcanism at this level, and a minimum age for the top of the Skye Lava Group.

Summary - Combined, these data indicate that the Skye Central complex is broadly coeval, to slightly younger than the emplacement of the Mull Central Complex, and that Skye Central Complex magmatism continued for ~2 Myr. Non-published dates from the Skye Lava Group (Table 2) constrain the basaltic magmatism continued to at least 56.1 Ma.

6.1.3   Northern Ireland

Background - In order to develop a regional model for the chronostratigraphic development of the NAIP lithologies for the Paleogene of the Northern Ireland (the Antrim Lava Group) were targeted as part of this study for combined palynolgoical and radio-isotopic dating. The samples processed for palynology were barren therefore only a small number of samples were targeted for dating. The results are outlined below.

CWF-3 is a sample of the Clay with Flints deposit, a hetrolithic facies sampled from Corkey Quarry where the Clay with Flints is overlain by 200 m of Lower Basalt Formation of the Antrim Lava Group (*Figure 14*, *Figure 15*). Analyses of zircon from CWF-3 (^{230}Th corrected) ^{238}U/^{206}Pb dates that range between 61.74 and 61.49 Ma (n = 6) with 2σ uncertainties on the order of 0.06 to 0.22 Myr. These dates are statistically indistinguishable from one another, and given their uniform morphology, we interpret that the zircon represent a single age population with an interpreted geological (weighted mean) age of 61.57 ± 0.04 (MSWD = 2.1, n = 6; *Figure 36*). The sedimentology of the Clay with Flints (Cooper et al., 2017) involves karstifiaction and reworking of materials from contemporaneous basaltic volcanism at the base of the Antrim Lava Group and provides a constraint on volcanism at this level, and a minimum age for the Antrim Lava Group.

TARDREE is a sample of zircon from the Tardreee Rhyolite which occurs within between the Lower and Upper Basalt Formations (*Figure 14*, *Figure 15*). This is an aliquot of the zircon studied Analyses of zircon from the study of Ganerød et al., 2011. TARDREE yield (^{230}Th corrected) ^{238}U/^{206}Pb dates that range between 61.43 and 60.81 Ma (n = 8) with 2σ uncertainties on the order of 0.05 to 0.11 Myr. These dates are statistically distinguishable from one another and no single coherent population is obvious, with two end member clusters at 60.9 and 61.4 Ma (*Figure 36*). Given the current constraints both of these age interpretations are viable and without more information it is not possible to assign a more accurate age to this level.

Summary – These data constrain the onset of the formation of the Antrim Lava Group to ca. 61.5 Ma, broadly similar in age to the onset of mafic magmatism on Mull and the Small Isles**.**

6.2   FAROE ISLAND BASALT GROUP, FAROE ISLANDS

Background - A number of samples were collected from the FIBG and processed for zircon, including both volcanic and intratrappean sediments. The mafic nature of the volcanic lithologies of the FIBG meant that the potential to recover Paleogene zircon was low, hence a wide range of lithologies were targeted. Most sampled processed were barren with respect to zircon however two samples from the Hvannhagi Formation yielded a number of zircon that were clear and prismatic and looked like non-inherited zircon. These were targeted for U-Pb CA-ID-TIMS and the results are described below.

FSC-16-100 is a sample of the tuffaceous and pyroclastic rocks that occur within the Hvannhagi Formation of the FIBG (*Figure 24*). Analyses of zircon from FSC-16-100 yield (^{230}Th corrected) ^{238}U/^{206}Pb dates that range between 1363 and 56.6 Ma (n = 5) with 2σ uncertainties on the order of

0.6 Myr for Paleogene dates reflecting the low uranium content of the zircon and resultant low level of radiogenic Pb for analyses (0.3 to 0.6 pg). Two dates are old (235 and 1363 Ma) and reflect a reworked or inherited component. The remaining three dates are statistically indistinguishable from one another and we interpret that the zircon represent a single age population with an interpreted geological (weighted mean) age of 56.84 ± 0.42 (MSWD = 0.7, n = 3). This sample, from within the Hvannhagi Formation provides a constraint on volcanism at this level.

FSC-16-4930 is a sample of a volcanic tuff that occurs within the Hvannhagi Formation of the FIBG (Figure 25). Analyses of zircon from FSC-16-4930 yield (^{230}Th corrected) ^{238}U/^{206}Pb dates that range between 56.51 and 55.81 Ma (n = 8) with 2σ uncertainties on the order of 0.17 to 1.17 Myr reflecting the low uranium content of the zircon and resultant low level of radiogenic Pb for analyses (0.7 to 1.9 pg). All dates are statistically indistinguishable from one another and we interpret that the zircon represent a single age population with an interpreted geological (weighted mean) age of 56.378 ± 0.092 Ma (MSWD = 0.82, n = 8). This sample, from within the Hvannhagi Formation provides a constraint on volcanism at this level.
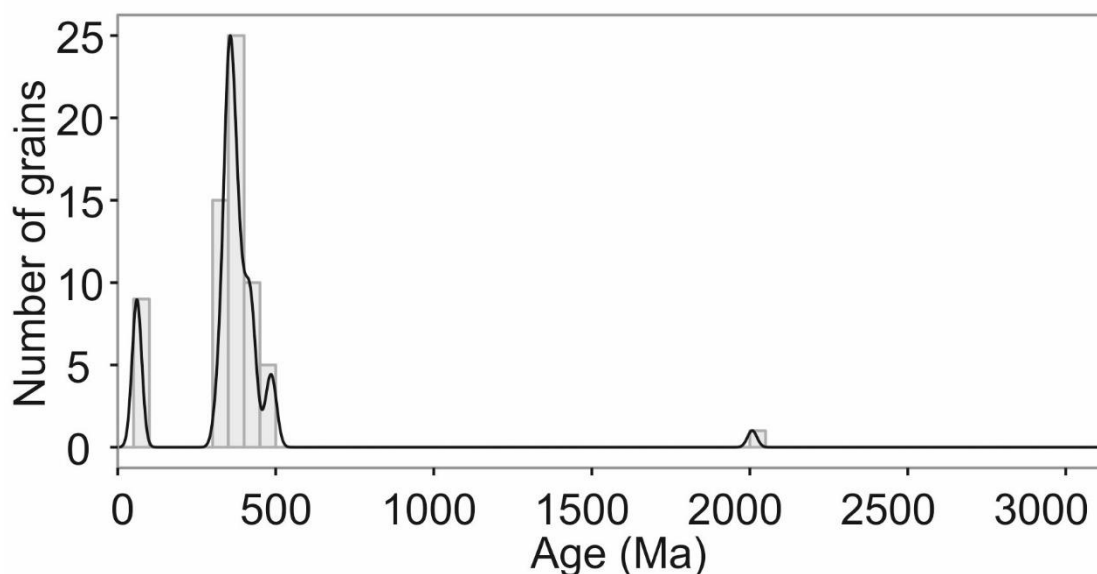
Figure 37 KDE plot and histogram showing the distribution of inherited / detrital zircons in Faroe Island Basalt Group samples.

During screening of the zircon populations using LA-ICPMS, a number of detrital zircon grains were identified (*Figure 37*). These have Palaeozoic ^{206}Pb/^{238}U ages, scattering between 500 and 330 Ma.

Summary – These new, and first zircon U/Pb ages, tighten the age constraints on the FIBG as a whole. These new data confirm the age of the syn-breakup volcanism to 56.378 ± 0.092 Ma (MSWD = 0.82, n = 8). These are the first zircons found in the FIBG, and also the first ages for the Hvannhagi Formation, and are some 0.8 Ma older than ^{40}Ar/^{39}Ar ages for the Malinstindur Fm (Storey et al, 2007; Wilkinson et al, 2017). Although they "only" give the most accurate the age for the onset of syn-breakup related volcanism, combined with good ^{40}Ar/^{39}Ar (e.g. Storey et al, 2007) and the magnethostratigraphy from the Beinisvørð Formation this has broad implications for the age constraints on the FIBG.

Looking at the wide ranges of ages from the SINDRI reports (i.e., Sherlock et al., 2010), these data are from the lavas themselves, and therefore also reflect the difficulties regarding interpretation of complex ^{40}Ar/^{39}Ar from these types of rocks (i.e., weathered Palaeogene basalts). Relating to the Storey et al (2007) ^{40}Ar/^{39}Ar ages, recently recalibrated by Wilkinson et al (2017), the new U/Pb data support and add to the age model presented. The outstanding debate whether models presented by e.g. Schofield and Jolley (2013) where the entire FIBG lava pile erupted within T45 and T40 (56.1Ma to 54.9 Ma) are therefore clearly flawed by these new data.

6.3   OFFSHORE VOLCANICS, FAROE-SHETLAND BASIN.

Background - During the course of the project it was suggested, based upon the success of dating the onshore volcanics from the Mull Lava Group, that samples from key offshore tuffs (i.e., the Kettla Tuff) be targeted for U-Pb (zircon) geochronology. A number of samples were collected a series of wells from the UK and Faroe sectors of the Faroe-Shetland Basin (Table 6A), targeting both volcanic and sedimentary lithologies, the hope being that the latter contain zircon reworked from broadly coeval volcanism in the hinterland (similar to the Ardtun Leaf Bed scenario). A total of 15 samples were processed from 7 wells (Table A6) and based upon the zircon recover and the zircon morphology a combined LA-ICP-MS screening and high-precision ID-TIMS analytical programme was undertaken and the results of key (i.e., successful) samples are outlined below.

SVÍNOY3216 is a sample from Well 6004 12/1 sampled at a depth between 3117 and 3126 metres and is comprises hand-picked fragments of tuff. Zircons from this sample were variable in their morphology, however, a population of clear faceted crystals was observed and U-Pb LA-ICP-MS screening indicated these were Paleogene in age. These young zircon were then selected for U-Pb ID-TIMS analyses which yield (^{230}Th corrected) ^{238}U/^{206}Pb dates that range between 57.8 and 56.9 Ma (n = 4) with 2σ uncertainties on the order of 0.3 to 2.1 Myr. These dates are statistically indistinguishable from one another, and given their uniform morphology, we interpret that the zircon represent a single age population with an interpreted geological (weighted mean) age of 57.75 ± 0.23 (MSWD = 0.33, n = 4). Given the reworked nature of this samples this is strictly a maximum constrain on the timing of sediment accumulation, however, given its young age it is likely that this age is an approximation of the sedimentation age at this level.

SSK76537 is a volcaniclastic sandstone samples from Well 213/27- 2 sampled at a depth of sampled 9664'0" at a level interpreted to be the 'Kettla Tuffite'. Zircons from this sample were variable in their morphology, however, a population of clear faceted crystals was observed and U-Pb LA-ICP-MS screening indicated these were Paleogene in age. These young zircon were then selected for U-Pb ID-TIMS analyses which yield (^{230}Th corrected) ^{238}U/^{206}Pb dates that range between 61.0 and 55.5 Ma (n = 5) with 2σ uncertainties on the order of 0.2 to 1.8 Myr. Two of the older data (z3 and z6, ~60 Ma) are distinctly older than the three remaining dates (~57 Ma). We interpret that the three youngest dates represent a single age population with an interpreted geological (weighted mean) age of 57.53 ± 0.21 (MSWD = 2.7, n = 3). Given the reworked nature of this samples this is strictly a maximum constrain on the timing of sediment accumulation, however, given its young age it is likely that this age is an approximation of the sedimentation age at this level.
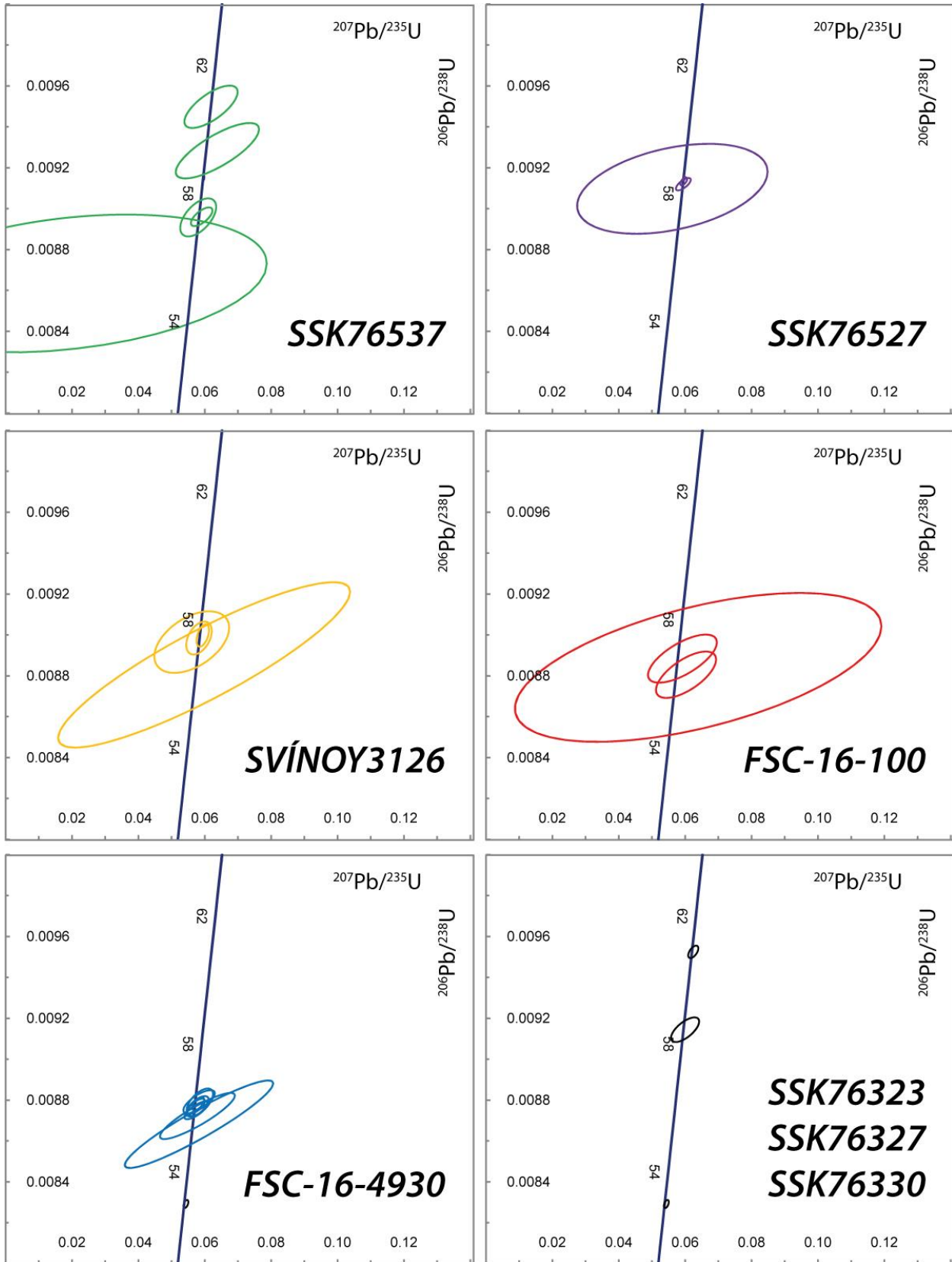
Figure 38 U-Pb (Wetherill) Concordia plots displaying the CA-ID-TIMS U-Pb results for zircon recovered from samples from wells within the Faroe-Shetland Basin and two samples from within the Faroe Islands Basalt Group stratigraphy.

SSK76527 is a volcaniclastic sandstone samples from Well 204/19-3A sampled at a depth of sampled at 1936.65m a level interpreted to be the 'Kettla Tuffite'. Zircons from this sample were variable in their morphology, however, a population of clear faceted crystals was observed and U-Pb LA-ICP-MS screening indicated these were Paleogene in age. These young zircon were then selected for U-Pb ID-TIMS analyses which yield (^{230}Th corrected) ^{238}U/^{206}Pb dates that range between 58.8 and 58.5

Ma (n = 4) with 2σ uncertainties on the order of 0.1 to 1.1 Myr. We interpret that the zircons represent a single age population with an interpreted geological (weighted mean) age of 58.75 ± 0.05 Ma (MSWD = 1.8, n = 4). Given the reworked nature of this samples this is strictly a maximum constrain on the timing of sediment accumulation, however, given its young age it is likely that this age is an approximation of the sedimentation age at this level.

During screening of the zircon populations using LA-ICPMS, a broad range of detrital / inherited zircon ages were identified (*Figure 39*). In addition to Archaean and Proterozoic populations, significant populations of grains with 'Caledonian' (c. 440 Ma) and Carboniferous / Permian ages were present.
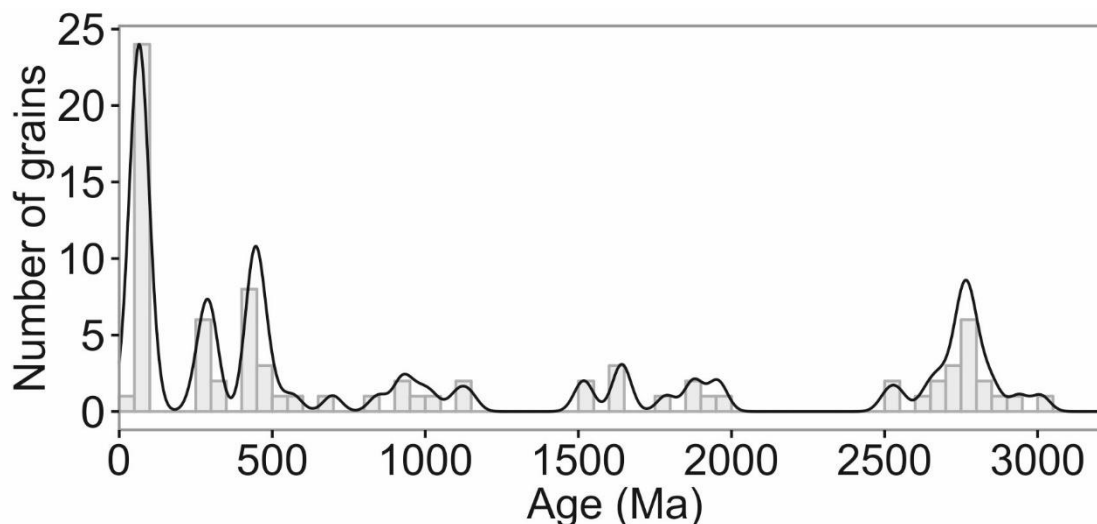
Figure 39 KDE plot and histogram showing the distribution of inherited / detrital zircons in Kettla Tuff core samples.

Combined, these data represent the first radio-isotopic (U-Pb zircon) age determinations for the Kettla Tuffite from the Faroe Shetland Basin. The dates obtained from these levels are from lithologic units that have been reworked and are strictly maximum age estimates for the levels sampled. Two of the Kettla Tuff samples yield similar ages, 57.53 ± 0.21 and 57.75 ± 0.23, however, the third yields a distinctly older date of 58.75 ± 0.05 Ma. Assuming these three levels are stratigraphically correlative, an age of 57.5 Ma is consider a maximum age for the Kettla Tuff and is a likely a good approximation to its numerical age. Importantly, these studies demonstrate the feasibility of obtaining high-precision U-Pb age constraints from these lithologies.

7 Discussion

Biostratigraphic data and zircon U/Pb radio-isotopic age dating of material from the Hebrides, Northern Ireland, Faroe-Shetland Basin and the Faroe Islands, emplaced during the formation of the North Atlantic Igneous Province, have been presented in the preceding sections. The present section reviews existing age models for Palaeogene formations and complexes of this region and establishes a revised chronostratigraphic framework based on new age constraints (this study) and accepted ages from the literature. The chronostratigraphy is presented relative to the 2016 Geologic Time Scale (GTS2016). The broader implications in terms of North Atlantic correlations, palaeo-environmental conditions and timing of tectono-magmatic and palaeoclimatic events are discussed.

7.1   PREVIOUS WORK

The lithostratigraphy of the Palaeogene succession west of Shetland, Sullom Formation thru Balder Formation, is well-established (Ritchie et al. 2011). This succession has been subdivided into a sequence stratigraphical framework based on biostratigraphy, heavy mineral analysis, lithofacies and

sedimentology (Ebdon et al. 1995). The Sullom Formation to the Balder Formation succession is assigned to T-sequences T10 to T50 of Danian to Ypresian age (Ebdon et al. 1995, Lamers and Carmichael, 1999).

On the basis of palynological evidence, Ellis et al. (2002) and Jolley and Whitham (2004) promoted that the pre-breakup volcanic formations in East Greenland (Nansen Fjord Formation) and on the Faroe Islands (Lopra and Beinissvørð formations) postdate the Lamba Formation of the FSB. Resultantly, the entire FIBG (and the pre- and syn-breakup equivalent formations in East Greenland; in total, a 6-7 km composite stratigraphic section) was constrained to T40 and T45 with the vast majority of the volcanic succession erupted during C24r, between 56-55 Ma. This temporal relationship was largely constrained by biostratigraphic correlation to palynofloral assemblages recovered from immediately beneath and in-between a ca. 70 m thick volcanic succession in well 205/9-1. From this stratigraphic level (Flett Formation; unit F1b; T40.2-40.3) in well 205/9-1 a post-PETM thermophylic palynofloral assemblage was reported and concluded to be equivalent to palynofloral assemblages in clastic sediments below the Nansen Formation and in interbasaltic sediments of the Beinisvørð Formation. In recent years this chronostratigraphic model (Model 1) driven by biostratigraphic correlations has been promoted further (e.g. Passey and Jolley, 2009; Schoefield and Jolley, 2013).

Magnetostratigraphic studies on the Faroe Islands document four reversals in the 6.5 km composite stratigraphic section; three zones with reverse polarity (R1, R2, R3) and two zones with normal polarity (N1, N2) (Waagstein, 1988; Riisager et al. 2002; Abrahamsen, 2006). R1 is determined from segments of the cored Lopra-1 borehole (Abrahamsen, 2006). Aided by K-Ar and ^{40}Ar/^{39}Ar radio-isotopic age determinations (Waagstein et al., 2002), the observed magnetostratigraphy has been correlated to C26r, C26n, C25r, C25n and C24r. The reversal between C25n and C24r is located in upper Beinisvørð Formation less than <50 m below the boundary to the Prestfjall Formation. Interpretation of some of the published K-Ar and ^{40}Ar/^{39}Ar age determinations of the pre-breakup volcanics, hydrothermally altered during burial metamorphism, is difficult due to the effects of argon loss and recoil (Waagstein et al., 2002; Storey et al., 2007). The combined radio-isotopic age data and magnetostratigraphy support a chronostratigraphic model (Model 2) with protracted pre-breakup volcanism between 61-56.5 Ma (T25-T40) followed by a hiatus and subsequently renewed, syn-breakup volcanism between 56-55 Ma (Storey et al., 2007).

The disparity between chronostratigraphic age models 1 and 2 is non-trivial, and especially the chronostratigraphy of the FIBG remain controversial. Biostratigraphy, magnetostratigraphy and radio-isotopic dating have failed to provide a consensus as to the absolute age range for this group. The observed two normal polarity zones in the pre-breakup volcanic succession of the FIBG are discarded by proponents of age model 1 as cryptochrons in C24r (Jolley and Bell, 2002).

The role of the formation of the NAIP as a potential trigger for the Palaeocene-Eocene thermal maximum (PETM) has received attention for more than two decades. Despite significant advances in geochronometry the absolute timing of the onset of the PETM relative to the (protracted) emplacement of the NAIP has not been firmly established until now. Chronostratigraphic age Model 1 predicts that the syn-breakup volcanism and most (if not all) of the pre-breakup volcanism postdate the PETM event. Model 2 predicts that the pre-breakup volcanism pre-dated the PETM and that the syn-breakup volcanism was concomitant with the PETM event.

The role of the BPIP in developing a chronostratigraphy for the Faroe-Shetland Basin revolves around a suite of radio-isotopic data/dates that have been obtained for volcanic rocks and associated intrusives that are used to constrain the age of palynomorph bearing sediments (e.g., Jolley et al., 2002), and in some studies assumed biostratigraphic constraints have been used to inform interpretative models for the interpretation of complex radio-isotopic data (Sherlock et al., 2010). As a result of these studies, inference from the BPIP are often exported to the FSB and FIBG, and as such these BPIP data and models require evaluation and testing.

The BPIP has been subject to a number of radio-isotopic dating studies and these continue to refine the chronology of the province. Critically, for this issue of a testing and developing

chronostratigraphic models, these studies have employed a variety of radio-isotopic dating systems (e.g., Rb-Sr, ^{40}Ar/^{39}Ar and U-Pb) using a range of analytical approaches (microbeam and isotope dilution) and from a number of different laboratories. This approach introduces age uncertainty related to a number of issues: (1) the systematics of a given chronometer system (i.e., assumptions made in determining a sample age); (2) inter-laboratory bias (remain poorly quantified within the geochronology community but has been demonstrated to be significant, % level in some relevant instances), and (3) inter-chronometer bias (i.e., calibration of specific parent/daughter systems and decay constants). Up until this studies, models for the chronology of the BPIP and NAIP have used dates from a wide variety of sources (Fig. 8), and therefore needed to address these issues. Most recently (Wilkinson et al, 2017) attempted to compile the NAIP database of published geochronology explicitly dealing with the issue of U-Pb and ^{40}Ar/^{39}Ar inter-calibration, however the exact level of temporal resolution that can be used for these legacy data sets.

Evaluating both the radio-isotopic and palynological data at the end of the Phase 2 Paleogene project revealed a number of issues. ^{40}Ar/^{39}Ar from the SINDRI projects (Sherlock et al., 2010) combined with inference based upon palynological studies have been used to suggest a young (ca. 55 Ma) age for the Staffa Lava Formation, to support an interpretative framework for de-convolving ^{40}Ar/^{39}Ar dates from complex spectra which was then applied to the FIBG. This young age for the Staffa Lava Formation is in conflict with a number of prior radio-isotopic dating studies (e.g., Chambers and Pringle, 2001) hence the need for new experiments (i.e., this study).

7.2   FAROE ISLANDS BASALT GROUP

We have presented a stratigraphic section (c. 12 m) from Holid í Helli, Faroe Islands, with palynological data and a high-precision zircon U/Pb age of a late Thanetian sediment-dominated sequence located between the pre- and syn-breakup flood basalts of the Faroe Islands Basalt Group. Thirteen samples yielded 34 different pollen and spores (most samples had <120 counted specimens). Gymnosperm pollen of *Inaperturopollenites hiatus* are dominant and other important elements include spores, *Momipites annellus/tenuipolus*, and members of the birch family (*Triatriopollenites spp.*, *Triporopollenites mullensis*). Labrapollis is absent, but *Caryapollenites circulus* and *Caryapollenites spp.* are present in low numbers. The pollen and spore flora contains a generic suite of taxa that conform to the NAIP flora but no taxa that are informative for age determination. No in-situ dinoflagellate cysts, such as the *Apectodinium* acme, are present in the section. A population of igneous zircons from the lower tuff bed yields a U/Pb age of 56.38 ± 0.09 Ma. The tuff beds correlate with explosive activity in local volcanic complexes exposed on the Faroe Islands and represent the earliest syn-breakup volcanism of the NAIP. These deposits, previously referred to as the tuff-agglomerate zone (Rasmussen and Noe-Nygaard, 1970), have more recently been lithostratigraphically formalized as the Hvannhagi Formation (Passey and Jolley, 2009). Promotion of these deposits as the Hvannhagi Formation is unfortunate since they are laterally discontinuous with significant local variability in lithology. Furthermore, the basaltic pyroclastic deposits of the Hvannhagi Formation share geochemical affinity with the Malinstindur Formation. At Jardfeingi, work is underway that will reassign the tuff-agglomerate zone as a member of the Malinstindur Formation.

Jolley and Whitham (2004) Ellis et al. (2002) and Passey and Jolley (2009) used palynofloral assemblages found in sub- and interbasaltic sedimentary sequences in central East Greenland, Northeast Greenland and on the Faroe Islands as evidence of post-PETM emplacement of both the pre- and syn-breakup volcanic piles. From central East Greenland (Jolley and Whitham, 2004) and the Faroe Islands (Ellis et al., 2002; Passey and Jolley, 2009) only long-ranging floral taxa were reported. These observations corroborate with the palynological results from Faroese interbasaltic sediments presented in this report; generic NAIP floral assemblages with no taxa that are informative for accurate age determination. Importantly, Jolley and Whitham (2004) reported on several occurrences of *Apectodinium augustum* that is diagnostic for the PETM, along with the generic NAIP palynofloral assemblage in lacustrine mudstones and fluvial sandstones underlying Lower and Upper Plateau Lava Series in Northeast Greenland. The biostratigraphy-driven chronostratigraphy of Model

1, assigning both the pre- and syn-breakup volcanic formations in East Greenland and the Faroe Islands to early Eocene (post-PETM), hinges on two findings: (1) the occurrence of *Apectodinium augustum* in Northeast Greenland and (2) a Palaeocene age of ca. 59 Ma for a 'lava flow' in the Lower Plateau Lava Series reported by Upton et al. (1995). Today the lava pile preserved in Northeast Greenland is referred to as the Lower and Upper Plateau Lava Series (Larsen et al., 2014). Recently, Larsen et al. (2014) have demonstrated that this lava pile is of early Eocene age (55.5-53.5 Ma) and erupted contemporaneous with the more well-known Plateau Basalts (e.g. Storey et al., 2007) exposed along the Blosseville coast in central East Greenland (*Figure 40*). The 'lava flow' dated by Upton et al. (1995) has been shown to be a nephelinitic sill (with geochemical affinity to the Upper Plateau Lava Series) that intruded the Lower Plateau Lava Series. The sill is affected by excess argon and the reported total fusion age should be discarded. The Lower and Upper Plateau Lava Series cannot be correlated geochemically to the Main Basalts (located 400-800 km further south) and the FIBG, as the mantle source was compositionally distinct. The pre-breakup volcanic formations known from central East Greenland and the Faroe Islands are not present in Northeast Greenland (Fig. 40, Larsen et al., 2014). In this report, we have presented the to-date most accurate radio-isotopic age for the earliest syn-break volcanism (56.38 ± 0.09 Ma). The radio-isotopic age for the onset of the PETM is 55.87 ± 0.09 Ma [U-Pb zircon age and cyclostratigraphy of key stratigraphic section on Svalbard, Charles et al., 2011]. Resultantly, the PETM and the syn-breakup volcanism of the NAIP were coeval, and the onset of the hyperthermal aberration occurred 510 ± 130 kyr after initiation of volcanism at ca. 56.4 Ma. The (protracted) pre-breakup volcanism had ceased prior to the onset of the PETM. We draw two significant conclusions from the above observations: (1) The observations on which the biostratigraphic correlations of Model 1 is based are flawed. (2) The palynology results are not in conflict with the magnetostratigraphic record and radio-isotopic geochronology of the terrestrial volcanic archives in support of Model 2. In particular, the occurrences of *Apectodinium augustum* in Northeast Greenland corroborate with an early Eocene age for the Lower Plateau Lava Series (ca. 55.5 Ma) (*Figure 40*). We attribute the lack of taxa diagnostic to the PETM in central East Greenland and on the Faroe Islands to the complete lack of sedimentary catchments for pollen and spores in the extreme volcanic environment that dominated during deposition of the Milne Land and Malinstindur formations. The results are of such importance that they should be disseminated among the global PETM-related research community. Equally important are the implications for the regional absolute chronostratigraphic framework of the FSB and bordering elevated terranes for the Palaeocene and early Eocene.

7.3   BRITISH PALAEOGENE IGNEOUS PROVINCE

We have determined U-Pb (zircon) ages for a range of units across the BPIP in order to develop a robust chronology for the province. The ages of the BPIP has developed based upon a developing dataset of radio-isotopic age from intrusive and extrusive igneous rocks using a rage of radio-isotope decay schemes (i.e., U-Pb, K-Ar, $^{40}Ar/^{39}Ar$ and Rb-Sr) and analytical approaches (whole rock vs. mineral, microbean vs. isotope dilution). These dates are combined with biostratigraphic information from inter-bedded sediments where palynomorphs have been recovered. There is an extensive literature on this province however their remains controversy due to conflicting age models based upon differential emphasis on different data sets. King (2016) provides the most recent and comprehensive review and appraisal of this dataset.

The results of this project provide an internally consistent chronology; the base of the Staff Lava Formation is now dated at 61.74 ± 0.14 Ma and is similar in age to the base of the Eigg Lava Formation (61.64 ± 0.17 Ma). The Ardtun Leaf Bed is constrained as being younger than 61.65 ± 0.13 Ma (the age of reworked zircons in the Ardtun Leaf Bed sediments), and a tuff from the overlying Mull Plateau Lava Formation (dated at 61.098 ± 0.090 Ma) provide a minimum age on the Staffa Lava Formation. The Sgurr of Eigg Pitchstone Formation, dated at 60.12 ± 0.38 Ma, is broadly coeval with Mull Plateau Lava Formation. A final constraint is provided by the age of the Loch Ba Felsite that is dated at 58.936 ± 0.072 and intrudes the Mull Plateau Lava Formation, hence providing firm constraint on the minimum age. These data are all internally consistent when considered in their

geological context and the analytical program is comparable to the data quality included in the GTS 2016, where the assumptions have been minimised and are explicit.

Units within Staffa Lava Formation that were used in the SINDRI ^{40}Ar/^{39}Ar study (Sherlock et al 2010) that concluded that the Staffa Lava Formation is ca. 55 Ma based upon an interpretation of complex ^{40}Ar/^{39}Ar data and an inferred palynological age. This is in contrast to ^{40}Ar/^{39}Ar analyses of Chambers and Pringle (2001) who obtained older dates (~58 to 60 Ma) for the Palaoegene rocks of Mull. Our new data provide a clear test of these models and indicate that the ca. 55 Ma age assignment (Sherlock et al., 2010) is not correct as the coherent data set of U-Pb (zircon) age determinations from this study constrain the age of the Staffa Lava Formation between 61.7 and 61.1 Ma. These data have implications for the ^{40}Ar/^{39}Ar (basalt) data using a similar approach but applied to FIBG rocks.

Whilst many of the palynological data obtained in this studay (and prior work) are not age diagnostic it is possible derive bio zonation data for the Artdun Leaf Bed, which when combined with the radio-isotopic dating permits an improved calibration of the numerical range of certain taxa. Palynological data from the Ardtun Leaf Bed strongly indicate that this unit is older than middle Thanetian, hence probably early Thanetian in age, however, radio-isotopic dates indicate a Selandian (GTS 2016) and this geochronological assessment provides a reliable calibration for the pollen biostratigraphy and information about their geographic and temporal range.

7.4   FAROE-SHETLAND BASIN

As a preliminary test of the application of zircon U/Pb geochronology to better constrain the chronostratigraphy of the FSB, we have reported on six zircon U/Pb ages of tuff/volcaniclastic sandstone intervals in the Kettla Tuff Member (Eidesgaard et al., 2012) from four wells (6004/12-1, 205/9-1, 204/19-3A (three samples), 213/27-2). A single grain analysis from 205/9-1 is anomalously young (53.3 Ma) and is discarded (lead loss, probable analytical outlier). The youngest zircon populations for each of the remaining five samples give ages between 64.0 and 57.5 Ma. With a conservative approach all five samples are interpreted as representing detrital zircons. However, the two samples from 6004/12-1 and 213/27-2 give the youngest ages, 57.75 ± 0.23 Ma and 57.53 ± 0.21 Ma respectively, and the ages overlap at 2sd errors (outside of 2sd error of the remaining three samples). We cautiously consider that the two young ages from 6004/12-1 and 213/27-2 are close to the emplacement age of the reworked volcaniclastic material of the Kettla Tuff Member. The Kettla Tuff Member is located near the base of the Lamba Formation (T36-38), and according to Schofield and Jolley (2013) the age of the Kettla Tuff Member is biostratigraphically constrained at ca. 58.8-58.4 Ma (lower T36). If we interpret all of the dated zircon populations as detrital, the Kettla Tuff Member should be not older than ca. 57.5 Ma. Considering the current biostratigraphic age range for Kettla Tuff Member, we argue that the two young ages reported here (57.75 ± 0.23 Ma and 57.53 ± 0.21 Ma) are very close to the emplacement age of this member. The young dated intervals could indeed represent actual primary tuff beds deposited by volcanic processes, but this can be ascertained only after detailed characterization of the mineral assemblage, petrography, and mineral- and geochemistry (not part of the deliverables identified for this report). The reported zircon U/Pb ages at 57.8-57.5 Ma do contest the current accepted biostratigraphic age for the Kettla Tuff Member ca. 58.8-58.4 Ma.

The broader implication of this test concerns the general validity of the current Palaeocene-early Eocene chrono/biostratigraphic age model for the FSB. The interaction and feedback between volcanic and sedimentary emplacement processes and deposits in volcanic basins along rifted margins remain poorly understood while exerting significant control basin development and petroleum prospectivity. However, in order to forward our understanding of these processes that influenced the FSB, it is imperative to have absolute chronostratigraphic framework that will synchronize sedimentary and volcanic lithostratigraphic formations/sequences. We have addressed the biostratigraphic mis-calibration of the NAIP volcanism relative to the Palaeocene-Eocene boundary and T40, and we have raised concerns regarding the chronostratigraphic placement of the Kettla Tuff

Member. We conclude by recommending a complete revision of the Palaeocene-early Eocene chronostratigraphy for the FSB (not part of the deliverables identified for this report).

7.5   SYNTHESIS

The onset of pre-breakup volcanism belonging to the NAIP occurred in lower Selandian between 62-60 Myr ago (Fig. 41). Volcanism seemingly initiated simultaneously over a widespread area and is attributed to the arrival of the proto-Icelandic mantle plume at the base of the lithosphere under central Greenland. Eruptive products are preserved onshore in central West Greenland (not discussed here), central East Greenland, the Faroe Islands and the British Isles. Accurate, high-precision U/Pb zircon ages constrain the base of the Mull Lava Group and the Antrim Lava Group to 61.7-61.5 Ma. The volcanic products were deposited into rifted sedimentary basins along the emerging continental margins above already previously thinned lithosphere. Lower magma productivity near the British Isles in comparison to Greenland and the Faroe Islands, led to more intermittent volcanism with episodes of erosion and deposition of fluviatile and lacustrine sediments of both siliciclastic and volcaniclastic origin. The Ardtun Leaf Beds from the upper part of the Staffa Lava Formation were deposited in this environment. Our age determination of a tuff from the overlying Mull Plateau Lava Formation to 61.1 Ma provides a minimum age of the important paleofloral assemblage represented in the Ardtun Leaf Beds. The Mull Plateau Lava Formation was fully emplaced prior to 58.9 Ma. Younger activity in the Skye Central Complex and the Skye Lava Group continued until at least 56.1 Ma, immediately predating the Palaeocene-Eocene boundary.

The frequency of individual volcanic eruptions dwindled toward the end of the pre-breakup volcanism of the FIBG, and the termination of this phase is constrained from magnetostratigraphy and ^{40}Ar/^{39}Ar age determinations to 57-56.5 Ma in early C24r (*Figure 41*). The pre-breakup volcanism was followed by erosion and subsequently deposition of lacustrine sediments of the Prestfjall Formation. Emerging syn-break plumbing systems at the Faroe Islands encountered mature hydrologic systems below the lacustrine basins, causing ignimbrite-producing phreato-magmatic explosive eruptions during the earliest syn-breakup volcanism (Hvannhagi Formation) that we have constrained at 56.4 Ma. This activity predates the onset of the PETM by <500 kyr. These events produced local topographic high around volcanic complexes and mass wasting with deposition of debris flows and lahars. Upon complete disruption of the hydrologic system the style of volcanism returned to emplacement of effusive flood basalts of the Malinstindur and Enni formations. The available magnetostratigraphic and radio-isotopic data constrain the paleofloral assemblage of the Prestfjall Formation to ca. 57-56.5 Ma in the late Thenatian. The last stages of the syn-breakup volcanism is constrained by the Gronau alkaline tuff of the Skrænterne Formation in East Greenland (ash layer -17 in the Danish mo clay) at 55.5 Ma. During post-breakup times the embryonic rift zone between East Greenland and the Faroe Islands subsided below sea-level, producing violent phreatomagmatic eruptions preserved in the Balder Formation (the positive tephra series of the mo clay, the Fur Formation).

If we consider the Gronau alkaline tuff (equivalent to ash layer -17 in the Sele Formation) located in the Skrænterne Formation (uppermost formation of the Main Basalts in central East Greenland) dated at 55.48 ± 0.12 Ma [@ 28.201 Ma for FCT, Heister et al., 2001; Storey et al., 2007], and the age for the onset of the syn-breakup volcanism in the Faroe Islands reported here, then the bulk of the syn-breakup volcanism of the NAIP erupted within 0.7-1.1 Myrs. The collective age constraints (biostratigraphy and geochronology) support a proposed causal relationship of the NAIP magmatism as a trigger for the PETM event (e.g. Svensen et al., 2004). Based on the available data we predict that the PETM event was coeval with the emplacement of the syn-breakup succession of the FIBG.
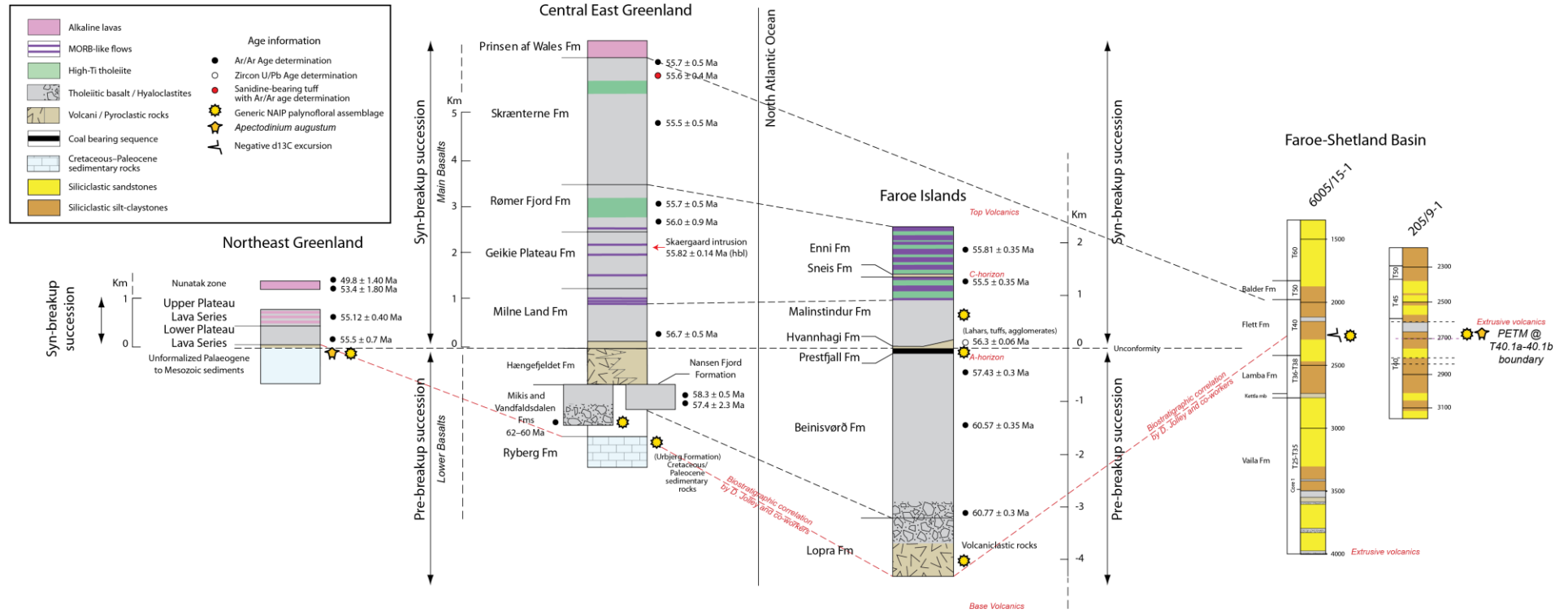
Figure 40 Regional lithostratigraphic log correlation chart for the NE Atlantic margins. Black stippled lines illustrate correlations based on radio-isotopic geochronology and basalt petrology. Red stippled lines illustrate biostratigraphic (mis)-correlations, based on misinterpretation of field relations in Northeast Greenland (see section 7.1.1 and 7.1.2 for further discussion).

Figure 41 Chronostratigraphic panel summarising the stratigraphic information and geochronology for regions of interest (BPIP, FSB, FIBG and North Sea) using the data from this project and other studies, plotted against the GTS 2016 timescale. NOTE –the chronostratigraphy for the T-sequences of the FSB is not calibrated against the U/Pb zircon geochronology, highlighted by the discrepancy regarding the age of the Kettla Tuff Member.

8 Conclusions

The overarching aim of this Phase 3 project was to test prior chronostratigraphical models for key regions of the NAIP that underpin the chronostratigraphy of the Faroes-Shetland Basin and adjacent volcanic province. Critical evaluation of cornerstone biostratigraphical and radio-isotopic data at the end of FSC Phase 2 (Smith et al., 2013) suggested that considerable uncertainty exists between proposed models. The aim of this Phase 3 project was to develop a new dataset of radio-isotopic (U-Pb zircon) and biostratigraphical (palynomorph) data to test the prior age models, primarily the young Staffa Formation (Sherlock et al., 2010), and the young FIBG model (Schofield and Jolley, 2013), and to develop a new data set that would allow construction of a new chronostratigraphical framework with tie points. In contrast to prior studies that have sought to use the ^{40}Ar/^{39}Ar system to provide direct age determinations of basalts, we have used the U-Pb (zircon) system targeting a wider range of lithologies, from basaltic to silicic volcanic units (tuff and ignimbrites), detrital zircon from sediments that broadly reflect the age of contemporaneous volcanism in the hinterland, and cross cutting felsic intrusive rocks. This approach has advantages in that the accuracy of the U-Pb (zircon) system is well demonstrated and quantified (e.g., Condon et al., 2015) and provides a level of accuracy that is directly comparable to the data used as input for the GTS 2016 (e.g., Charles et al., 2011).

The existing pollen biostratigraphy, which has been developed over several decades, is a robust scheme which allows the successions to be subdivided with a good stratigraphical resolution. It clearly is driven by evolutionary change coupled with extensive flora dynamics which was driven largely by palaeoclimatological fluctuations. The radio-isotopic conclusions in this study have allowed the refinement of the ages of some of the pollen based units.

Radio-isotopic dating from a range of lithologies at key stratigraphical intervals from the Inner Hebrides and Northern Ireland allow us to test prior models for the age of key intervals of the BPIP (e.g., Staffa Lava Formation) and are summarised in the following:

- Onset of NAIP volcanism is constrained to ca. 61.7 Ma and broadly coincident in the Antrim, Mull and Eigg Lava fields.
- Age of the Staffa Lava Formation (Isle of Mull) is robustly constrained to ≤61.7 Ma (age of ignimbrite from base of Staff Lava Formation) and to ≥61.1 Ma (age of tuff in overlying Mull Plateau Lava Formation).
- Prior studies that assign an age of ca. 55 Ma to the Staffa Lava formation based upon complex ^{40}Ar/^{39}Ar data and inferences based upon palynological data are incorrect and should be discounted.

In addition to testing the prior models for the chronology of the BPIP, we have obtained new data (U-Pb geochronology and palynology) from the FIBG and from cores from the FSB that provide the opportunity to further test the competing models for the chronostratigraphy of the region. These two contrasting models (Fig. 6) are i) the post-PETM emplacement model that has the entire FIBG erupted during a brief period (T40-45) of the Early Eocene, and ii) the alternative model of the FIBG being emplaced during a more protracted period of volcanism from the middle Palaeocene to early Eocene.

- Zircon U/Pb ages from volcanic deposits of the Hvannhagi Formation confirm the age for the earliest syn-breakup volcanism to 56.378 ± 0.092 Ma in the late Palaeocene; predating the onset of the PETM by ca. 500 kyr. The Lopra and Beinisvørð formations are therefore constrained to the middle-late Palaeocene in corroboration with peer-reviewed, robust ^{40}Ar/^{39}Ar data. Studies that assign an age an early Eocene age to the entire FIBG based upon complex ^{40}Ar/^{39}Ar data (including unpublished data) and correlations based upon palynological data are incorrect and should be discounted.
- Zircon U/Pb ages from the Kettla Tuff Member (57.8-57.5 Ma) are at odds with the current accepted biostratigraphic age for this member (c. 58.8-58.4 Ma).

We recommend a complete revision of the Palaeocene-early Eocene chronostratigraphy for the Faroe-Shetland Basin to allow for calibration against the emplacement of volcanic products and tectonic events relating to the bordering volcanic province. This will facilitate a better understanding of sedimentary depositional processes and general evolution of the FSB during the formation of the NAIP.

9 References

ANDERSON, F.W. and DUNHAM, K.C., (1966), *The geology of Northern Skye.* From Memoirs of the Geological Survey, Great Britain.

AUBRY, M.-P., SWISHER III, C.C., KENT, D.V. and BERGGREN, W.A.. (2003). *Paleogene time scale miscalibration: Evidence from the dating of the North Atlantic igneous province*: Comment. Geology, 31, 468–469.

BAILEY, E.B., CLOUGH, C.T., WRIGHT, W.B., RICHEY, J.E. and WILSON, G.V. (1924). *Tertiary and Post-Tertiary Geology of Mull, Loch Aline and Oban. Being a Description of Parts of Sheets 43, 44, 51 and 52 of the Geological Map.* Memoirs of the Geological Survey of Scotland: Edinburgh, Her Majesty's Stationery Office.

BELL, B.R. and JOLLEY, D.W. (1997). *Application of palynological data to the chronology of the Palaeogene lava fields of the British Province: implications for magmatic stratigraphy*. Journal of the Geological Society, London, 154, 701–708.

BELL, B.R. and WILLIAMSON, I.T. (2002). *Tertiary igneous activity*. In: Trewin, N.H. (editor). The Geology of Scotland. Fourth Edition. The Geological Society, London, 371–407.

BOULTER, M.C. and KVAČEK, Z. (1989). *The Palaeocene flora of the Isle of Mull*. Special Papers in Palaeontology, 42, 149 p.

BOULTER, M.C. and MANUM, S.B. (1989). *The Brito-Arctic Igneous Province flora around the Paleocene/Eocene boundary*. Proceedings of the Ocean Drilling Program Scientific Results, 104, 663–680.

BRITISH GEOLOGICAL SURVEY (2000). *Sheet 70. Minginish. 1:50,000 (Map)*. Solid and Drift Edition. British Geological Survey, Nottingham.

BROWN, D.J., HOLOHAN, E.P. and BELL B.R. (2009). *Sedimentary and volcano-tectonic processes in the British Paleocene Igneous Province: a review*. Geological Magazine, 146, 326–352.

CAMPBELL, G.D. (1851). *On Tertiary Leaf-Beds in the Isle of Mull: with a note on the vegetable remains* from Ardtum Head by Prof. E. Forbes, V.P.G.S. Quarterly Journal of the Geological Society of London, 7, 89–103.

CATTELL, A.C. (1989). *The Skye Main Lava Series: liquid density and the absence of basaltic hawaiites.* Geological Magazine, 126, 681–684.

CHALMERS, J,A, and WAAGSTEIN, R. (editors). (2006). *Scientific results from the deepened Lopra-1 Borehole, Faroe Islands*. Geological Survey of Denmark and Greenland Bulletin, No. 9, 156 p.

CHAMBERS, L.M. and PRINGLE, M.S. (2001). *Age and duration of activity at the Isle of Mull Tertiary igneous centre, Scotland, and confirmation of the existence of subchrons during Anomaly 26r.* Earth and Planetary Science Letters, 193, 333–345.

CHAMBERS, L. M., PRINGLE, M. S., and PARRISH, R. R., (2005), *Rapid formation of the Small Isles Tertiary centre constrained by precise* $^{40}Ar/^{39}Ar$ *and U–Pb ages: Lithos,* v. 79, no. 3, p. 367-384.

CHARLES, A. J., CONDON, D. J., HARDING, I. C., PÄLIKE, H., MARSHALL, J. E., CUI, Y., KUMP, L., and CROUDACE, I. W., (2011), *Constraints on the numerical age of the Paleocene-Eocene boundary*, Geochemistry, Geophysics, Geosystems, v. 12, no. 6.

CLEAL, C.J., THOMAS, B.A., BATTEN, D.J. and COLLINSON, M.E. (2001). *Mesozoic and Tertiary Palaeobotany of Great Britain*. Geological Conservation Review Series, 22. Joint Nature Conservation Committee, Peterborough.

CONDON, D. J., SCHOENE, B., MCLEAN, N. M., BOWRING, S. A. and PARRISH, R. R., (2015), *Metrology and traceability of U–Pb isotope dilution geochronology (EARTHTIME Tracer Calibration Part I)*: Geochimica et Cosmochimica Acta, v. 164, p. 464-480.

COOPER, J. (1979). *Lower Tertiary fresh-water Mollusca from Mull,* Argyllshire. Tertiary Research, 2, 69–74.

COOPER, M.R., TROLL, V.R. and LEMON, K (2017), *The 'Clay-with-Flints' deposit in Northern Ireland: reassessment of the evidence for an early Palaeocene ignimbrite*, Geological Magazine

CURRY, D., ADAMS, C.G., BOULTER, M.C., DILLEY, F.C., EAMES, F.E., FUNNELL B.M. and WELLS M.K. (1978). *A correlation of the Tertiary rocks in the British Isles*. Geological Society of London, Special Report, 12, 72 p.

EBDON, C.C., GRANGER, P.J., JOHNSON, H.D. and EVANS, A.M. (1995). *Early Tertiary evolution and stratigraphy of the Faeroe–Shetland Basin: implications for hydrocarbon prospectivity*. In: Scrutton, R.A., Stoker, M.S., Shimmield, G.B. and Tudhope, A.W. (editors). Sedimentation and Palaeoceanography of the North Atlantic Region. Geological Society, London, Special Publications, No. 90, 51–69.

EDWARDS, W.N. (1922). *An Eocene microthyriaceous fungus from Mull, Scotland*. Transactions of the British Mycological Society, 8, 66–72.

ELDHOLM, O. and GRUE, K. (1994). *North Atlantic volcanic margins: Dimensions and production rates*. Journal of Geophysical Research, 99, 2955–2968.

ELDRETT, J.S., GREENWOOD, D.R., POLLING, M., BRINKHUIS, H. and SLUIJS, A. (2014). *A seasonality trigger for carbon injection at the Paleocene–Eocene Thermal Maximum*. Climate of the Past, 10, 759–769.

ELLIS, D., BELL, B.R., JOLLEY, D.W. and O'CALLAGHAN, M. (2002). *The stratigraphy, environment of eruption and age of the Faroes Lava Group, NE Atlantic Ocean*. In: Jolley, D.W. and Bell, B.R. (editors). The North Atlantic Igneous Province: Stratigraphy, Tectonic, Volcanic and Magmatic Processes. Geological Society, London, Special Publications, 197, 253–269.

ELLIS, D. and STOKER, M.S. (2014). *The Faroe–Shetland Basin: a regional perspective from the Paleocene to the present day and its relationship to the opening of the North Atlantic Ocean*. In: Cannon, S.J.C. and Ellis, D. (editors). Hydrocarbon Exploration to Exploitation West of Shetlands. Geological Society, London, Special Publications, No. 397, 11–31.

ELSIK, W.C. and CRABAUGH, J.P. (2001). *Palynostratigraphy of the upper Paleocene and lower Eocene Wilcox Group in the Northwestern Gulf of Mexico Basin*. In: Goodman, D.K. and Clarke, R.T. (editors). Proceedings of the IX International Palynological Congress, Houston, Texas, U.S.A. 1996. American Association of Stratigraphic Palynologists Foundation, p. 233–237.

EMELEUS, C.H. and GYOPARI, M.C. (1992). *British Tertiary Volcanic Province*. Geological Conservation Review. London: Chapman and Hall on behalf of the Joint Nature Conservation Committee.

EMELEUS, C.H. and BELL, B.R. (2005). *British regional geology: the Palaeogene volcanic districts of Scotland (Fourth edition)*. British Geological Survey, Nottingham, 212 p.

EVANS, A.L. (1969). *On dating the British Tertiary Igneous Province*. Unpublished PhD Thesis, University of Cambridge.

GANERØD, M., SMETHURST, M.A., TORSVIK, T.H., PRESTVIK, T., ROUSSE, S., MCKENNA, C., VAN HINSBERGEN, D.J.J. and HENDRIKS, B.W.H. (2010). *The North Atlantic*

Igneous Province reconstructed and its relation to the Plume Generation Zone: the Antrim Lava Group revisited. Geophysical Journal International, 182, 183–202.

GANERØD, M., CHEW, D. M., SMETHURST, M. A., TROLL, V. R., CORFU, F., MEADE, F., and PRESTVIK, T., (2011), *Geochronology of the Tardree Rhyolite Complex, Northern Ireland: Implications for zircon fission track studies, the North Atlantic Igneous Province and the age of the Fish Canyon sanidine standard*: Chemical Geology, v. 286, no. 3, p. 222-228.

GARDNER, J.S. (1887). *On the Leaf-beds and Gravels of Ardtun, Carsaig, &c., in Mull.* Quarterly Journal of the Geological Society, 43, 270–300.

GRADSTEIN, F.M., OGG, J.G., SCHMITZ, M.D. and OGG, G.M. (editors). (2012). *The Geologic Time Scale* 2012. Elsevier, 1176 pp.

GRUAS-CAVAGNETTO, C. (1972). *Étude palynoplanctologique de deux gisements du Thanétian des environs de Reims.* Revue de Micropaléontologie, 15, 63–74.

GRUAS-CAVAGNETTO, C. (1976). *Étude palynologique du Paléogène du Sud de l'Angleterre.* Cahiers de Micropaléontologie, 1, 1–49.

HALD, N. and WAAGSTEIN, R. (1983). *Silicic basalts from the Faeroe Islands: evidence of crustal contamination.* In: Bott, M.H.P., Saxov, S., Talwani, M. and Thiede, J. (editors). Structure and Development of the Greenland–Scotland Ridge. New Methods and Concepts. New York: Plenum Press, 343–349.

HAMILTON, R.V. and MINSHELL, B.J. (2018). Hydrothermal vents and seismic anomalies: implications for the petroleum system NE of Shetland. Petroleum Geoscience, https://doi.org/10.1144/petgeo2017-072.

HARRINGTON, G.J., EBERLE, J., LE-PAGE, B.A. DAWSON, M. and HUTCHISON, J.H. (2012). Arctic plant diversity in the early Eocene greenhouse. Proceedings of the Royal Society of London B, 279, 1515–1521.

HEILMANN-CLAUSEN, C. (1985). Dinoflagellate stratigraphy of the uppermost Danian to Ypresian in the Viborg 1 borehole, central Jylland, Denmark. Danmarks Geologiske Undersøgelse Serie A, Nr. 7, 69 p.

HERNGREEN, G.F.W, FELDER, W.M., KEDVES, M., and MEESSEN, J.P.M.T. (1986). Micropaleontology of the Maestrichian Borehole Bunde, The Netherlands. Review of Palaeobotany and Palynology, 48, 1–70.

ITO, G., LIN, J. and GABLE, C.W. (1996). *Dynamics of mantle flow and melting at a ridge-centered hotspot: Iceland and the Mid-Atlantic Ridge*. Earth and Planetary Science Letters, 144, 53–74.

JARZEMBOWSKI, E.A., SIVETER, D.J., PALMER, D. and SELDEN, P.A. (2010). *Fossil Arthropods of Great Britain.* Geological Conservation Review Series, 35. Joint Nature Conservation Committee, Peterborough.

JOLLEY, D.W. and MORTON, A.C. (1992). *Palynological and petrological characterization of a North Sea Palaeocene volcaniclastic sequence*. Proceedings of the Geologists' Association, 103, 119–127.

JOLLEY, D.W. (1997). *Palaeosurface palynofloras of the Skye lava field and the age of the British Tertiary volcanic province.* In: Widdowson, M. (editor). Palaeosurfaces: Recognition, reconstruction and palaeoenvironmental interpretation. Geological Society Special Publication, 120, 67–94.

JOLLEY, D.W. and BELL, B.R. (editors). (2002). *The North Atlantic Igneous Province: Stratigraphy, Tectonic, Volcanic and Magmatic Processes*. Geological Society, London, Special Publications, 197, 331 p.

JOLLEY, D.W. and WHITHAM, A.G. (2004). *A stratigraphical and palaeoenvironmental analysis of the sub-basaltic Paleogene sediments of East Greenland.* Petroleum Geology, 10, 53–60.

JOLLEY, D.W., CLARKE, B. and KELLEY, S. (2002). *Paleogene time scale miscalibration: Evidence from the dating of the North Atlantic igneous province*. Geology, 30, 7–10.

KALKREUTH, W.D., RIEDIGER, C.L., MCINTYRE, D.J., RICHARDSON, R.J.H., FOWLER, M.G. and MARCHIONI, D. (1996). *Petrological, palynological and geochemical characteristics of Eureka Sound Group coals (Stenkul Fiord, southern Ellesmere Island, Arctic Canada)*. International Journal of Coal Geology, 30, 151–182.

KENDER, S., STEPHENSON, M.H., RIDING, J.B., LENG, M.J., KNOX, R.W.O'B., PECK, V.L., KENDRICK, C.P., ELLIS, M.A., VANE, C.H. and JAMIESON, R. (2012). *Marine and terrestrial environmental changes in NW Europe preceding carbon release at the Paleocene–Eocene transition*. Earth and Planetary Science Letters, 353-354, 108–120

KERR, A.C., KENT, R.W., BELL, B.R. and JOLLEY, D.W. (1998). *Discussion on application of palynological data to the chronology of the Paleogene lava fields of the British Province*. Journal of the Geological Society, London, 155, 733–735.

KERR, A.C., KENT, R.W., THOMSON, B.A., SEEDHOUSE, J.S. and DONALDSON, C.H. (1999). *Geochemical evolution of the Tertiary Mull volcano* Journal of Petrology, 40, 873–908.

KIMBELL, G.S. (2014). *Magnetic signatures of Palaeogene igneous rocks in the Faroe–Shetland area*. British Geological Survey Commissioned Report, CR/14/054, 98 p.

KING, C. (2016). *A revised correlation of Tertiary rocks in the British Isles and adjacent areas of NW Europe*. Gale, A.S. and Barry, T.L. (editors). Geological Society, London, Special Reports, No. 27, 719 p.

LAMERS, E. and CARMICHAEL, S.M.M. (1999). *The Paleocene deepwater sandstone play West of Shetland*. In: Fleet, A.J. and Boldy, S.A.R. (editors). Petroleum Geology of Northwest Europe: Proceedings of the 5th Conference. Geological Society, London, 645–659.

LARSEN, L.M., PEDERSEN, A.K., TEGNER, C. and DUNCAN, R.A. (2014). *Eocene to Miocene igneous activity in NE Greenland: northward younging of magmatism along the East Greenland margin.* Journal of the Geological Society, London, 171, 539–553.

LARSEN, L.M., PEDERSEN, A.K., TEGNER, C., DUNCAN, R.A., HALD, N. and LARSEN, J.G. (2016). *Age of Tertiary volcanic rocks on the West Greenland continental margin: volcanic evolution and event correlation to other parts of the North Atlantic Igneous Province*. Geological Magazine, 153, 487–511.

LEFFINGWELL, H.A. (1971). *Palynology of the Lance (Late Cretaceous) and Fort Union (Paleocene) formations of the type Lance area, Wyoming.* Geological Society of America Special Paper, 127, 1–64.

LUND, J. (1989). *A late Paleocene non-marine microflora from the interbasaltic coals of the Faeroe Islands*, North Atlantic. Bulletin of the Geological Society of Denmark, 37, 181–203.

MCINERNEY, F.A. and WING, S.L. (2011). *The Paleocene-Eocene Thermal Maximum: A perturbation of carbon cycle, climate, and biosphere with implications for the future.* Annual Review of Earth and Planetary Sciences, 39, 489–516.

MCINTYRE, D.J. (1989). *Paleocene palynoflora from northern Somerset Island, District of Franklin, N.W.T.* In: Current Research, Part G, Geological Survey of Canada Paper, 89-1G, 191–197.

MCINTYRE, D.J. (1991). *Pollen and spore flora of an Eocene forest, eastern Axel Heiberg Island, N.W.T.* In: Christie, R.L. and McMillian, N.J. (editors). Tertiary Fossil Forests of the Geodetic Hills, Axel Heiberg Islands, Arctic Archipelago. Geological Survey of Canada Bulletin, 403, 83–97.

MCINTYRE, D.J. (1994). *Appendix 1. Palynology*. In: Ricketts, B.D. (editor). Basin analysis, Eureka Sound Group, Axel Heiberg and Ellesmere Islands, Canadian Arctic archipelago. Geological Survey of Canada Memoir, 439, 85–101.

MITCHELL, W.I. (editor). (2004). *The Geology of Northern Ireland – Our Natural Foundation*. Geological Survey of Northern Ireland, Belfast, 318 p.

MUDGE, D.C. (2015). *Regional controls on Lower Tertiary sandstone distribution in the North Sea and NE Atlantic margin basins*. In: McKie, T., Rose, P.T.S., Hartley, A.J., Jones, D.W. and Armstrong, T.L. (editors). Tertiary Deep-Marine Reservoirs of the North Sea Region. Geological Society, London, Special Publications, No. 403, 17–42.

MUSSETT, A.E., BROWN, G.C., ECKFORD, M. and CHARLETON, S.R. (1972). *The British Tertiary Igneous Province: K-Ar ages of some dykes and lavas from Mull, Scotland*. Geophysical Journal of the Royal Astronomical Society, 30, 405–414.

MUSSETT, A.E. (1986). ^{40}Ar–^{39}Ar *step-heating ages of the Tertiary igneous rocks of Mull, Scotland*. Journal of the Geological Society, London, 143, 887–896.

MUSSETT, A.E., DAGLEY, P. and SKELHORN, R.R. (1988). *Time and duration of activity in the British Tertiary Igneous Province. Early Tertiary Volcanism and the Opening of the NE Atlantic*. Geological Society, London, Special Publications, No. 39, 337–348.

NAYLOR, P.H., BELL, B.R., JOLLEY, D.W., DURNALL, P. and FREDSTED, R. (1999). *Palaeogene magmatism in the Faroe-Shetland Basin: influences on uplift history and sedimentation*. In: Fleet, A.J. and Boldy, S.A.R. (editors). Petroleum Geology of Northwest Europe: Proceedings of the 5th Conference, 1, 545–558.

NORRIS, G. (1997). *Paleocene–Pliocene deltaic to inner shelf palynostratigraphic zonation, depositional environments and paleoclimates in the Imperial ADGO F-28 well, Beaufort-MacKenzie Basin*. Geological Survey of Canada Bulletin, 523, 71 p.

PASSEY, S.R. and BELL, B.R. (2007). *Morphologies and emplacement mechanisms of the lava flows of the Faroe Islands Basalt Group, Faroe Islands, NE Atlantic Ocean*. Bulletin of Volcanology, 70, 139–156.

PASSEY, S.R, (2008). *IGC Excursion No.6, Field Guide*, The Volcanic and Sedimentary Evolution of the Faroe Islands Basalt Group, 33 IGC Excursion No6, August 15-22, 2008

PASSEY, S.R. and JOLLEY, D.W. (2009). *A revised lithostratigraphic nomenclature for the Palaeogene Faroe Islands Basalt Group, NE Atlantic Ocean*. Earth and Environmental Science Transactions of the Royal Society of Edinburgh, 99, 127–158.

PHILLIPS, L. 1974. *Reworked Mesozoic spores in Tertiary leaf-beds on Mull, Scotland*. Review of Palaeobotany and Palynology, 17, 221–232.

PITMAN, W.C. III and TALWANI, M. (1972). *Sea-floor spreading in the North Atlantic*. GSA Bulletin, 83, 619–646.

POCKNALL, D.T. and NICHOLS, D.J. (1996). *Palynology of coal zones of the Tongue River Member (upper Paleocene) of the Fort Union Formation, Powder River Basin, Montana and Wyoming*. American Association of Stratigraphic Palynologists Contributions Series, 32, 58 p.

RASMUSSEN, J., NOE-NYGAARD, A. and TROELSEN, J.-C. (1956). *Faeröe Islands (Føroyar, Færøerne, îles Faeröe)*. In: Congrès Géologique International and Commission de Stratigraphie. Lexique Stratigraphique International, Europe, 1, 13–17. Centre National De La Recherche Scientifique, Paris.

RASMUSSEN, J. and NOE-NYGAARD, A. (1969). *Beskrivelse til Geologisk Kort over Færøerne i Ma lestok 1:50 000*, 1/24. Danmarks Geologiske Undersøgelse, København.

RASMUSSEN, J. and NOE-NYGAARD, A. (1970). *Geology of the Faeroe Islands (Pre-Quaternary) [Translated by Henderson, G.]* 1/25. Geological Survey of Denmark, Copenhagen.

RIISAGER, P., RIISAGER, J., ABRAHAMSEN, N. and WAAGSTEIN, R. (2002). *New paleomagnetic pole and magnetostratigraphy of Faroe Islands flood volcanics, North Atlantic igneous province.* Earth and Planetary Science Letters 201, 261–76.

RITCHIE, J.D., ZISKA, H., JOHNSON, H. and EVANS, D. (editors). (2011). *Geology of the Faroe–Shetland Basin and Adjacent Areas.* British Geological Survey, Nottingham.

ROUSE, G.E. (1977). *Paleogene palynomorph ranges in Western and Northern Canada.* American Association of Stratigraphic Palynologists Contributions Series, 5A, 48–65.

SAHY, D., CONDON, D. J., HILGEN, F. J., and KUIPER, K. F., (2017), *Reducing Disparity in Radio-Isotopic and Astrochronology-Based Time Scales of the Late Eocene and Oligocene: Paleoceanography,* v. 32, no. 10, p. 1018-1035.

SAUNDERS, A.D., FITTON, J.G., KERR, A.C., NORRY, M.J. and KENT, R.W. (1997). *The North Atlantic Igneous Province.* In: Mahoney, J.J. and M. F. Coffin, M.F. (editors). Large Igneous Provinces: Continental, Oceanic, and Planetary Flood Volcanism. American Geophysical Union, Washington, D.C., doi: 10.1029/GM100p0045.

SCHILLING, J.-G. (1973). *Iceland Mantle Plume: geochemical study of Reykjanes Ridge.* Nature, 242, 565–571.

SCHOFIELD, N. and JOLLEY, D.W. (2013). *Development of intra-basaltic lava-field drainage systems within the Faroe–Shetland Basin.* Petroleum Geoscience, 19, 273–288.

SCHOFIELD, N., HOLFORD, S. MILLETT, J., BROWN, D., JOLLEY, D., PASSEY, S.R., MUIRHEAD, D., GROVE, C., MAGEE, C., MURRAY, J., HOLE, M., JACKSON, C.A.-L. and STEVENSON, C. (2017). *Regional magma plumbing and emplacement mechanisms of the Faroe-Shetland Sill Complex: implications for magma transport and petroleum systems within sedimentary basins.* Basin Research, 29, 41–63.

SCHOUTEN, S., WOLTERING, M., RIJPSTRA, I.C., SLUIJS, A., BRIKHUIS, H. and SINNINGHE DAMSTÉ, J.S. (2007). *The Paleocene–Eocene carbon isotope excursion in higher plant organic matter: differential fractionation of angiosperms and conifers in the Arctic.* Earth and Planetary Science Letters, 258, 581–592.

SCHRÖDER, T. (1992). *A palynological zonation of the North Sea Basin.* Journal of Micropalaeontology, 11, 113–126.

SEWARD, A.C. and HOLTTUM, R.E. (1924). *Tertiary plants from Mull.* In: Bailey, E.B., Clough, C.T., Wright, W.B., Richey, J.E. and Wilson, G.V. Tertiary and Post-Tertiary Geology of Mull, Loch Aline and Oban. Being a Description of Parts of Sheets 43, 44, 51 and 52 of the Geological Map. Memoirs of the Geological Survey of Scotland: Edinburgh, Her Majesty's Stationery Office, p. 67–90.

SHERLOCK, S. C., JOLLEY, D.W., KELLEY, S.P., and WATSON, J. (2010). *A predictive model of the $^{40}Ar/^{39}Ar$ age dating system in Faroe Islands basalts to assist in well sampling and the positioning of sidewall core in future offshore drilling projects.* SindriMC Contract Number: C46-41-01

SIMPSON, J.B. (1961). *The Tertiary pollen flora of Mull and Ardnamurchan.* Transactions of the Royal Society of Edinburgh, 64, 421–468.

SKELHORN, R.R. (1969). *The Tertiary Igneous Geology of the Isle of Mull.* Geologists' Association Guide, No. 20.

SLUIJS, A., VAN ROIJ, L., HARRINGTON, G.J., SCHOUTEN, S., SESSA, J.A., LEVAY, L.J., REICHART, G.-J., and SLOMP, C.P. (2014). *Warming, euxinia and sea level rise during the Paleocene–Eocene Thermal Maximum on the Gulf Coastal Plain: implications for ocean oxygenation and nutrient cycling.* Climate of the Past, 10, 1421–1439.

SMITH, K., STOKER, M.S., JOHNSON, H. and EIDESGAARD, Ó. (2013). *Early Palaeogene stratigraphy, volcanism and tectonics of the Faroe–Shetland region.* British Geological Survey Commissioned Report, CR/13/006, 43 p.

STOKER, M.S. and VARMING, T. (2011). *The Cenozoic.* In: Ritchie, J.D., Ziska, H., Johnson, H. and Evans, D. (editors). Geology of the Faroe-Shetland Basin and Adjacent Areas. British Geological Survey Report RR/11/01.

STOKER, M.S., HOLFORD, S.P. and HILLIS, R.R. (2018). *A rift-to-drift record of vertical crustal motions in the Faroe–Shetland Basin, NW European margin: establishing constraints on NE Atlantic evolution.* Journal of the Geological Society, 175, 263–274.

STOREY, M., DUNCAN, R.A. and TEGNER, C. (2007). *Timing and duration of volcanism in the North Atlantic Igneous Province: implications for geodynamics and links to the Iceland hotspot.* Chemical Geology, 241, 264–281.

SRIVASTAVA, S.K. (1975). *Maastrichtian microspore assemblages from the interbasaltic lignites of Mull, Scotland.* Palaeontographica Abteilung B, 150, 125–156.

WAAGSTEIN, R. (1988). *Structure, composition and age of the Faeroe basalt plateau.* In: Morton, A.C. and Parson, L.M. (editors). Early Tertiary Volcanism and the Opening of the NE Atlantic. Geological Society, London, Special Publications, No. 39, 225–238.

WATSON, D., SCHOFIELD, N., JOLLEY, D., ARCHER, S., FINLAY, A.J., MARK, N., HARDMAN, J. and WATTON, T. (2017). *Stratigraphic overview of Palaeogene tuffs in the Faroe–Shetland Basin, NE Atlantic Margin*. Journal of the Geological Society, 174, 627–645.

WEI, W. (2003). *Paleogene time scale miscalibration: Evidence from the dating of the North Atlantic igneous province*: Comment. Geology, 31, 467–468.

WILLIAMSON, I.T. and BELL, B.R. (1994). *The Palaeocene lava field of west-central Skye, Scotland: Stratigraphy, palaeogeography and structure*. Transactions of the Royal Society of Edinburgh: Earth Sciences, 85, 39–75.

WILLIAMSON, I.T. and BELL, B.R. (2012). *The Staffa Lava Formation: graben-related volcanism, associated sedimentation and landscape character during the early development of the Palaeogene Mull Lava Field, NW Scotland*. Scottish Journal of Geology, 48, 1–46.

WILKINSON, C. M., GANERØD, M., HENDRIKS, B. W. H., and EIDE, E. A., (2017), *Compilation and appraisal of geochronological data from the North Atlantic Igneous Province (NAIP)*: Geological Society, London, Special Publications, v. 447, no. 1, p. 69-103.

WING, S.L. and CURRANO, E.D. (2013). *Plant responses to a global greenhouse event 56 million years ago*. American Journal of Botany, 100, 1234–1254.

ZEUNER, F.E. (1941). *The Eocene insects of the Ardtun Beds, Isle of Mull.* Annals and Magazine of Natural History, 7, 82–100.

ZEUNER, F.E. (1944). *Notes on Eocene Homoptera from the Isle of Mull, Scotland*. Annals and Magazine of Natural History, 11, 110–117.

10 Appendices

10.1   APPENDIX 1 – LIST OF SAMPLES

Table A1 – Samples from the Faroe Islands which were analysed for δ^{13}C.

No.	Registration No.	Collector's No.	Latitude	Longitude	Locality	Lithotype	Lithostratigraphical Formation
1	MPA 68205	FSC16 37	-7,177628	62,042790	Quarry Miðvágur (top)	Siltstone	Malinstindur Formation
2	MPA 68206	FSC16 38	-7,178177	62,043516	Quarry Miðvágur (base)	Fine red sandstone	Malinstindur Formation
3	MPA 68209	FSC16 41	-7,155968	62,084004	Sandavágshálsur	Fine sandstone	Malinstindur Formation
4	MPA 68211	FSC16 43	-7,023463	62,127286	Leynavatn, Klivarnir, road	Fine sandstone	Malinstindur Formation
5	MPA 68214	FSC16 46	-7,025025	62,125970	Leynavatn, Klivarnir, top	Coarse sandstone	Malinstindur Formation
6	MPA 68215	FSC16 47	-6,860917	62,051125	Sund Quarry	Very fine sandstone	Malinstindur Formation (Sund bed)
7	MPA 68218	FSC16 49 1	-6,748327	61,548303	Holið í Helli	Black mudstone	Hvannhagi Formation
8	MPA 68220	FSC16 49 3	-6,748327	61,548303	Holið í Helli	Black mudstone	Hvannhagi Formation
9	MPA 68222	FSC16 49 5	-6,748327	61,548303	Holið í Helli	Black mudstone	Hvannhagi Formation
10	MPA 68224	FSC16 49 7	-6,748327	61,548303	Holið í Helli	Black mudstone	Hvannhagi Formation
11	MPA 68226	FSC16 49 9	-6,748327	61,548303	Holið í Helli	Black mudstone	Hvannhagi Formation
12	MPA 68228	FSC16 49 11	-6,748327	61,548303	Holið í Helli	Black mudstone	Hvannhagi Formation
13	MPA 68230	FSC16 49 13	-6,748327	61,548303	Holið í Helli	Black mudstone	Hvannhagi Formation
14	MPA 68232	FSC16 49 15	-6,748327	61,548303	Holið í Helli	Black mudstone	Hvannhagi Formation
15	MPA 68234	FSC16 49 17	-6,748327	61,548303	Holið í Helli	Black mudstone	Hvannhagi Formation
16	MPA 68236	FSC16 49 19	-6,748327	61,548303	Holið í Helli	Black mudstone	Hvannhagi Formation
17	MPA 68238	FSC16 49 20B	-6,748327	61,548303	Holið í Helli	Coarse band	Hvannhagi Formation
18	MPA 68239	FSC16 49 21	-6,748327	61,548303	Holið í Helli	Rubbly mudstone	Hvannhagi Formation
19	MPA 68243	FSC16 49 25	-6,748327	61,548303	Holið í Helli	Rubbly mudstone	Hvannhagi Formation
20	MPA 68247	FSC16 49 29	-6,748327	61,548303	Holið í Helli	Dark mudstone	Hvannhagi Formation
22	MPA 68253	FSC16 49 35	-6,748327	61,548303	Holið í Helli	Dark mudstone	Hvannhagi Formation

23	MPA 68264	FSC16 49 46	-6,748327	61,548303	Holið í Helli	Black graphitic mudstone	Hvannhagi Formation
24	MPA 68267	FSC16 52 1	-6,748048	61,547741	Holið í Helli	Black mudstone	Hvannhagi Fm/Prestfjall Fm
25	MPA 68273	FSC16 52 7	-6,748048	61,547741	Holið í Helli	Black mudstone	Hvannhagi Fm/Prestfjall Fm
26	MPA 68280	FSC16 52 14	-6,748048	61,547741	Holið í Helli	Black mudstone	Hvannhagi Fm/Prestfjall Fm
27	MPA 68288	FSC16 52 22	-6,748048	61,547741	Holið í Helli	Dark mudstone w. Coal	Prestfjall Formation
28	MPA 68293	FSC16 52 27	-6,748048	61,547741	Holið í Helli	Coal	Prestfjall Formation
29	MPA 68301	FSC16 52 35	-6,748048	61,547741	Holið í Helli	Coal	Prestfjall Formation
30	MPA 68306	FSC16 52 40	-6,748048	61,547741	Holið í Helli	Clay w. Coal	Prestfjall Formation
31	MPA 68313	FSC16 52 47	-6,748048	61,547741	Holið í Helli	Black claystone	Prestfjall Formation
32	MPA 68316	FSC16 55	-6,747819	61,547522	Holið í Helli	Grey siltstone	Prestfjall Formation
33	MPA 68319	FSC16 58	-6,749749	61,545309	Ádalsmøl	Coal	Beinisvørð Formation
34	MPA 68327	FSC16 66	-6,819607	61,480389	Hvannfelli Profile	Siltstone	Beinisvørð Formation
35	MPA 68335	FSC16 74	-6,835096	61,492356	Hvannfelli Profile	Brown claystone	Beinisvørð Formation
36	MPA 68340	FSC16 79	-6,841627	61,492199	Hvannfelli Profile	Claystone	Beinisvørð Formation
37	MPA 68355	FSC16 88 4	-6,779110	61,455424	Núpur	Brown siltstone	Beinisvørð Formation
38	MPA 68362	FSC16 94	-6,836446	61,464537	Vágseiðið, Kleivin	Brown siltstone	Beinisvørð Formation
39	MPA 68365	FSC16 96 2	-6,780528	61,484033	Áin mikla, Porkeri	Black mudstone	Beinisvørð Formation
40	MPA 68366	FSC16 96 3	-6,780528	61,484033	Áin mikla, Porkeri	Dark grey claystone	Beinisvørð Formation
41	MPA 68375	FSC16 99 2	-6,770699	61,508256	Hov	Brown mudstone	Beinisvørð Formation
42	MPA 68378	FSC16 101	-6,929101	61,608001	Undir bergi	Tuff	Hvanhaga Formation
43	MPA 68379	FSC16 102	-6,925465	61,610488	Sandavíkartunnil, S	Red sandstone	Hvanhaga Formation

Table A2 – Mull (Hebrides) samples

No.	Registration No.	Collector's No.	Latitude	Longitude	Locality	Lithotype	Lithostratigraphical Unit (SLF)
1	MPA 67360	FSC-15-2	56.3426 N	-6.24577 W	Ardtun Head, north of Bunessan	silty mudstone	A6 Sedimentary Unit (ALB)
2	MPA 67361	FSC-15-3	56.3426 N	-6.24577 W	Ardtun Head, north of Bunessan	silty mudstone	A6 Sedimentary Unit (ALB)
3	MPA 67362	FSC-15-4	56.3426 N	-6.24577 W	Ardtun Head, north of Bunessan	silty mudstone	A6 Sedimentary Unit (ALB)
4	MPA 67363	FSC-15-5	56.3426 N	-6.24577 W	Ardtun Head, north of Bunessan	silty mudstone	A6 Sedimentary Unit (ALB)
5	MPA 67364	FSC-15-6	56.3426 N	-6.24577 W	Ardtun Head, north of Bunessan	silty mudstone	A6 Sedimentary Unit (ALB)
6	MPA 68177	FSC-16-07	56°19′09.52″N	005°57′21.38″W	Carraig Mhor, Carsaig Arches, Mull	siltstone	A5 Sedimentary Unit
7	MPA 68178	FSC-16-08	56°19′09.52″N	005°57′21.38″W	Carraig Mhor, Carsaig Arches, Mull	sandstone	A5 Sedimentary Unit
8	MPA 68179	FSC-16-09	56°19′09.52″N	005°57′21.38″W	Carraig Mhor, Carsaig Arches, Mull	siltstone	A5 Sedimentary Unit
9	MPA 68180	FSC-16-10	56°19′09.52″N	005°57′21.38″W	Carraig Mhor, Carsaig Arches, Mull	sandstone	A5 Sedimentary Unit
10	MPA 68181	FSC-16-12	56°19′08.35″N	005°57′16.31″W	Carraig Mhor, Carsaig Arches, Mull	siltstone	A5 Sedimentary Unit
11	MPA 68174	FSC-16-04	56°17′35.47″N	006°02′43.66″W	Malcolm's Point, west of Carsaig Bay	conglomerate	A4 Sedimentary Unit
12	MPA 68175	FSC-16-05	56°17′53.74″N	006°01′50.80″W	Malcolm's Point, west of Carsaig Bay	coal	A4 Sedimentary Unit
13	MPA 68176	FSC-16-06	56°17′53.74″N	006°01′50.80″W	Malcolm's Point, west of Carsaig Bay	coal	A4 Sedimentary Unit
14	MPA 68171	FSC-16-01	56° 17′41.08″N	006° 02′ 19.68″W	The Pulpit Rock, Carsaig Bay	sandstone-conglomerate	A2 Sedimentary Unit
15	MPA 68172	FSC-16-02	56° 17′41.08″N	006° 02′ 19.68″W	The Pulpit Rock, Carsaig Bay	sandstone	A2 Sedimentary Unit

Table A3 – Skye (Hebrides) samples

No.	Registration No.	Collector's No.	Latitude	Longitude	Locality	Lithotype	Lithostratigraphical Unit (and Surface No.)
1	MPA 68182	FSC-16-14	57°15′50.13″N	006°25′43.67″W	Preshal Beag, Talisker	sandstone	Preshal Beag Conglomerate Formation (E5)
2	MPA 68183	FSC-16-15	57°15′39.23″N	006°25′35.13″W	Preshal Beag, Talisker	sandstone-conglomerate	Preshal Beag Conglomerate Formation (E5)
3	MPA 68184	FSC-16-16	57°15′39.36″N	006°25′36.10″W	Preshal Beag, Talisker	coarse-grained sandstone	Preshal Beag Conglomerate Formation (E5)
4	MPA 68185	FSC-16-17	57°15′39.36″N	006°25′36.10″W	Preshal Beag, Talisker	sandstone	Preshal Beag Conglomerate Formation (E5)
5	MPA 68186	FSC-16-18	57°15′39.36″N	006°25′36.10″W	Preshal Beag, Talisker	sandstone	Preshal Beag Conglomerate Formation (E5)
6	MPA 68187	FSC-16-19	57°15′39.36″N	006°25′36.10″W	Preshal Beag, Talisker	sandstone	Preshal Beag Conglomerate Formation (E5)
7	MPA 68188	FSC-16-20	57°15′39.36″N	006°25′36.10″W	Preshal Beag, Talisker	sandstone	Preshal Beag Conglomerate Formation (E5)
8	MPA 68189	FSC-16-21	57°15′39.59″N	006°25′35.77″W	Preshal Beag, Talisker	sandstone	Preshal Beag Conglomerate Formation (E5)
9	MPA 68190	FSC-16-23	57°16′43.33″N	006°26′23.85″W	West of Preshal Mhor, Talisker	siltstone	Preshal Beag Conglomerate Formation (E5)
10	MPA 68195	FSC-16-30	57°21′39.26″N	006°25′56.61″W	Dunn Beag, Loch Harport	coal	Eynort Mudstone Formation (E4)
11	MPA 68196	FSC-16-31	57°21′39.26″N	006°25′56.61″W	Dunn Beag, Loch Harport	sandy siltstone	Eynort Mudstone Formation (E4)
12	MPA 68197	FSC-16-32	57°21′39.26″N	006°25′56.61″W	Dunn Beag, Loch Harport	carbonaceous siltstone	Eynort Mudstone Formation (E4)
13	MPA 68198	FSC-16-33	57°21′39.26″N	006°25′56.61″W	Dunn Beag, Loch Harport	sandy siltstone	Eynort Mudstone Formation (E4)
14	MPA 68199	FSC-16-34	57°21′39.26″N	006°25′56.61″W	Dunn Beag, Loch Harport	carbonaceous siltstone	Eynort Mudstone Formation (E4)

15	MPA 68192	FSC-16-27	57°17'37.46"N	006°21'38.59"W	Carbost Burn Waterfall, Carbost	shaly sandstone	Below the Fiskavaig Group (E3)
16	MPA 68193	FSC-16-28	57°17'37.46"N	006°21'38.59"W	Carbost Burn Waterfall, Carbost	coal	Below the Fiskavaig Group (E3)
17	MPA 68194	FSC-16-29	57°17'37.60"N	006°21'39.39"W	Carbost Burn Waterfall, Carbost	red sandstone	Below the Fiskavaig Group (E3)
18	MPA 68200	FSC-16-35	57°22'19.73"N	006°08'18.12"W	near Camas Tianavaig, Sound of Raasay	sandstone	Palagonite Tuff Plant Beds (E1)
19	MPA 68201	FSC-16-36	57°22'19.73"N	006°08'18.12"W	near Camas Tianavaig, Sound of Raasay	carbonaceous sandstone	Palagonite Tuff Plant Beds (E1)

Table A4 – Northern Ireland samples

No.	Reg. No. (MPA)	Collector's No.	Easting	Northing	Locality	Lithotype	Lithostratigraphical Unit
1	68839	NMC 497	310455	407219	Clinty Quarry	Organic pisolithic clay	Interbasaltic Formation
2	68840	NMC 498	310418	407167	Clinty Quarry	Organic pisolithic clay	Interbasaltic Formation
3	68841	NMC 499	332540	381085	Belfast Zoo	Organic pisolitic clay	Clay-with-Flints
4	68842	NMC 500	332540	381085	Belfast Zoo	Purple pisolitic clay	Clay-with-Flints
5	68843	NMC 501	332723	380747	Belfast Zoo	Organic pisolitic clay	Clay-with-Flints
6	68844	NMC 503	288083	439154	Craigahulliar Quarry	Lignite	Port na Spaniagh Mb.
7	68845	NMC 504	288083	439154	Craigahulliar Quarry	Pisolitic clay	Port na Spaniagh Mb.
8	68846	NMC 505	288214	438985	Craigahulliar Quarry	Pisolitic clay	Port na Spaniagh Mb.
9	68847	NMC 506	274270	417940	Donald's Hill	Red clay	Clay-with-Flints (lowermost)
10	68848	NMC 507	274270	417940	Donald's Hill	Basalt with organic matter	Upper Basalt Fm. (lowermost)
11	68849	NI 212	287934	436679	Ballylagan	Pisolitic clay	Ballylagan Member

Table A5 – FIBG samples

No.	Registration No.	Collector's No.	Latitude	Longitude	Locality	Lithotype	Lithostratigraphical Formation
1	MPA 68205	FSC16 37	-7,177628	62,042790	Quarry Miðvágur (top)	Siltstone	Malinstindur Formation
2	MPA 68206	FSC16 38	-7,178177	62,043516	Quarry Miðvágur (base)	Fine red sandstone	Malinstindur Formation
3	MPA 68209	FSC16 41	-7,155968	62,084004	Sandavágshálsur	Fine sandstone	Malinstindur Formation
4	MPA 68211	FSC16 43	-7,023463	62,127286	Leynavatn, Klivarnir, road	Fine sandstone	Malinstindur Formation
5	MPA 68214	FSC16 46	-7,025025	62,125970	Leynavatn, Klivarnir, top	Coarse sandstone	Malinstindur Formation
6	MPA 68215	FSC16 47	-6,860917	62,051125	Sund Quarry	Very fine sandstone	Malinstindur Formation (Sund bed)
7	MPA 68218	FSC16 49 1	-6,748327	61,548303	Holið í Helli	Black mudstone	Hvannhagi Formation
8	MPA 68220	FSC16 49 3	-6,748327	61,548303	Holið í Helli	Black mudstone	Hvannhagi Formation
9	MPA 68222	FSC16 49 5	-6,748327	61,548303	Holið í Helli	Black mudstone	Hvannhagi Formation
10	MPA 68224	FSC16 49 7	-6,748327	61,548303	Holið í Helli	Black mudstone	Hvannhagi Formation
11	MPA 68226	FSC16 49 9	-6,748327	61,548303	Holið í Helli	Black mudstone	Hvannhagi Formation
12	MPA 68228	FSC16 49 11	-6,748327	61,548303	Holið í Helli	Black mudstone	Hvannhagi Formation
13	MPA 68230	FSC16 49 13	-6,748327	61,548303	Holið í Helli	Black mudstone	Hvannhagi Formation

14	MPA 68232	FSC16 49 15	-6,748327	61,548303	Holið í Helli	Black mudstone	Hvannhagi Formation
15	MPA 68234	FSC16 49 17	-6,748327	61,548303	Holið í Helli	Black mudstone	Hvannhagi Formation
16	MPA 68236	FSC16 49 19	-6,748327	61,548303	Holið í Helli	Black mudstone	Hvannhagi Formation
17	MPA 68238	FSC16 49 20B	-6,748327	61,548303	Holið í Helli	Coarse band	Hvannhagi Formation
18	MPA 68239	FSC16 49 21	-6,748327	61,548303	Holið í Helli	Rubbly mudstone	Hvannhagi Formation
19	MPA 68243	FSC16 49 25	-6,748327	61,548303	Holið í Helli	Rubbly mudstone	Hvannhagi Formation
20	MPA 68247	FSC16 49 29	-6,748327	61,548303	Holið í Helli	Dark mudstone	Hvannhagi Formation
21	MPA 68248	FSC16 49 30	-6,748327	61,548303	Holið í Helli	Volcaniclastic sandstone	Hvannhagi Formation
22	MPA 68253	FSC16 49 35	-6,748327	61,548303	Holið í Helli	Dark mudstone	Hvannhagi Formation
23	MPA 68264	FSC16 49 46	-6,748327	61,548303	Holið í Helli	Black graphitic mudstone	Hvannhagi Formation
24	MPA 68267	FSC16 52 1	-6,748048	61,547741	Holið í Helli	Black mudstone	Hvannhagi Fm/Prestfjall Fm
25	MPA 68273	FSC16 52 7	-6,748048	61,547741	Holið í Helli	Black mudstone	Hvannhagi Fm/Prestfjall Fm
26	MPA 68280	FSC16 52 14	-6,748048	61,547741	Holið í Helli	Black mudstone	Hvannhagi Fm/Prestfjall Fm
27	MPA 68288	FSC16 52 22	-6,748048	61,547741	Holið í Helli	Dark mudstone w. Coal	Prestfjall Formation
28	MPA 68293	FSC16 52 27	-6,748048	61,547741	Holið í Helli	Coal	Prestfjall Formation
29	MPA 68301	FSC16 52 35	-6,748048	61,547741	Holið í Helli	Coal	Prestfjall Formation
30	MPA 68306	FSC16 52 40	-6,748048	61,547741	Holið í Helli	Clay w. Coal	Prestfjall Formation
31	MPA 68313	FSC16 52 47	-6,748048	61,547741	Holið í Helli	Black claystone	Prestfjall Formation
32	MPA 68316	FSC16 55	-6,747819	61,547522	Holið í Helli	Grey siltstone	Prestfjall Formation
33	MPA 68319	FSC16 58	-6,749749	61,545309	Ádalsmøl	Coal	Beinisvørð Formation
34	MPA 68327	FSC16 66	-6,819607	61,480389	Hvannfelli Profile	Siltstone	Beinisvørð Formation
35	MPA 68335	FSC16 74	-6,835096	61,492356	Hvannfelli Profile	Brown claystone	Beinisvørð Formation
36	MPA 68340	FSC16 79	-6,841627	61,492199	Hvannfelli Profile	Claystone	Beinisvørð Formation
37	MPA 68355	FSC16 88 4	-6,779110	61,455424	Núpur	Brown siltstone	Beinisvørð Formation
38	MPA 68362	FSC16 94	-6,836446	61,464537	Vágseiðið, Kleivin	Brown siltstone	Beinisvørð Formation
39	MPA 68365	FSC16 96 2	-6,780528	61,484033	Áin mikla, Porkeri	Black mudstone	Beinisvørð Formation
40	MPA 68366	FSC16 96 3	-6,780528	61,484033	Áin mikla, Porkeri	Dark grey claystone	Beinisvørð Formation
41	MPA 68375	FSC16 99 2	-6,770699	61,508256	Hov	Brown mudstone	Beinisvørð Formation
42	MPA 68378	FSC16 101	-6,929101	61,608001	Undir bergi	Tuff	Hvanhaga Formation
43	MPA 68379	FSC16 102	-6,925465	61,610488	Sandavíkartunnil, S	Red sandstone	Hvanhaga Formation

Table A6 – FSB (UK Sector) samples

Well ID	BGS Sub-sample ID	Depth	Lithology	Purpose
205/01-1	SSK76525	9635"	Sandstone	Geochronology
213/26-1	SSK76526	9472"	Tuff	Geochronology
204/19-3A	SSK76527	1936.65m	Sandstone	Geochronology
204/19-3A	SSK76528	1976.81m	Mudstone	Palynology
204/19-3A	SSK76529	1999.6m	Sandstone	Geochronology
204/19-3A	SSK76530	2036.55m	Sandstone	Geochronology
204/19-3A	SSK76531	2081.77m	Sandstone	Geochronology
204/19-3A	SSK76532	2091.71m	Siltstone	Palynology
204/19-3A	SSK76533	2249.76m	Sandstone	Geochronology

204/19-3A	SSK76534	2238.81m	Siltstone	Palynology
213/27-2	SSK76538	9437"	Breccia	CaCO$_3$ Geochronology
213/27-2	SSK76537	9640"	Siltstone	Geochronology
213/27-2	SSK76536	9660"	Mudstone	Palynology
213/27-2	SSK76535	9664"	Sandstone	Geochronology
205/09-1	SSK76524	3470m	Sandstone	Geochronology
205/09-1	SSK76523	3611m	Sandstone	Geochronology
205/09-1	SSK76522	3617m	Siltstone	Palynology
205/09-1	SSK76521	3716m	Sandstone	Geochronology
205/09-1	SSK76520	3721m	Carbonaceous Sst	Palynology
SVÍNOY 6004 12/1		3431m	Tuff/Volc.cl sst. Cuttings	Geochronology
SVÍNOY 6004 12/1		3117m	Tuff/Volc.cl sst. Cuttings	Geochronology
SVÍNOY 6004 12/1		3604,65m	Sandstone	Palynology
SVÍNOY 6004 12/1		3602,8m	Sandstone	Palynology
SVÍNOY 6004 12/1		3601,85m	Sandstone	Palynology
SVÍNOY 6004 12/1		3597,61m	Sandstone	Palynology
SVÍNOY 6004 12/1		3593,44m	Sandstone / mm coal ly	Palynology
SVÍNOY 6004 12/1		3591,48m	Sandstone (w burrows)	Palynology
SVÍNOY 6004 12/1		3588,87m	Sandstone	Palynology
SVÍNOY 6004 12/1		3587,52m	Siltstone	Palynology
SVÍNOY 6004 12/1		3585,69m	Sandstone (carbonaceous)	Palynology
SVÍNOY 6004 12/1		3584,68m	Sandstone (carbonaceous)	Palynology
SVÍNOY 6004 12/1		3582,2m	Sandstone	Palynology
SVÍNOY 6004 12/1		3579,32m	Siltstone	Palynology
MARIMAS 6004/17-1		3189,8m	Siltstone	Palynology
MARIMAS 6004/17-1		3189,35m	Siltstone	Palynology
MARIMAS 6004/17-1		3181,6m	Siltstone	Palynology
MARIMAS 6004/17-1		3180,8m	Siltstone	Palynology
MARIMAS 6004/17-1		3177,3m	Siltstone	Palynology
MARJUN 6004/16-1Z		4181,7m	Mudstone	Palynology
MARJUN 6004/16-1Z		4181,54m	Mudstone	Palynology
MARJUN 6004/16-1Z		3461,16m	Sand/Siltst	Palynology
MARJUN 6004/16-1Z		3460,7m	Sand/Siltst	Palynology
MARJUN 6004/16-1Z		3456,67m	Carbonaceous Sst	Palynology
MARJUN 6004/16-1Z		3455,09m	Mudstone	Palynology
LONGAN 6005/15-1		3513,8m	Tuff, coarse	Geochronology
LONGAN 6005/15-1		3512,39m	Mudstone	Palynology
LONGAN 6005/15-1		3511,65m	Intraclast / Siltst	Palynology
LONGAN 6005/15-1		3511,7m	Siltstone	Palynology
LONGAN 6005/15-1		3510,72m	Siltstone	Palynology
LONGAN 6005/15-1		3509,93m	Siltstone	Palynology
LONGAN 6005/15-1		3508,39m	Siltstone	Palynology

10.2   APPENDIX 2 – RADIO-ISOTOPE DATING METHODOLOGIES

Sample preparation and zircon separation

Samples were crushed using a steel jaw crusher and disk mill.   The < 500 µ fraction was processed using a Gemini table and/or Haultain Superpanner in order to extract a heavy mineral concentrate, which was further purified by passing through di-iodomethane with a specific gravity of 3.3. The most magnetic material was extracted using a hand magnet and a Frantz magnetic separator.

Zircons were hand-picked from the non-magnetic fraction onto double-sided tape and mounted in epoxy, then polished to expose the interior of the grains. For screening analysis prior to ID-TIMS analysis, zircons were mounted on sticky tape and analysed directly in the mass spectrometer, without polishing.

LA-MC-ICPMS

Data were acquired using a Nu Plasma HR multi-collector inductively coupled mass spectrometer. The sample was introduced into the mass spectrometer using a New Wave Research UP193SS solid state laser ablation system. All analyses were carried out using a 20 µm spot and a frequency of 10 Hz, resulting in a fluence of ca. 2.0-2.5 J/cm2. Samples were ablated for 30 seconds. Ablated sample material was transported to the mass spectrometer by a flow of He gas, which was continuously passed through the sample cell.

Data were acquired and processed using the Nu Instruments time resolved analysis software, with an in-house Excel spreadsheet for data reduction and error propagation. The matrix matched zircon standard 91500 was analysed at regular intervals throughout each session. The deviation of the average $^{207}Pb/^{206}Pb$ and $^{206}Pb/^{238}U$ values obtained for 91500 were compared to the known values for this standard, and were used to establish a fractionation factor for each session. Unknown samples were then normalised using the appropriate fractionation factor. The analytical uncertainties reported for each of the sample ratios are also propagated relative to the respective reproducibility of this standard. Two additional zircon standards (Plesovice and GJ1) were analysed at regular intervals to prove the validity of the procedure. Data and plots for all standards are presented in the accompanying spreadsheets.

Only data < 5% discordant are plotted. For kernel density estimate plots, $^{207}Pb/^{206}Pb$ ages are used for ages > 1200 Ma, and $^{206}Pb/^{238}U$ ages are used for ages < 1200 Ma.

ID-TIMS

Zircons selected for analysis were chemically abraded following a modified procedure to remove damaged parts of the crystal that were likely to have experienced open-system behaviour. Firstly, the zircons were thermally annealed at 900°C for 60 hours in quartz crucibles before being individually selected, photographed and loaded into FEP Teflon beakers. Single zircon crystals, or fragments, were selected for dissolution using transmitted light microscopy. Zircons were selected based upon their external morphology and observation of internal feature (i.e., visible cores).

Zircons were then refluxed in 4 M HNO_3 on a hotplate at 120°C for > 2 hours, followed by ultrasonic cleaning for at least 20 minutes. The zircon crystals were rinsed with acetone and 4 M HNO_3 and loaded into individual 300 µl FEP Teflon microcapsules and leached in 29 M HF inside a Parr vessel (a self-sealing stainless-steel jacket) for 12 hours at 180 °C. The zircons were rinsed with 4 M HNO_3 and refluxed in 6 M HCl at 120°C for 2-5 hours, before a final rinsing with 4 M HNO_3 several times.

The leached zircons and all total procedural blanks were spiked with mixed ^{205}Pb–^{233}U–^{235}U (ET535) EARTHTIME tracer solution and dissolved in ~150 µl 29 M HF and trace HNO_3 in a Parr vessel at 220°C for at least 60 hours. Complete dissolution was checked by visual inspection of some larger crystals and assumed for smaller grains, following standard protocol for dissolution at NIGL. The solutions were dried down as fluorides and re-dissolved in 3 M HCl in a Parr vessel overnight at

180°C. U and Pb fractions were isolated by HCl-based anion exchange procedure using Bio-Rad AG-1 resin in Teflon columns. Pb and U fractions were then recombined and dried down with ~10 µl of H_3PO_4. The dried samples were then loaded onto zone-refined Re filaments in a silica gel matrix to enhance ionisation.

Isotope ratios were measured on a Thermo-Electron Triton thermal ionisation mass spectrometer (TIMS). Pb was measured in dynamic mode on a MassCom secondary electron multiplier; Pb mass bias corrections were made using a fractionation factor of 0.14 ± 0.02 % amu-1 (1 sigma) for samples spiked using ET535. Dead-time and linearity of the secondary electron multiplier were monitored using repeated analyses of the standards NBS 982, NBS 981 and U 500. U oxide (UO_2) was measured, and corrected for isobaric interferences using a $^{18}O/^{16}O$ value of 0.00205 (IUPAC value and measured in-house at NIGL). U was measured in dynamic mode and a mass bias fractionation correction calculated in real-time using the ^{233}U-^{235}U ratio of the ET535 tracer solutions. Corrections for the addition of Pb and U during the procedure (i.e., laboratory contamination) were made using the long-term measured isotopic composition and variability of blanks using an amount that is based upon contemporary total procedural blanks. The U/Pb ratio for each analyses was determined via isotope dilution principles and the ET535 mixed ^{205}Pb-^{233}U-^{235}U tracer. A $^{238}U/^{235}U$ value of 137.818 was assumed and used in the data reduction algorithm.

Data Reduction

Due to the slightly larger ionic radius of Th the intermediate daughter ^{230}Th is excluded during zircon crystallisation such that a correction is required to account for ^{230}Th disequilibrium and resulting in deficit ^{206}Pb. This disequilibrium correction requires a priori knowledge of the Th/U of the magma coexisting with the crystal during growth. A sensitivity analysis of the choice of Th/U ratio in the Th-correction shows an inverse exponential relationship between the magnitude of the Th-correction and Th/U ratio that plateaus between Th/U = 3-4 (Figure 1). A value of Th/U = 3.5 was selected for the Th-correction in this study.

See Sahy et al., 2017 for full ID-TIMS methods, references and discussion of age interpretation.

10.3   APPENDIX 3 – ID-TIMS ANALYTICAL DATA

Group	Sample/fraction ID (a)	Th/U (b)	$^{206}Pb^*$ x10^{-13} mol (c)	mol% $^{206}Pb^*$ (c)	Pb*/Pb$_c$ (c)	Pb$_c$ (pg) (c)	^{206}Pb/^{204}Pb (d)	^{208}Pb/^{206}Pb (e)	^{207}Pb/^{206}Pb (e)	% err (f)	^{207}Pb/^{235}U (g)	% err (f)	^{206}Pb/^{238}U (g)	% err (f)	corr. coef.	^{207}Pb/^{206}Pb (h)	± (f)	^{207}Pb/^{235}U (h)	± (f)	^{206}Pb/^{238}U (h)	± (h)
	AMASE	0.59	0.5567	96.7%	9	1.58	546	0.190	0.04804	1.8	0.100533	1.9	0.015177	0.17	0.74	99	42	97.3	1.8	97.2	0.2
Faroe Island Basalt Group	FSC16-100 z7	0.65	0.0198	82.5%	1.49	0.35	103	0.220	0.04962	11.6	0.060245	12.3	0.008805	1.1	0.66	174	271	59.4	7.1	**56.60**	**0.59**
	FSC16-100 z6	0.57	0.0110	53.2%	0.35	0.80	39	0.201	0.05242	68.8	0.063903	70.6	0.008841	3.36	0.55	300	1568	62.9	43.1	**56.83**	**1.90**
	FSC16-100 z1	0.77	0.0213	81.1%	1.39	0.41	96	0.253	0.04830	13.6	0.059164	14.3	0.008884	1.08	0.68	111	321	58.4	8.1	**57.10**	**0.61**
	FSC16-100 z4	0.48	0.6594	99.2%	38.94	0.42	2374	0.152	0.05103	0.4	0.262031	0.5	0.037242	0.16	0.59	241	9	236.3	1.0	235.80	0.38
	FSC16-100 z3	0.49	0.2562	80.2%	1.25	5.21	93	0.145	0.08507	5.8	2.762807	6.6	0.235556	1.69	0.57	1317	113	1345.6	49.5	1363.63	20.81
	FSC16-4930 z6	0.57	0.0644	63.2%	0.5	3.12	49	0.190	0.04868	29.5	0.058274	31.4	0.008682	2.02	0.93	129	694	57.5	17.5	**55.81**	**1.12**
	FSC16-4930 z2	0.59	0.0427	77.7%	1.1	1.02	81	0.192	0.04805	15.0	0.057788	16.0	0.008722	1.06	0.89	98	356	57.0	8.9	**56.07**	**0.59**
	FSC16-4930 z4	1.12	0.0636	91.9%	4.0	0.47	223	0.361	0.04755	4.7	0.057365	5.0	0.008750	0.40	0.76	74	111	56.6	2.7	**56.23**	**0.23**
	FSC16-4930 z5	0.67	0.0636	93.7%	4.7	0.35	288	0.218	0.04748	3.5	0.057405	3.8	0.008770	0.35	0.70	70	84	56.7	2.1	**56.37**	**0.19**
	FSC16-4930 z11	0.58	0.0473	92.5%	3.8	0.32	241	0.189	0.04785	4.5	0.057850	4.8	0.008769	0.47	0.64	88	106	57.1	2.6	**56.37**	**0.26**
	FSC16-4930 z7	1.06	0.0618	95.7%	7.7	0.23	421	0.346	0.04789	2.4	0.057997	2.5	0.008783	0.30	0.60	91	56	57.2	1.4	**56.44**	**0.17**
	FSC16-4930 z1	0.64	0.0292	90.9%	3.1	0.24	199	0.211	0.04828	5.2	0.058514	5.6	0.008790	0.62	0.60	110	123	57.7	3.1	**56.50**	**0.35**
	FSC16-4930 z3	0.63	0.0736	90.7%	3.0	0.63	195	0.207	0.04810	6.3	0.058305	6.7	0.008792	0.53	0.73	100	148	57.5	3.7	**56.51**	**0.30**
Offshore cores	SSK76330 z6m	0.35	0.0769	96.7%	8	0.22	545	0.112	0.04753	1.9	0.062423	2.0	0.009525	0.26	0.56	72	44	61.5	1.2	61.2	0.2
	SSK76525 z3m	0.12	0.0406	91.0%	3	0.33	202	0.037	0.04755	5.4	0.059957	5.8	0.009144	0.54	0.67	73	129	59.1	3.3	58.8	0.3
	SSK76523 z8m	0.37	0.0974	98.3%	17	0.14	1090	0.120	0.04750	1.0	0.054306	1.1	0.008292	0.20	0.48	70	24	53.7	0.6	53.3	0.1
	SSK76527 z4m	0.71	0.0107	72.9%	1	0.33	67	0.216	0.04474	41.1	0.056119	41.8	0.009097	1.98	0.38	-73	1003	55.4	22.5	**58.5**	**1.1**
	SSK76527 z2Am	0.51	0.0997	94.9%	6	0.44	357	0.164	0.04726	2.9	0.059426	3.1	0.009120	0.27	0.72	59	69	58.62	1.75	**58.6**	**0.2**
	SSK76527 z2Bm	0.46	0.1398	97.6%	12	0.29	750	0.146	0.04728	1.3	0.059546	1.4	0.009133	0.17	0.61	60	32	58.73	0.82	**58.7**	**0.1**
	SSK76527 z1m	0.74	0.8404	99.7%	95	0.23	5417	0.236	0.04733	0.2	0.059695	0.3	0.009148	0.10	0.64	63	6	58.87	0.17	**58.8**	**0.1**
	SSK76532 z10m	0.69	0.1407	83.2%	2	2.35	108	0.227	0.04827	10.3	0.066340	10.9	0.009968	0.71	0.92	109	242	65.2	6.9	64.0	0.5
	SSK76532 z8m	0.64	0.1266	97.6%	13	0.25	766	0.203	0.04773	1.4	0.098007	1.5	0.014891	0.25	0.50	84	34	94.9	1.4	95.4	0.2
	SSK76537 z2m	3.14	0.0065	61.6%	1	0.33	47	0.351	0.01618	251.2	0.019263	252.1	0.008634	3.19	0.29	-3704	14457	19.4	48.4	**55.5**	**1.8**
	SSK76537 z6am	1.10	0.0219	89.1%	3	0.22	167	0.350	0.04698	7.2	0.058022	7.6	0.008957	0.85	0.56	45	172	57.3	4.2	**57.6**	**0.5**

Group	Sample/fraction ID	Th/U	206Pb* x10⁻¹³ mol	mol% 206Pb*	Pb*/Pbc	Pbc (pg)	206Pb/204Pb	208Pb/206Pb	207Pb/206Pb	% err	207Pb/235U	% err	206Pb/238U	% err	corr. coef.	207Pb/206Pb	±	207Pb/235U	±	206Pb/238U	±
	(a)	(b)	(c)	(c)	(c)	(c)	(d)	(e)	(e)	(f)	(g)	(f)	(g)	(f)		(h)	(f)	(h)	(f)	(h)	(h)
	SSK76537 z16m	1.22	0.0555	92.9%	4.7	0.35	255	0.396	0.04782	4.2	0.059074	4.5	0.008960	0.42	0.67	88	100	58.3	2.5	**57.6**	**0.2**
	SSK76537 z6m	1.19	0.0256	77.8%	1	0.61	82	0.403	0.04985	15.2	0.063803	16.1	0.009283	1.19	0.77	185	353	62.8	9.8	59.6	0.7
	SSK76537 z3m	1.18	0.0262	84.6%	2	0.40	117	0.379	0.04725	10.0	0.061882	10.6	0.009498	0.89	0.70	59	238	61.0	6.3	61.0	0.5
	SVÍNOY3126 z14m	1.22	0.0258	48.4%	0.3	2.28	35	0.406	0.04901	56.8	0.059826	60.1	0.008853	3.73	0.88	146	1332	59.0	34.4	**56.9**	**2.1**
	SVÍNOY3126 z9m	1.36	0.0135	82.9%	1.8	0.23	106	0.420	0.04537	15.8	0.056083	16.4	0.008965	1.37	0.47	-38	384	55.4	8.9	**57.6**	**0.8**
	SVÍNOY3126 z5m	1.20	0.0250	93.7%	5.3	0.14	285	0.382	0.04704	5.1	0.058268	5.4	0.008985	0.73	0.43	48	123	57.5	3.0	**57.7**	**0.4**
	SVÍNOY3126 zXm	1.30	0.0333	95.9%	9	0.12	443	0.424	0.04788	2.4	0.059400	2.6	0.008998	0.50	0.47	91	57	58.6	1.5	**57.8**	**0.3**
Skye Lava Group	SG16-00 z4	1.07	0.2294	98.7%	25.9	0.25	1376	0.343	0.04726	0.8	0.057811	0.9	0.008871	0.16	0.49	60	19	57.1	0.5	**57.00**	**0.09**
	SG16-00 z2	1.43	0.9926	99.4%	65.5	0.47	3178	0.459	0.04724	0.3	0.057910	0.4	0.008890	0.10	0.63	59	8	57.16	0.21	**57.11**	**0.05**
	SG16-00 z1	1.52	1.2543	99.7%	113.4	0.35	5383	0.489	0.04724	0.2	0.057912	0.3	0.008891	0.09	0.72	59	5	57.16	0.15	**57.12**	**0.05**
	FSC-16-26 z5	1.430	0.2258	97.13%	13	0.55	630	0.456	0.046960	1.808	0.057429	1.925	0.008869	0.227	0.559	44.83	43.19	56.70	1.06	**56.98**	**0.13**
	FSC-16-26 z5	1.408	0.1546	97.75%	16	0.30	804	0.455	0.047535	1.278	0.058154	1.372	0.008873	0.166	0.609	73.80	30.36	57.40	0.77	**57.00**	**0.09**
	Hugh-1 z1	2.37	1.2075	94.0%	7.1	6.34	307	0.761	0.04730	1.6	0.059802	1.7	0.009169	0.19	0.66	63	38	59.0	1.0	**58.87**	**0.11**
	Hugh-1 z2	1.17	0.4911	90.6%	3.4	4.21	194	0.377	0.04754	4.2	0.060151	4.4	0.009176	0.29	0.95	74	99	59.3	2.6	**58.95**	**0.17**
	Hugh-1 z3	1.40	1.3581	97.3%	13.5	3.11	674	0.449	0.04725	1.4	0.059875	1.5	0.009190	0.15	0.71	60	33	59.0	0.9	**59.03**	**0.09**
	LB1 z2	0.64	0.2165	98.7%	23.0	0.24	1356	0.203	0.04691	0.8	0.059209	0.8	0.009154	0.13	0.57	41	18	58.4	0.5	**58.83**	**0.08**
	LB1 z9	0.62	0.3002	97.9%	14.7	0.52	877	0.199	0.04719	1.2	0.059660	1.3	0.009170	0.14	0.67	55	28	58.8	0.7	**58.93**	**0.08**
	LB1 z4	0.57	0.1616	98.3%	18.1	0.23	1088	0.183	0.04728	1.0	0.059814	1.1	0.009176	0.17	0.51	60	23	59.0	0.6	**58.97**	**0.10**
Mull Lava Group and Mull Central Complex	LB1 z8	0.61	0.4139	98.5%	20.6	0.51	1225	0.197	0.04739	0.8	0.059964	0.9	0.009177	0.12	0.61	65	19	59.1	0.5	**58.97**	**0.07**
	LB1 z7	0.59	0.1714	95.3%	6.2	0.70	384	0.190	0.04758	2.6	0.060210	2.8	0.009179	0.22	0.79	75	62	59.4	1.6	**58.99**	**0.13**
	LB1 z6	0.64	0.5013	97.3%	11.2	1.16	666	0.207	0.04757	1.5	0.060223	1.6	0.009182	0.19	0.60	74	36	59.4	0.9	**59.01**	**0.11**
	LB1 z1	0.62	0.7542	97.7%	13.0	1.49	778	0.197	0.04709	1.4	0.059754	1.5	0.009202	0.21	0.54	50	34	58.9	0.9	59.14	0.12
	LB1 z5	0.59	0.2400	97.6%	12.3	0.50	744	0.189	0.04737	1.3	0.060131	1.4	0.009207	0.15	0.69	64	31	59.3	0.8	59.17	0.09
	LB1 z3	0.60	0.2375	98.2%	16.4	0.37	983	0.191	0.04678	1.1	0.059441	1.1	0.009215	0.13	0.66	35	25	58.6	0.6	59.22	0.08
	FSC15-2 z2	0.96	0.1017	97.1%	11.3	0.25	621	0.310	0.04750	1.6	0.062845	1.7	0.009596	0.21	0.59	71	38	61.9	1.0	**61.64**	**0.13**
	FSC15-2 z4	0.94	0.0221	77.0%	1.1	0.55	79	0.321	0.05035	15.7	0.067000	16.6	0.009652	1.28	0.75	208	364	65.8	10.6	**61.99**	**0.79**
	FSC15-6 z1	0.91	0.1117	96.1%	8.3	0.37	468	0.293	0.04727	2.2	0.062446	2.4	0.009582	0.25	0.61	60	53	61.5	1.4	**61.55**	**0.15**
	FSC15-6 z2	0.18	2.0858	99.7%	111.8	0.46	6862	0.073	0.11704	0.1	2.888126	0.2	0.178975	0.18	0.89	1911	2	1378.8	1.8	1061.5	1.7

		Compositional Parameters						Radiogenic Isotope Ratios								Isotopic Ages					
	Sample/fraction ID	Th/U	$^{206}Pb^*$ x10^{-13} mol	mol% $^{206}Pb^*$	Pb*/Pbc	Pbc (pg)	$^{206}Pb/^{204}Pb$	$^{208}Pb/^{206}Pb$	$^{207}Pb/^{206}Pb$	% err	$^{207}Pb/^{235}U$	% err	$^{206}Pb/^{238}U$	% err	corr. coef.	$^{207}Pb/^{206}Pb$	±	$^{207}Pb/^{235}U$	±	$^{206}Pb/^{238}U$	±
	(a)	(b)	(c)	(c)	(c)	(c)	(d)	(e)	(e)	(f)	(g)	(f)	(g)	(f)		(h)	(f)	(h)	(f)	(h)	(h)
	FSC15-7 z6	1.40	0.0842	86.4%	2.4	1.10	133	0.444	0.04655	8.6	0.060397	9.1	0.009410	0.59	0.89	24	206	59.5	5.3	60.43	0.36
	FSC15-7 z5	1.86	0.0418	90.2%	3.7	0.38	184	0.583	0.04610	6.3	0.060344	6.6	0.009495	0.57	0.66	1	151	59.5	3.8	**60.96**	**0.34**
	FSC15-7 z2	1.70	0.1772	92.7%	5.0	1.16	248	0.543	0.04717	4.1	0.061830	4.4	0.009507	0.31	0.87	56	99	60.9	2.6	**61.05**	**0.19**
	FSC15-7 z4	2.35	0.0795	93.9%	6.9	0.43	295	0.761	0.04772	3.5	0.062600	3.7	0.009514	0.32	0.73	85	83	61.7	2.2	**61.07**	**0.20**
	FSC15-7 z9	1.45	0.0671	86.3%	2.4	0.88	132	0.463	0.04730	8.4	0.062017	8.9	0.009510	0.61	0.86	62	200	61.1	5.3	**61.07**	**0.37**
	FSC15-7 z7	1.77	0.1473	95.4%	8.3	0.60	390	0.569	0.04742	2.6	0.062285	2.8	0.009527	0.23	0.76	69	62	61.4	1.6	**61.17**	**0.14**
	FSC16-11 z4	0.92	0.0270	89.1%	2.7	0.27	166	0.294	0.04715	6.8	0.062409	7.2	0.009599	0.75	0.61	54	162	61.5	4.3	**61.66**	**0.46**
	FSC16-11 z5	1.16	0.0486	89.7%	3.1	0.46	175	0.385	0.04888	6.0	0.064730	6.4	0.009605	0.54	0.74	140	140	63.7	3.9	**61.68**	**0.33**
	FSC16-11 z2	0.92	0.0537	90.8%	3.3	0.45	196	0.299	0.04808	5.3	0.063685	5.6	0.009606	0.47	0.75	100	124	62.7	3.4	**61.71**	**0.29**
	FSC16-11 z1	0.97	0.0683	94.3%	5.6	0.34	319	0.313	0.04748	3.2	0.062959	3.4	0.009617	0.33	0.67	71	77	62.0	2.1	**61.77**	**0.20**
	FSC16-11 z3	1.10	0.0229	87.8%	2.5	0.26	149	0.352	0.04721	7.6	0.062638	8.1	0.009623	0.87	0.59	57	181	61.7	4.8	**61.81**	**0.53**
Small Isles Volcanics	EP1-98 z3	1.36	0.0232	85.0%	2.1	0.34	120	0.438	0.04752	10.5	0.061280	11.1	0.009352	0.9	0.64	73	250	60.4	6.5	**60.07**	**0.56**
	EP1-98 z4	1.33	0.0185	79.3%	1.4	0.40	88	0.437	0.04854	15.6	0.062604	16.4	0.009355	1.27	0.65	123	367	61.7	9.8	**60.08**	**0.76**
	EP1-98 z2	0.99	0.0095	62.9%	0.6	0.47	49	0.329	0.04886	56.7	0.063166	57.8	0.009376	2.64	0.43	138	1331	62.2	34.9	**60.23**	**1.58**
	EP1-98 z5	1.02	0.0315	73.5%	0.9	0.94	68	0.323	0.04683	20.8	0.060556	21.9	0.009377	1.4	0.82	38	498	59.7	12.7	**60.24**	**0.82**
	ET1-100 z1	1.077	0.1191	95.23%	7	0.49	380	0.345	0.047287	2.642	0.062424	2.819	0.009574	0.281	0.663	60.82	62.91	61.48	1.68	**61.50**	**0.17**
	ET1-100 z7	1.112	0.1003	97.06%	12	0.25	616	0.358	0.047432	1.703	0.062724	1.824	0.009591	0.232	0.565	68.43	40.51	61.77	1.09	**61.60**	**0.14**
	ET1-100 z9	0.985	0.3523	98.28%	19	0.51	1054	0.317	0.047475	0.979	0.062778	1.058	0.009590	0.133	0.631	70.41	23.29	61.82	0.63	**61.60**	**0.08**
	ET1-100 z6	1.037	0.1077	95.64%	8	0.41	416	0.339	0.048212	3.516	0.063783	3.734	0.009595	0.296	0.756	107.01	83.01	62.78	2.27	**61.63**	**0.18**
	ET1-100 z3	1.495	0.2183	95.07%	7	0.94	367	0.483	0.047678	2.729	0.063237	2.911	0.009620	0.266	0.707	81.23	64.76	62.26	1.76	**61.77**	**0.16**
	MT2 z1	1.07	0.3978	90.9%	3.5	3.31	199	0.344	0.04740	4.8	0.062570	5.1	0.009573	0.34	0.89	67	114	61.6	3.0	**61.50**	**0.21**
	MT2 z5	1.39	0.2456	97.2%	13.1	0.58	656	0.450	0.04787	1.5	0.063286	1.6	0.009589	0.16	0.70	90	36	62.3	1.0	**61.58**	**0.10**
	MT2 z3	0.98	0.1293	89.5%	2.9	1.26	172	0.322	0.04850	6.0	0.064175	6.4	0.009597	0.44	0.88	121	142	63.2	3.9	**61.65**	**0.27**
	MT2 z2	1.25	0.2162	96.6%	10.4	0.63	538	0.408	0.04811	1.8	0.063791	1.9	0.009616	0.18	0.74	102	43	62.8	1.2	**61.76**	**0.11**
	MT2 z4	1.11	0.4512	98.2%	18.9	0.70	992	0.365	0.04891	1.0	0.067907	1.0	0.010070	0.13	0.65	141	23	66.7	0.7	64.66	0.08
Northern Ireland	Tardree z6	0.45	1.1272	99.4%	49.5	0.56	3038	0.146	0.04755	0.4	0.062042	0.4	0.009463	0.11	0.51	73	9	61.1	0.3	**60.81**	**0.07**
	Tardree z1	0.31	4.8860	99.6%	78.9	1.46	5031	0.099	0.04742	0.2	0.061949	0.3	0.009475	0.09	0.74	66	5	61.0	0.2	**60.89**	**0.05**
	Tardree z7	0.66	1.0831	99.4%	53.0	0.53	3077	0.213	0.04750	0.3	0.062144	0.4	0.009488	0.10	0.62	71	8	61.2	0.2	**60.96**	**0.06**

Sample/fraction ID	Th U	$^{206}Pb^*$ x10^{-13} mol	mol% $^{206}Pb^*$	Pb* Pb$_c$	Pb$_c$ (pg)	^{206}Pb ^{204}Pb	^{208}Pb ^{206}Pb	^{207}Pb ^{206}Pb	% err	^{207}Pb ^{235}U	% err	^{206}Pb ^{238}U	% err	corr. coef.	^{207}Pb ^{206}Pb	±	^{207}Pb ^{235}U	±	^{206}Pb ^{238}U	±
(a)	(b)	(c)	(c)	(c)	(c)	(d)	(e)	(e)	(f)	(g)	(f)	(g)	(f)		(h)	(f)	(h)	(f)	(h)	(h)
Tardree z8	0.35	1.2427	99.7%	91.0	0.33	5731	0.112	0.04744	0.2	0.062185	0.3	0.009507	0.09	0.75	68	5	61.3	0.2	61.09	0.05
Tardree z3	0.55	0.6295	97.8%	13.3	1.19	810	0.178	0.04746	1.2	0.062266	1.3	0.009516	0.13	0.70	69	29	61.3	0.8	61.14	0.08
Tardree z4	0.71	0.1937	97.1%	10.7	0.47	631	0.226	0.04729	1.6	0.062087	1.7	0.009521	0.19	0.64	61	38	61.2	1.0	61.17	0.11
Tardree z5	0.62	0.5582	97.2%	10.9	1.32	652	0.198	0.04738	1.5	0.062428	1.6	0.009556	0.14	0.75	65	36	61.5	1.0	61.39	0.09
Tardree z2	0.43	0.6564	97.6%	11.9	1.35	748	0.137	0.04750	1.3	0.062607	1.4	0.009560	0.13	0.75	71	31	61.7	0.8	61.43	0.08
CWF z2	1.45	0.5130	97.2%	13.1	1.22	649	0.464	0.04737	1.5	0.062545	1.6	0.009576	0.14	0.75	66	36	61.6	1.0	**61.49**	**0.09**
CWF z6	1.45	0.7849	99.1%	39.7	0.62	1926	0.466	0.04739	0.5	0.062598	0.6	0.009581	0.10	0.61	67	12	61.7	0.3	**61.52**	**0.06**
CWF z4	1.46	0.5771	99.3%	53.6	0.34	2586	0.469	0.04746	0.4	0.062785	0.4	0.009594	0.09	0.62	71	9	61.8	0.3	**61.61**	**0.06**
CWF z5	1.35	0.2234	96.2%	9.5	0.72	482	0.435	0.04763	2.1	0.063011	2.2	0.009595	0.19	0.75	79	49	62.0	1.3	**61.62**	**0.12**
CWF z1	0.93	0.1686	91.8%	3.7	1.26	220	0.302	0.04770	4.7	0.063095	5.0	0.009593	0.35	0.86	82	112	62.1	3.0	**61.62**	**0.22**
CWF z3	0.92	0.0757	93.6%	4.9	0.43	282	0.298	0.04776	3.7	0.063294	3.9	0.009612	0.34	0.73	84	87	62.3	2.4	**61.74**	**0.21**

(a) z1, z2 etc. are labels for fractions composed of single zircon grains or fragments; all fractions annealed and chemically abraded after Mattinson (2005).

(d) Model Th/U ratio calculated from radiogenic 208Pb/206Pb ratio and 207Pb/235U age.

(b) Pb* and Pbc represent radiogenic and common Pb, respectively; mol % $^{206}Pb^*$ with respect to radiogenic, blank and initial common Pb.

(c) Measured ratio corrected for spike and fractionation only. Pb mass bias based on analysis of NBS-981 and 202Pb-205Pb age solutions

(e) Corrected for fractionation, spike, and common Pb; up to 1 pg of common Pb was assumed to be procedural blank: 206Pb/204Pb = 18.62 ± 0.80%; 207Pb/204Pb = 15.63 ± 0.32%;
    208Pb/204Pb = 38.54 ± 0.74% (all uncertainties 1-sigma). Excess over blank was assigned to initial common Pb.

(f) Errors are 2-sigma, propagated using the algorithms of Schmitz and Schoene (2007) and Crowley et al. (2007).

(g) Calculations are based on the decay constants of Jaffey et al. (1971). 206Pb/238U and 207Pb/206Pb ages corrected for initial disequilibrium in 230Th/238U using Th/U [magma] = 3.5.

10.4   APPENDIX 4 – LA-ICMPS ANALYTICAL DATA

		Tera-Wasserberg plot			Normal - Wetherill plot					Ages						Discordance	Preferred Ages		
Grain	$^{238}U/^{206}Pb$	± 1σ %	$^{207}Pb/^{206}Pb$	± 1σ %	$^{207}Pb/^{235}U$	± 1σ %	$^{206}Pb/^{238}U$	± 1σ %	ρ	$^{207}Pb/^{206}Pb$	± 2σ	$^{206}Pb/^{238}U$	± 2σ	$^{207}Pb/^{235}U$	± 2σ	6-38/7-35	Age	± 2σ	Notes
FSC-15-02 Ardtun leaf bed																			
14.1	86.01	2.47	0.19689	5.68	0.315	6.2	0.0116	2.5	0.40	2801	93	75	4	278	30	73.2	75	4	1
14.2	96.42	2.21	0.07760	3.04	0.111	3.8	0.0104	2.2	0.59	1137	61	67	3	107	8	37.7	67	3	1
16	104.36	1.10	0.04412	2.35	0.058	2.6	0.0096	1.1	0.42	-104	58	61	1	58	3	-6.9	61	1	1
23	105.24	0.74	0.04788	4.26	0.063	4.3	0.0095	0.7	0.17	93	101	61	1	62	5	1.3	61	1	1
34	103.37	0.95	0.04752	1.96	0.063	2.2	0.0097	0.9	0.44	76	47	62	1	62	3	0.5	62	1	1
3	5.11	0.83	0.07845	0.52	2.116	1.0	0.1957	0.8	0.85	1158	10	1152	18	1154	13	0.2	1152	18	2
4	5.04	0.96	0.07894	0.54	2.159	1.1	0.1984	1.0	0.87	1171	11	1167	21	1168	15	0.1	1167	21	2
7	15.65	1.11	0.05361	0.60	0.472	1.3	0.0639	1.1	0.88	355	14	399	9	393	8	-1.7	399	9	2
9	22.49	0.90	0.04975	0.74	0.305	1.2	0.0445	0.9	0.77	183	17	280	5	270	6	-3.8	280	5	2
12	5.24	1.05	0.07606	0.52	2.000	1.2	0.1908	1.1	0.90	1097	10	1126	22	1116	16	-0.9	1126	22	2
17	14.89	0.66	0.05548	0.54	0.513	0.8	0.0671	0.7	0.77	431	12	419	5	421	6	0.4	419	5	2
25	6.01	0.75	0.07277	0.57	1.668	0.9	0.1664	0.7	0.80	1008	11	992	14	997	12	0.5	992	14	2
29	5.61	1.18	0.07526	0.55	1.848	1.3	0.1782	1.2	0.91	1075	11	1057	23	1063	17	0.5	1057	23	2
37	5.31	1.52	0.08279	0.79	2.150	1.7	0.1884	1.5	0.89	1264	15	1113	31	1165	24	4.5	1113	31	2
1	3.20	0.89	0.10848	0.52	4.677	1.0	0.3129	0.9	0.86	1774	9	1755	27	1763	17	0.5	1774	9	3
2	4.41	0.80	0.08580	0.51	2.679	1.0	0.2265	0.8	0.84	1334	10	1316	19	1323	14	0.5	1334	10	3
5	3.15	0.78	0.10782	0.51	4.718	0.9	0.3175	0.8	0.84	1763	9	1778	24	1770	16	-0.4	1763	9	3
6	3.42	0.78	0.10265	0.52	4.140	0.9	0.2926	0.8	0.84	1673	10	1655	23	1662	15	0.5	1673	10	3
8	3.13	0.96	0.10915	0.54	4.799	1.1	0.3190	1.0	0.87	1785	10	1785	30	1785	18	0.0	1785	10	3
10	2.07	1.63	0.19737	0.53	13.114	1.7	0.4821	1.6	0.95	2805	9	2537	68	2688	32	5.6	2805	9	3
11	3.19	1.07	0.11093	0.52	4.799	1.2	0.3139	1.1	0.90	1815	9	1760	33	1785	20	1.4	1815	9	3
13	1.91	0.84	0.19045	0.52	13.758	1.0	0.5242	0.8	0.85	2746	9	2717	37	2733	19	0.6	2746	9	3
15	3.47	0.90	0.10174	0.52	4.041	1.0	0.2882	0.9	0.87	1656	10	1632	26	1642	17	0.6	1656	10	3
18	2.48	2.85	0.15397	2.23	8.542	3.6	0.4025	2.9	0.79	2391	38	2181	105	2290	64	4.8	2391	38	3
19	3.10	0.92	0.11082	0.51	4.926	1.1	0.3225	0.9	0.87	1813	9	1802	29	1807	18	0.3	1813	9	3

		Tera-Wasserberg plot			Normal - Wetherill plot					Ages						Discordance	Preferred Ages		
Grain	$^{238}U/^{206}Pb$	$\pm 1\sigma$ %	$^{207}Pb/^{206}Pb$	$\pm 1\sigma$ %	$^{207}Pb/^{235}U$	$\pm 1\sigma$ %	$^{206}Pb/^{238}U$	$\pm 1\sigma$ %	ρ	$^{207}Pb/^{206}Pb$	$\pm 2\sigma$	$^{206}Pb/^{238}U$	$\pm 2\sigma$	$^{207}Pb/^{235}U$	$\pm 2\sigma$	6-38/7-35	Age	$\pm 2\sigma$	Notes
20.1	3.24	0.99	0.11109	0.53	4.729	1.1	0.3089	1.0	0.88	1817	10	1735	30	1772	19	2.1	1817	10	3
20.2	3.66	2.59	0.11111	0.52	4.179	2.6	0.2729	2.6	0.98	1818	9	1555	71	1670	42	6.9	1818	9	3
21	3.12	0.87	0.11071	0.51	4.883	1.0	0.3200	0.9	0.86	1811	9	1790	27	1799	17	0.5	1811	9	3
22	2.09	1.76	0.21592	2.26	14.239	2.9	0.4785	1.8	0.61	2951	37	2521	73	2766	53	8.9	2951	37	3
24	1.93	1.38	0.18891	0.53	13.513	1.5	0.5190	1.4	0.93	2733	9	2695	61	2716	28	0.8	2733	9	3
26	2.07	0.87	0.17931	0.98	11.957	1.3	0.4839	0.9	0.66	2646	16	2544	36	2601	24	2.2	2646	16	3
27	3.21	1.20	0.10958	0.52	4.698	1.3	0.3111	1.2	0.92	1792	9	1746	37	1767	22	1.2	1792	9	3
28	3.21	1.35	0.10821	0.52	4.639	1.5	0.3111	1.4	0.93	1770	10	1746	41	1756	24	0.6	1770	10	3
30	3.19	1.01	0.10958	0.52	4.727	1.1	0.3130	1.0	0.89	1792	9	1755	31	1772	19	0.9	1792	9	3
31	2.04	1.51	0.18310	0.51	12.344	1.6	0.4892	1.5	0.95	2681	9	2567	63	2631	29	2.4	2681	9	3
32	4.36	1.00	0.08888	0.54	2.808	1.1	0.2293	1.0	0.88	1402	10	1331	24	1358	17	2.0	1402	10	3
33	3.12	1.01	0.11019	0.53	4.874	1.1	0.3209	1.0	0.89	1803	10	1794	32	1798	19	0.2	1803	10	3
35	3.42	0.98	0.10141	0.67	4.085	1.2	0.2922	1.0	0.83	1650	12	1653	29	1651	19	-0.1	1650	12	3
36	3.72	0.64	0.09426	0.53	3.490	0.8	0.2687	0.6	0.77	1513	10	1534	17	1525	13	-0.6	1513	10	3
39	1.83	0.96	0.19467	0.51	14.645	1.1	0.5459	1.0	0.88	2782	8	2808	44	2792	21	-0.6	2782	8	3
40	3.23	1.30	0.10589	0.62	4.519	1.4	0.3097	1.3	0.90	1730	11	1739	39	1735	24	-0.3	1730	11	3
41	3.20	1.13	0.10569	0.54	4.555	1.3	0.3128	1.1	0.90	1726	10	1754	35	1741	21	-0.8	1726	10	3
43	3.39	0.94	0.10137	0.53	4.124	1.1	0.2952	0.9	0.87	1649	10	1667	28	1659	18	-0.5	1649	10	3

FSC-15-06 Sand above Ardtun leaf bed

8.1	102.79	0.94	0.03228	4.45	0.043	4.6	0.0097	0.9	0.21	-939	130	62	1	43	4	-45.1	62	1	1
8.2	100.29	0.94	0.04777	0.53	0.066	1.1	0.0100	0.9	0.87	88	13	64	1	65	1	0.9	64	1	1
8.3	98.16	1.22	0.06374	2.70	0.089	3.0	0.0102	1.2	0.41	733	57	65	2	87	5	24.9	65	2	1
33	106.41	0.53	0.04901	1.41	0.063	1.5	0.0094	0.5	0.35	148	33	60	1	62	2	3.5	60	1	1
36	107.97	0.62	0.04883	2.45	0.062	2.5	0.0093	0.6	0.24	140	58	59	1	61	3	3.2	59	1	1
72.1	101.94	0.87	0.04370	4.20	0.059	4.3	0.0098	0.9	0.20	-128	104	63	1	58	5	-8.0	63	1	1
72.2	100.83	1.15	0.04793	0.65	0.066	1.3	0.0099	1.1	0.87	96	15	64	1	64	2	1.3	64	1	1

			Tera-Wasserberg plot			Normal - Wetherill plot					Ages						Discordance	Preferred Ages		
Grain	^{238}U/^{206}Pb	±1σ %	^{207}Pb/^{206}Pb	±1σ %	^{207}Pb/^{235}U	±1σ %	^{206}Pb/^{238}U	±1σ %	ρ	^{207}Pb/^{206}Pb	±2σ	^{206}Pb/^{238}U	±2σ	^{207}Pb/^{235}U	±2σ	6-38/7-35	Age	±2σ	Notes
72.3	98.36	0.88	0.05029	1.01	0.070	1.3	0.0102	0.9	0.66	208	23	65	1	69	2	5.7	65	1	1
6	21.78	0.84	0.05112	0.80	0.323	1.2	0.0459	0.8	0.72	246	19	289	5	285	6	-1.7	289	5	2
9	26.12	0.79	0.04740	1.30	0.250	1.5	0.0383	0.8	0.52	69	31	242	4	227	6	-6.9	242	4	2
11	21.83	0.62	0.05143	0.41	0.325	0.7	0.0458	0.6	0.83	260	9	289	4	285	4	-1.1	289	4	2
12	5.59	1.05	0.07358	0.73	1.814	1.3	0.1789	1.0	0.82	1030	15	1061	20	1051	17	-1.0	1061	20	2
13	22.26	0.93	0.05080	0.82	0.315	1.2	0.0449	0.9	0.75	232	19	283	5	278	6	-2.0	283	5	2
18.1	22.76	0.57	0.05125	0.54	0.310	0.8	0.0439	0.6	0.72	252	12	277	3	274	4	-1.0	277	3	2
18.2	22.51	0.62	0.04954	0.76	0.303	1.0	0.0444	0.6	0.64	173	18	280	3	269	5	-4.2	280	3	2
20	23.22	0.71	0.05045	0.35	0.299	0.8	0.0431	0.7	0.90	216	8	272	4	266	4	-2.2	272	4	2
21	4.98	0.88	0.07816	0.72	2.163	1.1	0.2008	0.9	0.78	1151	14	1180	19	1169	16	-0.9	1180	19	2
24	20.35	0.66	0.05216	0.80	0.353	1.0	0.0491	0.7	0.63	292	18	309	4	307	5	-0.7	309	4	2
25	5.65	0.76	0.07409	0.72	1.806	1.0	0.1768	0.8	0.73	1044	15	1050	15	1048	14	-0.2	1050	15	2
26	5.35	0.78	0.07455	0.73	1.921	1.1	0.1870	0.8	0.73	1056	15	1105	16	1088	14	-1.5	1105	16	2
28	14.27	0.77	0.05504	0.73	0.532	1.1	0.0701	0.8	0.72	414	16	437	7	433	7	-0.9	437	7	2
28	23.49	0.54	0.05175	0.41	0.304	0.7	0.0426	0.5	0.80	274	9	269	3	269	3	0.2	269	3	2
29	22.83	0.74	0.05266	0.35	0.318	0.8	0.0438	0.7	0.90	314	8	276	4	280	4	1.4	276	4	2
38	5.91	0.68	0.07272	0.32	1.697	0.8	0.1693	0.7	0.90	1006	7	1008	13	1007	10	-0.1	1008	13	2
40	5.45	0.86	0.07641	0.28	1.933	0.9	0.1836	0.9	0.95	1106	6	1086	17	1093	12	0.6	1086	17	2
48	20.68	1.17	0.05247	0.56	0.350	1.3	0.0484	1.2	0.90	306	13	304	7	305	7	0.0	304	7	2
59	5.60	0.94	0.07344	0.19	1.806	1.0	0.1785	0.9	0.98	1026	4	1059	18	1048	12	-1.0	1059	18	2
60	5.71	0.90	0.07323	0.44	1.766	1.0	0.1750	0.9	0.90	1020	9	1040	17	1033	13	-0.6	1040	17	2
64	14.53	0.86	0.05593	0.59	0.530	1.0	0.0688	0.9	0.83	449	13	429	7	432	7	0.7	429	7	2
74	22.48	1.38	0.05147	1.03	0.316	1.7	0.0445	1.4	0.80	262	24	281	8	279	8	-0.7	281	8	2
75	20.92	0.74	0.05362	1.00	0.353	1.2	0.0478	0.7	0.59	355	23	301	4	307	7	2.0	301	4	2
80	21.95	1.17	0.05253	0.67	0.330	1.3	0.0455	1.2	0.87	308	15	287	7	289	7	0.8	287	7	2
1	1.88	0.89	0.18801	0.24	13.747	0.9	0.5305	0.9	0.97	2725	4	2744	39	2732	17	-0.4	2725	4	3
2	3.10	0.58	0.10996	0.71	4.891	0.9	0.3227	0.6	0.63	1799	13	1803	18	1801	15	-0.1	1799	13	3
2	3.07	1.04	0.10966	0.22	4.923	1.1	0.3257	1.0	0.98	1794	4	1818	33	1806	18	-0.6	1794	4	3

Grain	Tera-Wasserberg plot				Normal - Wetherill plot					Ages						Discordance	Preferred Ages		
	$^{238}U/^{206}Pb$	±1σ %	$^{207}Pb/^{206}Pb$	±1σ %	$^{207}Pb/^{235}U$	±1σ %	$^{206}Pb/^{238}U$	±1σ %	ρ	$^{207}Pb/^{206}Pb$	±2σ	$^{206}Pb/^{238}U$	±2σ	$^{207}Pb/^{235}U$	±2σ	6-38/7-35	Age	±2σ	Notes
3	3.68	0.80	0.09675	0.78	3.623	1.1	0.2717	0.8	0.72	1562	15	1549	22	1555	18	0.3	1562	15	3
3	1.92	1.15	0.19030	0.32	13.679	1.2	0.5216	1.1	0.96	2745	5	2706	50	2728	22	0.8	2745	5	3
4	1.73	0.61	0.21239	0.70	16.961	0.9	0.5794	0.6	0.66	2924	11	2946	29	2933	18	-0.5	2924	11	3
6	1.80	1.17	0.19135	0.21	14.653	1.2	0.5556	1.2	0.98	2754	3	2849	54	2793	22	-2.0	2754	3	3
7	3.27	0.81	0.10325	0.71	4.358	1.1	0.3063	0.8	0.75	1683	13	1722	25	1704	18	-1.1	1683	13	3
7	3.03	1.16	0.10898	0.23	4.954	1.2	0.3298	1.2	0.98	1782	4	1838	37	1812	20	-1.4	1782	4	3
8	3.22	1.08	0.10303	0.26	4.410	1.1	0.3106	1.1	0.97	1679	5	1744	33	1714	18	-1.7	1679	5	3
9	1.67	0.99	0.21841	0.21	18.014	1.0	0.5985	1.0	0.98	2969	3	3024	48	2990	19	-1.1	2969	3	3
10	2.48	1.16	0.13055	0.71	7.262	1.4	0.4036	1.2	0.85	2105	12	2186	43	2144	24	-1.9	2105	12	3
10	2.50	0.87	0.13080	0.22	7.224	0.9	0.4008	0.9	0.97	2109	4	2173	32	2140	16	-1.5	2109	4	3
11	3.17	0.92	0.10514	0.73	4.569	1.2	0.3154	0.9	0.79	1717	13	1767	28	1744	19	-1.3	1717	13	3
12	2.67	0.57	0.12966	0.21	6.683	0.6	0.3740	0.6	0.94	2093	4	2048	20	2070	11	1.1	2093	4	3
13	2.82	0.65	0.12587	0.21	6.141	0.7	0.3540	0.7	0.95	2041	4	1954	22	1996	12	2.1	2041	4	3
14	2.98	0.80	0.11711	0.70	5.425	1.1	0.3361	0.8	0.75	1913	13	1868	26	1889	18	1.1	1913	13	3
15	2.90	0.75	0.11436	0.72	5.431	1.0	0.3446	0.8	0.72	1870	13	1909	25	1890	18	-1.0	1870	13	3
16	3.09	0.90	0.10941	0.71	4.874	1.1	0.3232	0.9	0.79	1790	13	1805	28	1798	19	-0.4	1790	13	3
17	3.07	0.92	0.10922	0.71	4.908	1.2	0.3261	0.9	0.79	1786	13	1819	29	1804	19	-0.9	1786	13	3
17	1.93	0.84	0.20443	0.21	14.595	0.9	0.5181	0.8	0.97	2862	3	2691	37	2789	16	3.5	2862	3	3
18	2.54	0.77	0.12985	0.73	7.049	1.1	0.3939	0.8	0.73	2096	13	2141	28	2118	19	-1.1	2096	13	3
19	3.03	1.10	0.10931	0.71	4.974	1.3	0.3302	1.1	0.84	1788	13	1839	35	1815	22	-1.3	1788	13	3
19	3.22	0.71	0.10951	0.22	4.684	0.7	0.3103	0.7	0.96	1791	4	1742	22	1764	12	1.2	1791	4	3
20	2.99	0.81	0.11064	0.72	5.099	1.1	0.3344	0.8	0.75	1810	13	1860	26	1836	18	-1.3	1810	13	3
21	3.13	0.72	0.11145	0.16	4.903	0.7	0.3192	0.7	0.98	1823	3	1786	23	1803	12	0.9	1823	3	3
22	1.80	0.93	0.20358	0.71	15.610	1.2	0.5564	0.9	0.79	2855	12	2852	43	2853	22	0.1	2855	12	3
22	1.97	0.64	0.18467	0.19	12.932	0.7	0.5081	0.6	0.96	2695	3	2649	28	2675	12	1.0	2695	3	3
23	3.36	1.12	0.11478	0.71	4.702	1.3	0.2973	1.1	0.85	1876	13	1678	33	1768	22	5.1	1876	13	3
23	2.63	0.56	0.12812	0.23	6.713	0.6	0.3802	0.6	0.93	2072	4	2077	20	2074	11	-0.1	2072	4	3
24	3.17	0.64	0.10837	0.24	4.716	0.7	0.3158	0.6	0.94	1772	4	1769	20	1770	11	0.1	1772	4	3

			Tera-Wasserberg plot				Normal - Wetherill plot					Ages					Discordance	Preferred Ages		
Grain	^{238}U/^{206}Pb	±1σ %	^{207}Pb/^{206}Pb	±1σ %	^{207}Pb/^{235}U	±1σ %	^{206}Pb/^{238}U	±1σ %	ρ	^{207}Pb/^{206}Pb	±2σ	^{206}Pb/^{238}U	±2σ	^{207}Pb/^{235}U	±2σ	6-38/7-35	Age	±2σ	Notes
25	3.15	0.76	0.11079	0.17	4.845	0.8	0.3173	0.8	0.98	1812	3	1776	23	1793	13	0.9	1812	3	3
26	2.60	0.53	0.13718	0.34	7.260	0.6	0.3840	0.5	0.84	2192	6	2095	19	2144	11	2.3	2192	6	3
27	2.54	1.03	0.12963	0.71	7.022	1.3	0.3931	1.0	0.82	2093	12	2137	37	2114	22	-1.1	2093	12	3
27	2.60	0.46	0.13441	0.51	7.121	0.7	0.3844	0.5	0.67	2156	9	2097	16	2127	12	1.4	2156	9	3
29	1.92	0.86	0.18441	0.70	13.265	1.1	0.5219	0.9	0.77	2693	12	2707	38	2699	21	-0.3	2693	12	3
30	2.40	0.50	0.15015	1.58	8.610	1.7	0.4161	0.5	0.30	2348	27	2243	19	2298	30	2.4	2348	27	3
30	2.72	0.48	0.12934	0.25	6.543	0.5	0.3671	0.5	0.89	2089	4	2016	17	2052	9	1.8	2089	4	3
31	1.93	0.71	0.18478	0.09	13.208	0.7	0.5187	0.7	0.99	2696	1	2693	31	2695	13	0.0	2696	1	3
31	1.86	0.57	0.20595	0.18	15.291	0.6	0.5388	0.6	0.95	2874	3	2778	25	2834	11	2.0	2874	3	3
32	3.22	0.64	0.10711	0.17	4.587	0.7	0.3107	0.6	0.97	1751	3	1744	20	1747	11	0.2	1751	3	3
32	3.61	0.50	0.10027	0.34	3.829	0.6	0.2771	0.5	0.83	1629	6	1577	14	1599	10	1.4	1629	6	3
33	1.92	0.77	0.18472	0.12	13.240	0.8	0.5201	0.8	0.99	2696	2	2699	34	2697	15	-0.1	2696	2	3
34	3.21	0.88	0.10970	0.18	4.706	0.9	0.3113	0.9	0.98	1794	3	1747	27	1768	15	1.2	1794	3	3
34	1.97	0.64	0.20743	0.19	14.516	0.7	0.5078	0.6	0.96	2886	3	2647	28	2784	13	4.9	2886	3	3
35	1.87	0.61	0.18828	0.13	13.857	0.6	0.5340	0.6	0.98	2727	2	2758	27	2740	12	-0.7	2727	2	3
35	1.96	0.42	0.20697	0.18	14.584	0.5	0.5113	0.4	0.92	2882	3	2662	18	2788	9	4.5	2882	3	3
36	3.07	0.58	0.10698	0.28	4.803	0.6	0.3258	0.6	0.90	1749	5	1818	18	1785	11	-1.8	1749	5	3
37	3.27	0.65	0.10941	0.15	4.609	0.7	0.3057	0.7	0.98	1790	3	1719	20	1751	11	1.8	1790	3	3
37	2.09	0.56	0.19774	0.19	13.040	0.6	0.4785	0.6	0.95	2808	3	2521	23	2683	11	6.0	2808	3	3
38	2.71	0.50	0.13141	0.18	6.680	0.5	0.3688	0.5	0.94	2117	3	2024	17	2070	9	2.2	2117	3	3
39	2.94	0.93	0.11628	0.08	5.445	0.9	0.3398	0.9	1.00	1900	1	1886	30	1892	16	0.3	1900	1	3
39	3.55	0.69	0.10511	0.18	4.079	0.7	0.2816	0.7	0.97	1716	3	1599	19	1650	12	3.1	1716	3	3
40	1.98	0.66	0.19225	0.21	13.403	0.7	0.5058	0.7	0.95	2762	3	2639	28	2708	13	2.6	2762	3	3
42	3.48	1.79	0.10549	0.13	4.179	1.8	0.2874	1.8	1.00	1723	2	1629	51	1670	29	2.5	1723	2	3
43	1.93	1.56	0.19079	0.20	13.608	1.6	0.5175	1.6	0.99	2749	3	2689	68	2723	29	1.3	2749	3	3
44	3.64	1.11	0.09625	0.26	3.644	1.1	0.2747	1.1	0.97	1553	5	1565	31	1559	18	-0.4	1553	5	3
45	1.87	1.16	0.19006	0.12	14.024	1.2	0.5354	1.2	0.99	2743	2	2764	52	2751	22	-0.5	2743	2	3
46	2.06	1.04	0.17726	0.09	11.857	1.0	0.4854	1.0	1.00	2627	2	2551	44	2593	19	1.6	2627	2	3

	Tera-Wasserberg plot				Normal - Wetherill plot					Ages						Discordance	Preferred Ages		
Grain	$^{238}U/^{206}Pb$	± 1σ %	$^{207}Pb/^{206}Pb$	± 1σ %	$^{207}Pb/^{235}U$	± 1σ %	$^{206}Pb/^{238}U$	± 1σ %	ρ	$^{207}Pb/^{206}Pb$	± 2σ	$^{206}Pb/^{238}U$	± 2σ	$^{207}Pb/^{235}U$	± 2σ	6-38/7-35	Age	± 2σ	Notes
47	2.11	1.28	0.20134	0.13	13.164	1.3	0.4744	1.3	0.99	2837	2	2503	53	2691	24	7.0	2837	2	3
49	1.93	0.91	0.18842	0.09	13.432	0.9	0.5173	0.9	1.00	2728	1	2688	40	2711	17	0.8	2728	1	3
50	1.67	1.29	0.22074	0.11	18.249	1.3	0.5999	1.3	1.00	2986	2	3029	62	3003	25	-0.9	2986	2	3
51	3.25	1.12	0.10846	0.15	4.599	1.1	0.3077	1.1	0.99	1774	3	1729	34	1749	19	1.1	1774	3	3
52	1.85	0.93	0.19326	0.05	14.432	0.9	0.5419	0.9	1.00	2770	1	2791	42	2779	18	-0.5	2770	1	3
53	1.88	2.76	0.20851	0.06	15.289	2.8	0.5320	2.8	1.00	2894	1	2750	122	2833	51	2.9	2894	1	3
54	1.82	0.76	0.19917	0.11	15.068	0.8	0.5489	0.8	0.99	2819	2	2821	35	2820	15	0.0	2819	2	3
55	1.91	0.96	0.20138	0.09	14.562	1.0	0.5247	1.0	1.00	2837	1	2719	42	2787	18	2.4	2837	1	3
56	2.04	1.09	0.17992	0.12	12.172	1.1	0.4909	1.1	0.99	2652	2	2575	46	2618	20	1.7	2652	2	3
57	2.10	1.45	0.16596	0.22	10.903	1.5	0.4767	1.5	0.99	2517	4	2513	60	2515	27	0.1	2517	4	3
58	1.86	0.51	0.21108	0.10	15.668	0.5	0.5386	0.5	0.98	2914	2	2778	23	2857	10	2.8	2914	2	3
61	1.99	0.60	0.18480	0.16	12.831	0.6	0.5038	0.6	0.96	2696	3	2630	26	2667	12	1.4	2696	3	3
62	3.08	1.19	0.10988	0.54	4.911	1.3	0.3243	1.2	0.91	1797	10	1811	37	1804	22	-0.4	1797	10	3
65	1.87	1.19	0.18177	0.69	13.395	1.4	0.5347	1.2	0.87	2669	11	2761	53	2708	26	-2.0	2669	11	3
66	3.42	1.10	0.10152	0.51	4.096	1.2	0.2928	1.1	0.91	1652	10	1655	32	1654	20	-0.1	1652	10	3
67	3.13	1.11	0.10918	0.54	4.808	1.2	0.3195	1.1	0.90	1786	10	1787	35	1786	21	-0.1	1786	10	3
68	3.08	1.19	0.10991	0.51	4.920	1.3	0.3248	1.2	0.92	1798	9	1813	37	1806	22	-0.4	1798	9	3
69	3.09	1.06	0.10858	0.57	4.843	1.2	0.3236	1.1	0.88	1776	10	1807	33	1792	20	-0.8	1776	10	3
70	2.57	0.83	0.13064	0.55	6.999	1.0	0.3887	0.8	0.83	2107	10	2117	30	2111	18	-0.3	2107	10	3
71	2.07	0.65	0.18064	0.52	12.051	0.8	0.4841	0.6	0.78	2659	9	2545	27	2608	15	2.4	2659	9	3
73	1.86	1.71	0.19008	0.85	14.062	1.9	0.5368	1.7	0.89	2743	14	2770	76	2754	36	-0.6	2743	14	3
76	2.58	0.75	0.13115	0.53	7.001	0.9	0.3873	0.8	0.82	2113	9	2110	27	2112	16	0.1	2113	9	3
77	1.99	0.52	0.19496	0.52	13.517	0.7	0.5031	0.5	0.70	2784	9	2627	22	2716	14	3.3	2784	9	3
78	1.84	1.15	0.19736	0.51	14.765	1.3	0.5428	1.2	0.92	2804	8	2795	52	2800	24	0.2	2804	8	3

FSC-16-04 Conglomerate, Malcolm's Point, Carsaig Bay

3	105.19	1.10	0.03170	5.81	0.042	5.9	0.0095	1.1	0.19	-992	172	61	1	41	5	-47.6	61	1	1
2	5.02	1.06	0.07787	0.97	2.138	1.4	0.1993	1.1	0.74	1143	19	1171	23	1161	20	-0.9	1171	23	2

			Tera-Wasserberg plot			Normal - Wetherill plot						Ages						Discordance	Preferred Ages		
Grain	^{238}U/^{206}Pb	± 1σ %	^{207}Pb/^{206}Pb	± 1σ %	^{207}Pb/^{235}U	± 1σ %	^{206}Pb/^{238}U	± 1σ %	ρ	^{207}Pb/^{206}Pb	± 2σ	^{206}Pb/^{238}U	± 2σ	^{207}Pb/^{235}U	± 2σ	6-38/7-35	Age	± 2σ	Notes
4	5.09	1.10	0.07791	0.96	2.110	1.5	0.1965	1.1	0.76	1145	19	1157	23	1152	20	-0.4	1157	23	2
6	14.24	0.95	0.05508	1.03	0.533	1.4	0.0702	1.0	0.68	415	23	438	8	434	10	-0.8	438	8	2
7	11.79	1.17	0.05775	0.96	0.675	1.5	0.0848	1.2	0.77	520	21	525	12	524	12	-0.2	525	12	2
13	5.20	1.16	0.07540	0.97	1.998	1.5	0.1923	1.2	0.77	1079	19	1134	24	1115	20	-1.7	1134	24	2
20	14.22	1.12	0.05567	0.96	0.540	1.5	0.0703	1.1	0.76	439	21	438	10	438	10	0.0	438	10	2
22	20.42	1.16	0.05064	1.05	0.342	1.6	0.0490	1.2	0.74	224	24	308	7	298	8	-3.2	308	7	2
27	5.43	1.15	0.07491	0.97	1.902	1.5	0.1842	1.2	0.77	1066	19	1090	23	1082	20	-0.8	1090	23	2
30	13.88	1.17	0.05487	0.97	0.545	1.5	0.0720	1.2	0.77	407	22	448	10	442	11	-1.5	448	10	2
31	13.90	0.92	0.05445	0.98	0.540	1.3	0.0719	0.9	0.69	390	22	448	8	438	10	-2.2	448	8	2
34	14.17	0.89	0.05458	0.98	0.531	1.3	0.0705	0.9	0.67	395	22	439	8	432	9	-1.7	439	8	2
35	13.84	0.98	0.05332	1.08	0.531	1.5	0.0723	1.0	0.67	342	24	450	8	433	10	-4.0	450	8	2
39	20.77	1.21	0.05075	0.98	0.337	1.6	0.0481	1.2	0.78	229	23	303	7	295	8	-2.9	303	7	2
42	5.30	1.17	0.07641	1.01	1.988	1.6	0.1888	1.2	0.76	1106	20	1115	24	1111	21	-0.3	1115	24	2
46	5.65	1.18	0.07427	0.96	1.813	1.5	0.1771	1.2	0.78	1049	19	1051	23	1050	20	-0.1	1051	23	2
51	20.46	1.31	0.05002	0.84	0.337	1.6	0.0489	1.3	0.84	196	19	308	8	295	8	-4.3	308	8	2
52	6.54	1.60	0.07064	0.59	1.489	1.7	0.1529	1.6	0.94	947	12	917	27	926	21	0.9	917	27	2
54	14.06	1.41	0.05494	0.55	0.539	1.5	0.0711	1.4	0.93	410	12	443	12	438	11	-1.3	443	12	2
55	5.20	1.31	0.07584	0.48	2.010	1.4	0.1923	1.3	0.94	1091	10	1134	27	1119	19	-1.3	1134	27	2
58	4.90	1.27	0.07879	0.49	2.218	1.4	0.2042	1.3	0.93	1167	10	1198	28	1187	19	-1.0	1198	28	2
59	13.90	1.26	0.05423	0.56	0.538	1.4	0.0720	1.3	0.91	381	13	448	11	437	10	-2.5	448	11	2
62	5.62	1.44	0.07323	0.51	1.795	1.5	0.1778	1.4	0.94	1020	10	1055	28	1043	20	-1.1	1055	28	2
71	5.07	1.33	0.07847	0.48	2.132	1.4	0.1971	1.3	0.94	1159	9	1160	28	1159	19	-0.1	1160	28	2
81	14.16	1.37	0.05454	0.67	0.531	1.5	0.0706	1.4	0.90	393	15	440	12	432	11	-1.7	440	12	2
84	5.27	1.22	0.07617	0.50	1.992	1.3	0.1898	1.2	0.93	1100	10	1120	25	1113	18	-0.7	1120	25	2
85	13.37	1.36	0.05555	0.57	0.573	1.5	0.0748	1.4	0.92	434	13	465	12	460	11	-1.1	465	12	2
98	9.66	1.24	0.05994	0.59	0.855	1.4	0.1035	1.2	0.90	601	13	635	15	627	13	-1.2	635	15	2
100	4.94	1.25	0.07875	0.48	2.196	1.3	0.2023	1.2	0.93	1166	9	1188	27	1180	18	-0.7	1188	27	2
101	6.11	1.32	0.07009	0.49	1.580	1.4	0.1636	1.3	0.94	931	10	977	24	962	17	-1.5	977	24	2

			Tera-Wasserberg plot				Normal - Wetherill plot				Ages						Discordance	Preferred Ages		
Grain	$^{238}U/^{206}Pb$	± 1σ %	$^{207}Pb/^{206}Pb$	± 1σ %	$^{207}Pb/^{235}U$	± 1σ %	$^{206}Pb/^{238}U$	± 1σ %	ρ	$^{207}Pb/^{206}Pb$	± 2σ	$^{206}Pb/^{238}U$	± 2σ	$^{207}Pb/^{235}U$	± 2σ	6-38/7-35	Age	± 2σ	Notes
102	5.36	1.29	0.07476	0.60	1.920	1.4	0.1864	1.3	0.90	1062	12	1102	26	1088	19	-1.2	1102	26	2
105	5.43	1.26	0.07522	0.58	1.909	1.4	0.1841	1.3	0.91	1075	12	1089	25	1084	18	-0.5	1089	25	2
106	14.10	1.26	0.05594	0.46	0.547	1.3	0.0709	1.3	0.94	450	10	442	11	443	10	0.3	442	11	2
107	5.28	1.24	0.07296	0.69	1.906	1.4	0.1895	1.2	0.87	1013	14	1119	25	1083	19	-3.3	1119	25	2
108	13.53	1.17	0.05597	0.49	0.570	1.3	0.0739	1.2	0.92	451	11	460	10	458	9	-0.3	460	10	2
110	6.83	1.24	0.06790	0.56	1.370	1.4	0.1464	1.2	0.91	865	12	881	20	876	16	-0.5	881	20	2
112	4.90	1.24	0.07949	0.47	2.234	1.3	0.2039	1.2	0.94	1184	9	1196	27	1192	18	-0.4	1196	27	2
116	5.25	1.35	0.07722	0.47	2.027	1.4	0.1905	1.3	0.95	1127	9	1124	28	1125	19	0.1	1124	28	2
117	6.02	1.35	0.07071	0.57	1.618	1.5	0.1660	1.3	0.92	949	12	990	25	977	18	-1.3	990	25	2
5	3.00	0.97	0.10906	0.95	5.003	1.4	0.3329	1.0	0.71	1784	17	1852	31	1820	23	-1.8	1784	17	3
8	3.31	1.03	0.10249	0.96	4.271	1.4	0.3024	1.0	0.73	1670	18	1703	31	1688	23	-0.9	1670	18	3
9	1.83	1.16	0.19138	0.95	14.404	1.5	0.5461	1.2	0.77	2754	16	2809	53	2777	28	-1.2	2754	16	3
10	1.74	1.06	0.19648	0.96	15.575	1.4	0.5752	1.1	0.74	2797	16	2929	50	2851	27	-2.7	2797	16	3
11	2.31	1.28	0.16004	0.98	9.552	1.6	0.4331	1.3	0.79	2456	17	2319	50	2393	29	3.1	2456	17	3
12	2.60	0.97	0.12440	1.03	6.596	1.4	0.3847	1.0	0.68	2020	18	2098	35	2059	25	-1.9	2020	18	3
14	2.95	1.04	0.11058	0.96	5.160	1.4	0.3386	1.0	0.74	1809	17	1880	34	1846	24	-1.8	1809	17	3
15	2.98	1.09	0.11007	0.96	5.085	1.5	0.3352	1.1	0.75	1801	18	1863	35	1834	24	-1.6	1801	18	3
16	3.30	0.98	0.10134	0.96	4.229	1.4	0.3028	1.0	0.71	1649	18	1705	29	1680	22	-1.5	1649	18	3
17	3.02	0.93	0.11147	0.96	5.081	1.3	0.3307	0.9	0.70	1824	17	1842	30	1833	22	-0.5	1824	17	3
18	4.74	0.92	0.07977	0.96	2.319	1.3	0.2110	0.9	0.69	1191	19	1234	21	1218	19	-1.3	1191	19	3
19	3.03	1.00	0.11025	0.96	5.011	1.4	0.3298	1.0	0.72	1804	17	1837	32	1821	23	-0.9	1804	17	3
21	4.51	1.02	0.08357	0.99	2.552	1.4	0.2215	1.0	0.72	1283	19	1290	24	1287	21	-0.2	1283	19	3
23	2.13	1.57	0.17098	0.99	11.073	1.9	0.4699	1.6	0.85	2567	17	2483	65	2529	34	1.8	2567	17	3
24	3.11	1.15	0.11079	0.96	4.917	1.5	0.3221	1.1	0.77	1812	17	1800	36	1805	25	0.3	1812	17	3
25	2.54	1.28	0.12961	0.98	7.031	1.6	0.3936	1.3	0.79	2093	17	2140	46	2115	28	-1.1	2093	17	3
26	3.38	1.24	0.10146	0.96	4.141	1.6	0.2962	1.2	0.79	1651	18	1672	37	1662	25	-0.6	1651	18	3
28	2.02	1.54	0.19056	0.95	13.000	1.8	0.4950	1.5	0.85	2747	16	2592	65	2680	34	3.3	2747	16	3
33	3.39	1.07	0.10063	0.96	4.087	1.4	0.2947	1.1	0.74	1636	18	1665	31	1652	23	-0.8	1636	18	3

Grain	Tera-Wasserberg plot				Normal - Wetherill plot						Ages						Discordance	Preferred Ages		Notes
	$^{238}U/^{206}Pb$	$\pm 1\sigma$ %	$^{207}Pb/^{206}Pb$	$\pm 1\sigma$ %	$^{207}Pb/^{235}U$	$\pm 1\sigma$ %	$^{206}Pb/^{238}U$	$\pm 1\sigma$ %	ρ	$^{207}Pb/^{206}Pb$	$\pm 2\sigma$	$^{206}Pb/^{238}U$	$\pm 2\sigma$	$^{207}Pb/^{235}U$	$\pm 2\sigma$	6-38/7-35	Age	$\pm 2\sigma$	
36	3.29	1.02	0.10286	0.96	4.312	1.4	0.3042	1.0	0.73	1676	18	1712	31	1696	23	-1.0	1676	18	3
37	1.86	0.86	0.18371	1.16	13.593	1.4	0.5369	0.9	0.60	2687	19	2770	39	2722	27	-1.8	2687	19	3
38	2.00	1.08	0.18345	0.96	12.660	1.4	0.5008	1.1	0.75	2684	16	2617	46	2655	27	1.4	2684	16	3
41	3.12	0.93	0.11119	0.96	4.917	1.3	0.3209	0.9	0.70	1819	17	1794	29	1805	22	0.6	1819	17	3
43	3.16	1.11	0.10890	0.96	4.747	1.5	0.3163	1.1	0.76	1781	18	1771	34	1776	24	0.2	1781	18	3
44	1.92	1.13	0.18768	0.97	13.503	1.5	0.5221	1.1	0.76	2722	16	2708	50	2716	28	0.3	2722	16	3
45	1.85	1.11	0.20086	0.96	14.992	1.5	0.5416	1.1	0.76	2833	16	2790	50	2815	28	0.9	2833	16	3
47	2.93	1.22	0.11451	0.96	5.380	1.6	0.3409	1.2	0.78	1872	17	1891	40	1882	26	-0.5	1872	17	3
49	2.88	1.13	0.11467	0.96	5.485	1.5	0.3471	1.1	0.76	1875	17	1921	38	1898	25	-1.2	1875	17	3
50	3.65	1.53	0.09885	0.97	3.733	1.8	0.2740	1.5	0.84	1602	18	1561	42	1578	29	1.1	1602	18	3
53	4.40	1.34	0.08417	0.47	2.637	1.4	0.2273	1.3	0.94	1297	9	1320	32	1311	21	-0.7	1297	9	3
57	2.98	1.33	0.10965	0.55	5.068	1.4	0.3354	1.3	0.92	1794	10	1864	43	1831	24	-1.8	1794	10	3
60	2.86	1.32	0.11230	0.47	5.405	1.4	0.3492	1.3	0.94	1837	9	1931	44	1886	24	-2.4	1837	9	3
61	1.89	1.32	0.20935	0.47	15.271	1.4	0.5293	1.3	0.94	2901	8	2738	59	2832	26	3.3	2901	8	3
63	1.78	1.15	0.19209	0.49	14.889	1.2	0.5624	1.1	0.92	2760	8	2877	53	2808	23	-2.4	2760	8	3
64	4.89	1.25	0.07804	0.47	2.201	1.3	0.2046	1.2	0.94	1148	9	1200	27	1181	18	-1.6	1148	9	3
65	2.65	1.57	0.12669	0.55	6.593	1.7	0.3776	1.6	0.94	2053	10	2065	55	2058	29	-0.3	2053	10	3
66	3.22	1.47	0.10347	0.46	4.434	1.5	0.3109	1.5	0.96	1687	8	1745	45	1719	25	-1.5	1687	8	3
68	3.60	1.33	0.10066	0.48	3.853	1.4	0.2778	1.3	0.94	1636	9	1580	37	1604	23	1.5	1636	9	3
69	1.98	1.68	0.18260	0.53	12.705	1.8	0.5048	1.7	0.95	2677	9	2635	72	2658	33	0.9	2677	9	3
70	1.89	1.44	0.18523	0.47	13.535	1.5	0.5302	1.4	0.95	2700	8	2742	64	2718	28	-0.9	2700	8	3
72	3.76	1.39	0.09396	0.46	3.447	1.5	0.2662	1.4	0.95	1507	9	1522	37	1515	23	-0.4	1507	9	3
73	1.86	1.45	0.19552	0.48	14.464	1.5	0.5368	1.4	0.95	2789	8	2770	65	2781	29	0.4	2789	8	3
73	1.86	1.45	0.19552	0.48	14.464	1.5	0.5368	1.4	0.95	2789	8	2770	65	2781	29	0.4	2789	8	3
74	3.43	1.38	0.10047	0.46	4.041	1.5	0.2919	1.4	0.95	1633	9	1651	40	1643	23	-0.5	1633	9	3
74	3.43	1.38	0.10047	0.46	4.041	1.5	0.2919	1.4	0.95	1633	9	1651	40	1643	23	-0.5	1633	9	3
75	1.85	1.44	0.18791	0.46	14.034	1.5	0.5419	1.4	0.95	2724	8	2791	65	2752	28	-1.4	2724	8	3
76	3.29	1.57	0.10269	0.47	4.308	1.6	0.3044	1.6	0.96	1673	9	1713	47	1695	27	-1.1	1673	9	3

Grain	Tera-Wasserberg plot				Normal - Wetherill plot					Ages						Discordance 6-38/7-35	Preferred Ages		Notes
	$^{238}U/^{206}Pb$	±1σ %	$^{207}Pb/^{206}Pb$	±1σ %	$^{207}Pb/^{235}U$	±1σ %	$^{206}Pb/^{238}U$	±1σ %	ρ	$^{207}Pb/^{206}Pb$	±2σ	$^{206}Pb/^{238}U$	±2σ	$^{207}Pb/^{235}U$	±2σ		Age	±2σ	
77	1.94	1.18	0.18991	0.52	13.512	1.3	0.5162	1.2	0.92	2741	9	2683	52	2716	24	1.2	2741	9	3
78	3.94	1.26	0.09173	0.50	3.211	1.4	0.2540	1.3	0.93	1462	10	1459	33	1460	21	0.0	1462	10	3
79	3.37	1.37	0.10032	0.49	4.100	1.5	0.2966	1.4	0.94	1630	9	1674	40	1654	23	-1.2	1630	9	3
80	2.89	1.36	0.11611	0.46	5.531	1.4	0.3456	1.4	0.95	1897	8	1914	45	1905	24	-0.4	1897	8	3
82	2.90	1.24	0.11451	0.47	5.450	1.3	0.3453	1.2	0.94	1872	8	1912	41	1893	23	-1.0	1872	8	3
86	4.10	1.28	0.08716	0.48	2.933	1.4	0.2441	1.3	0.94	1364	9	1408	32	1390	20	-1.3	1364	9	3
88	3.36	1.39	0.10180	0.45	4.172	1.5	0.2974	1.4	0.95	1657	8	1678	41	1669	24	-0.6	1657	8	3
89	2.50	1.36	0.13079	0.47	7.223	1.4	0.4007	1.4	0.94	2109	8	2172	50	2139	25	-1.5	2109	8	3
90	1.82	1.36	0.19403	0.47	14.697	1.4	0.5496	1.4	0.95	2777	8	2824	62	2796	27	-1.0	2777	8	3
91	3.07	1.25	0.10947	0.46	4.915	1.3	0.3257	1.3	0.94	1791	8	1818	40	1805	22	-0.7	1791	8	3
92	2.51	1.54	0.13012	0.49	7.151	1.6	0.3987	1.5	0.95	2100	9	2163	57	2130	28	-1.5	2100	9	3
93	3.22	2.69	0.11000	0.52	4.705	2.7	0.3104	2.7	0.98	1799	9	1743	82	1768	45	1.4	1799	9	3
94	3.77	1.31	0.09242	0.51	3.379	1.4	0.2653	1.3	0.93	1476	10	1517	35	1499	22	-1.2	1476	10	3
95	3.09	1.40	0.11049	0.46	4.921	1.5	0.3232	1.4	0.95	1808	8	1805	44	1806	25	0.0	1808	8	3
96	2.81	1.50	0.11624	0.49	5.710	1.6	0.3564	1.5	0.95	1899	9	1965	51	1933	27	-1.7	1899	9	3
97	1.88	1.20	0.18875	0.47	13.826	1.3	0.5315	1.2	0.93	2731	8	2748	54	2738	24	-0.4	2731	8	3
99	1.88	1.13	0.21061	0.85	15.454	1.4	0.5324	1.1	0.80	2910	14	2752	50	2844	27	3.2	2910	14	3
103	1.79	1.30	0.19516	0.46	15.005	1.4	0.5579	1.3	0.94	2786	7	2858	60	2816	26	-1.5	2786	7	3
104	1.79	1.37	0.19564	0.45	15.104	1.4	0.5602	1.4	0.95	2790	7	2867	63	2822	27	-1.6	2790	7	3
109	1.96	1.24	0.16977	0.64	11.958	1.4	0.5111	1.2	0.89	2555	11	2661	54	2601	26	-2.3	2555	11	3
111	2.49	1.35	0.13011	0.51	7.196	1.4	0.4013	1.4	0.93	2099	9	2175	50	2136	25	-1.8	2099	9	3
113	1.90	1.39	0.18122	0.48	13.152	1.5	0.5266	1.4	0.95	2664	8	2727	61	2691	27	-1.4	2664	8	3
114	1.78	1.32	0.19876	0.45	15.389	1.4	0.5618	1.3	0.95	2816	7	2874	61	2840	26	-1.2	2816	7	3
115	3.02	1.33	0.11156	0.46	5.089	1.4	0.3310	1.3	0.94	1825	8	1843	42	1834	24	-0.5	1825	8	3
118	3.17	1.34	0.10894	0.46	4.740	1.4	0.3157	1.3	0.95	1782	8	1769	41	1774	23	0.3	1782	8	3
119	2.71	1.20	0.13076	0.52	6.659	1.3	0.3695	1.2	0.92	2108	9	2027	42	2067	23	1.9	2108	9	3

Grain	Tera-Wasserberg plot ^{238}U/^{206}Pb	±1σ %	^{207}Pb/^{206}Pb	±1σ %	Normal - Wetherill plot ^{207}Pb/^{235}U	±1σ %	^{206}Pb/^{238}U	±1σ %	ρ	Ages ^{207}Pb/^{206}Pb	±2σ	^{206}Pb/^{238}U	±2σ	^{207}Pb/^{235}U	±2σ	Discordance 6-38/7-35	Preferred Ages Age	±2σ	Notes

FSC-16-11 Carraig Mhor ignimbrite, Carsaig Bay

Grain	^{238}U/^{206}Pb	±1σ %	^{207}Pb/^{206}Pb	±1σ %	^{207}Pb/^{235}U	±1σ %	^{206}Pb/^{238}U	±1σ %	ρ	^{207}Pb/^{206}Pb	±2σ	^{206}Pb/^{238}U	±2σ	^{207}Pb/^{235}U	±2σ	6-38/7-35	Age	±2σ	Notes
3.1	101.82	2.30	0.04364	2.78	0.059	3.6	0.0098	2.3	0.64	-131	69	63	3	58	4	-8.1	63	3	1
3.2	85.45	1.83	0.15437	7.89	0.249	8.1	0.0117	1.8	0.23	2395	134	75	3	226	32	66.8	75	3	1
10.1	102.48	2.31	0.04115	3.42	0.055	4.1	0.0098	2.3	0.56	-278	87	63	3	55	4	-14.4	63	3	1
10.2	93.31	1.35	0.07040	8.50	0.104	8.6	0.0107	1.4	0.16	940	174	69	2	100	16	31.6	69	2	1
15	100.69	2.21	0.04866	2.12	0.067	3.1	0.0099	2.2	0.72	131	50	64	3	65	4	2.7	64	3	1
16.2	98.80	1.09	0.04670	1.14	0.065	1.6	0.0101	1.1	0.69	34	27	65	1	64	2	-1.3	65	1	1
99.1	101.98	2.22	0.03911	3.09	0.053	3.8	0.0098	2.2	0.58	-409	81	63	3	52	4	-20.3	63	3	1
99.2	96.20	1.10	0.04721	0.75	0.068	1.3	0.0104	1.1	0.83	60	18	67	1	66	2	-0.3	67	1	1
110.1	102.62	0.88	0.04766	2.20	0.064	2.4	0.0097	0.9	0.37	82	52	63	1	63	3	0.8	63	1	1
110.2	99.21	1.12	0.04755	0.78	0.066	1.4	0.0101	1.1	0.82	77	19	65	1	65	2	0.5	65	1	1
138.1	100.90	1.32	0.04657	1.52	0.064	2.0	0.0099	1.3	0.66	27	36	64	2	63	2	-1.5	64	2	1
138.2	99.21	1.04	0.04726	0.62	0.066	1.2	0.0101	1.0	0.86	62	15	65	1	65	2	-0.1	65	1	1
4	14.32	2.30	0.05475	0.87	0.527	2.5	0.0698	2.3	0.94	402	20	435	19	430	17	-1.3	435	19	2
8	5.79	2.23	0.07342	0.66	1.747	2.3	0.1727	2.2	0.96	1026	13	1027	42	1026	30	-0.1	1027	42	2
12	5.07	3.44	0.07916	1.21	2.151	3.6	0.1971	3.4	0.94	1176	24	1160	73	1165	49	0.5	1160	73	2
23	14.58	2.23	0.05500	0.65	0.520	2.3	0.0686	2.2	0.96	412	15	428	18	425	16	-0.6	428	18	2
25	5.45	2.37	0.07573	0.63	1.914	2.5	0.1834	2.4	0.97	1088	13	1086	47	1086	32	0.0	1086	47	2
27	13.91	2.21	0.05491	0.82	0.544	2.4	0.0719	2.2	0.94	409	18	448	19	441	17	-1.5	448	19	2
33	14.23	2.32	0.05568	1.25	0.539	2.6	0.0703	2.3	0.88	439	28	438	20	438	19	0.0	438	20	2
36	14.05	2.13	0.05574	0.63	0.547	2.2	0.0712	2.1	0.96	442	14	443	18	443	16	-0.1	443	18	2
37	13.87	2.16	0.05572	0.72	0.554	2.3	0.0721	2.2	0.95	441	16	449	19	447	16	-0.3	449	19	2
39	6.27	3.00	0.07274	0.88	1.598	3.1	0.1594	3.0	0.96	1007	18	954	53	969	38	1.6	954	53	2
42	14.12	2.14	0.05545	0.69	0.541	2.3	0.0708	2.1	0.95	430	15	441	18	439	16	-0.4	441	18	2
43	14.05	2.24	0.05907	0.86	0.579	2.4	0.0712	2.2	0.93	570	19	443	19	464	18	4.5	443	19	2
45	14.27	2.30	0.05542	0.64	0.535	2.4	0.0701	2.3	0.96	429	14	437	19	435	17	-0.3	437	19	2
48	14.02	2.34	0.05579	0.64	0.548	2.4	0.0713	2.3	0.96	444	14	444	20	444	17	0.0	444	20	2

			Tera-Wasserberg plot							Ages						Discordance	Preferred Ages		
Grain	^{238}U/^{206}Pb	±1σ %	^{207}Pb/^{206}Pb	±1σ %	^{207}Pb/^{235}U	±1σ %	^{206}Pb/^{238}U	±1σ %	ρ	^{207}Pb/^{206}Pb	±2σ	^{206}Pb/^{238}U	±2σ	^{207}Pb/^{235}U	±2σ	6-38/7-35	Age	±2σ	Notes
52	5.72	2.19	0.07293	0.68	1.756	2.3	0.1747	2.2	0.96	1012	14	1038	42	1029	29	-0.8	1038	42	2
55	14.28	2.21	0.05521	0.70	0.533	2.3	0.0700	2.2	0.95	421	16	436	19	434	16	-0.6	436	19	2
61	14.22	2.21	0.05553	0.80	0.538	2.4	0.0703	2.2	0.94	434	18	438	19	437	17	-0.2	438	19	2
67	5.43	2.18	0.07475	0.71	1.897	2.3	0.1841	2.2	0.95	1062	14	1089	43	1080	30	-0.9	1089	43	2
70	14.31	2.19	0.05483	0.75	0.528	2.3	0.0699	2.2	0.95	405	17	435	18	430	16	-1.1	435	18	2
71	4.99	2.19	0.07788	0.65	2.150	2.3	0.2003	2.2	0.96	1144	13	1177	47	1165	31	-1.0	1177	47	2
72	13.92	2.27	0.05621	0.78	0.557	2.4	0.0718	2.3	0.95	461	17	447	20	449	17	0.4	447	20	2
79	5.61	2.13	0.07363	0.62	1.807	2.2	0.1781	2.1	0.96	1031	13	1057	41	1048	29	-0.8	1057	41	2
88	5.25	2.28	0.07739	0.63	2.030	2.4	0.1903	2.3	0.96	1131	12	1123	47	1126	32	0.2	1123	47	2
91	14.73	2.26	0.05551	0.67	0.520	2.4	0.0679	2.3	0.96	433	15	424	18	425	16	0.3	424	18	2
95	5.43	2.32	0.07527	0.64	1.910	2.4	0.1841	2.3	0.96	1076	13	1090	46	1085	32	-0.4	1090	46	2
96	6.02	2.33	0.07083	0.66	1.621	2.4	0.1660	2.3	0.96	953	13	990	43	978	30	-1.2	990	43	2
97	13.83	2.11	0.05543	0.72	0.552	2.2	0.0723	2.1	0.95	429	16	450	18	446	16	-0.8	450	18	2
100	14.15	2.30	0.05428	0.76	0.529	2.4	0.0707	2.3	0.95	383	17	440	20	431	17	-2.1	440	20	2
102	13.87	0.88	0.05588	0.64	0.555	1.1	0.0721	0.9	0.81	447	14	449	8	449	8	-0.1	449	8	2
103	5.91	0.95	0.07150	0.60	1.667	1.1	0.1692	1.0	0.85	972	12	1008	18	996	14	-1.2	1008	18	2
107	14.13	1.12	0.05542	0.68	0.541	1.3	0.0708	1.1	0.85	429	15	441	10	439	9	-0.5	441	10	2
109	5.42	1.09	0.07477	0.68	1.900	1.3	0.1843	1.1	0.85	1062	14	1091	22	1081	17	-0.9	1091	22	2
115	13.91	1.06	0.05569	0.76	0.552	1.3	0.0719	1.1	0.81	440	17	448	9	446	9	-0.3	448	9	2
119	5.11	0.87	0.08067	0.86	2.176	1.2	0.1958	0.9	0.71	1213	17	1153	18	1174	17	1.8	1153	18	2
122	9.87	1.29	0.05971	0.59	0.834	1.4	0.1014	1.3	0.91	593	13	622	15	616	13	-1.1	622	15	2
124	4.97	0.85	0.07859	0.56	2.181	1.0	0.2014	0.9	0.83	1162	11	1183	18	1175	14	-0.7	1183	18	2
127	13.97	1.01	0.05518	0.62	0.544	1.2	0.0716	1.0	0.85	419	14	446	9	441	8	-1.0	446	9	2
129	14.26	0.96	0.05503	0.62	0.532	1.1	0.0701	1.0	0.84	413	14	437	8	433	8	-0.9	437	8	2
137	12.67	1.05	0.05583	1.02	0.608	1.5	0.0790	1.0	0.72	446	23	490	10	482	11	-1.6	490	10	2
144	5.60	0.73	0.07398	0.66	1.819	1.0	0.1785	0.7	0.75	1041	13	1059	14	1052	13	-0.6	1059	14	2
148	13.90	1.01	0.05521	0.62	0.547	1.2	0.0719	1.0	0.85	421	14	448	9	443	8	-1.0	448	9	2
1	1.76	2.34	0.19906	0.61	15.548	2.4	0.5667	2.3	0.97	2818	10	2894	108	2849	45	-1.6	2818	10	3

	Tera-Wasserberg plot				Normal - Wetherill plot					Ages						Discordance	Preferred Ages		
Grain	^{238}U/^{206}Pb	±1σ %	^{207}Pb/^{206}Pb	± 1σ %	^{207}Pb/^{235}U	±1σ %	^{206}Pb/^{238}U	±1σ %	ρ	^{207}Pb/^{206}Pb	± 2σ	^{206}Pb/^{238}U	± 2σ	^{207}Pb/^{235}U	± 2σ	6-38/7-35	Age	± 2σ	Notes
2	3.16	2.25	0.10767	0.62	4.703	2.3	0.3169	2.3	0.96	1760	11	1775	69	1768	38	-0.4	1760	11	3
5	3.97	2.39	0.09307	0.63	3.232	2.5	0.2520	2.4	0.97	1489	12	1449	62	1465	38	1.1	1489	12	3
6	1.77	2.16	0.19608	0.63	15.252	2.2	0.5644	2.2	0.96	2794	10	2885	100	2831	42	-1.9	2794	10	3
7	3.25	2.12	0.10413	0.61	4.419	2.2	0.3079	2.1	0.96	1699	11	1730	64	1716	36	-0.8	1699	11	3
9	3.33	2.61	0.10204	0.61	4.223	2.7	0.3003	2.6	0.97	1662	11	1693	77	1678	43	-0.8	1662	11	3
11	4.12	2.35	0.09354	0.62	3.129	2.4	0.2427	2.4	0.97	1499	12	1401	59	1440	37	2.7	1499	12	3
13	3.11	2.27	0.11012	0.61	4.874	2.4	0.3211	2.3	0.97	1801	11	1795	71	1798	39	0.1	1801	11	3
14	3.35	2.41	0.10229	0.62	4.202	2.5	0.2981	2.4	0.97	1666	11	1682	71	1674	40	-0.4	1666	11	3
17	3.51	2.32	0.09968	0.61	3.916	2.4	0.2851	2.3	0.97	1618	11	1617	66	1617	38	0.0	1618	11	3
19	4.66	2.30	0.08202	0.62	2.425	2.4	0.2146	2.3	0.97	1246	12	1253	52	1250	34	-0.2	1246	12	3
20	3.42	2.33	0.10100	0.62	4.066	2.4	0.2921	2.3	0.97	1643	12	1652	67	1648	38	-0.3	1643	12	3
21	3.28	2.64	0.11108	0.62	4.662	2.7	0.3046	2.6	0.97	1817	11	1714	79	1761	44	2.6	1817	11	3
22	1.92	2.25	0.19490	0.62	13.981	2.3	0.5205	2.2	0.96	2784	10	2701	98	2748	43	1.7	2784	10	3
24	3.05	2.53	0.11194	0.61	5.052	2.6	0.3275	2.5	0.97	1831	11	1826	80	1828	43	0.1	1831	11	3
26	2.99	2.38	0.11067	0.61	5.109	2.5	0.3350	2.4	0.97	1810	11	1863	76	1838	41	-1.4	1810	11	3
29	4.19	2.47	0.08648	0.61	2.846	2.5	0.2388	2.5	0.97	1349	12	1381	61	1368	38	-0.9	1349	12	3
31	1.81	2.28	0.20132	0.63	15.287	2.4	0.5510	2.3	0.96	2837	10	2829	104	2833	44	0.1	2837	10	3
32	2.55	2.26	0.13176	0.62	7.117	2.3	0.3920	2.3	0.96	2122	11	2132	82	2126	41	-0.3	2122	11	3
34	4.09	3.50	0.08868	0.71	2.990	3.6	0.2446	3.5	0.98	1397	14	1411	88	1405	53	-0.4	1397	14	3
35	3.45	2.12	0.10152	0.61	4.054	2.2	0.2898	2.1	0.96	1652	11	1640	61	1645	35	0.3	1652	11	3
38	3.80	2.13	0.09466	0.61	3.430	2.2	0.2629	2.1	0.96	1521	12	1505	57	1511	34	0.4	1521	12	3
40	2.56	2.24	0.15806	0.63	8.522	2.3	0.3912	2.2	0.96	2435	11	2128	81	2288	41	7.0	2435	11	3
41	1.79	2.08	0.19289	0.76	14.873	2.2	0.5595	2.1	0.94	2767	13	2864	95	2807	41	-2.0	2767	13	3
44	1.82	2.36	0.18936	0.61	14.329	2.4	0.5491	2.4	0.97	2737	10	2821	107	2772	45	-1.8	2737	10	3
46	3.22	2.22	0.11001	0.65	4.707	2.3	0.3105	2.2	0.96	1800	12	1743	67	1769	38	1.4	1800	12	3
46	1.99	2.80	0.18636	0.67	12.920	2.9	0.5030	2.8	0.97	2710	11	2627	120	2674	53	1.8	2710	11	3
47	1.91	2.16	0.18564	0.67	13.401	2.3	0.5238	2.2	0.96	2704	11	2715	95	2708	42	-0.3	2704	11	3
49	1.88	2.49	0.19151	0.63	14.006	2.6	0.5307	2.5	0.97	2755	10	2744	110	2750	48	0.2	2755	10	3

			Tera-Wasserberg plot				Normal - Wetherill plot				Ages						Discordance	Preferred Ages		
Grain	$^{238}U/^{206}Pb$	±1σ %	$^{207}Pb/^{206}Pb$	± 1σ %	$^{207}Pb/^{235}U$	±1σ %	$^{206}Pb/^{238}U$	±1σ %	ρ	$^{207}Pb/^{206}Pb$	± 2σ	$^{206}Pb/^{238}U$	± 2σ	$^{207}Pb/^{235}U$	± 2σ	6-38/7-35	Age	± 2σ	Notes
50	3.45	2.33	0.10078	0.63	4.030	2.4	0.2901	2.3	0.97	1639	12	1642	67	1640	38	-0.1	1639	12	3
51	4.09	2.38	0.09158	0.62	3.088	2.5	0.2446	2.4	0.97	1459	12	1411	60	1430	37	1.3	1459	12	3
54	3.63	3.24	0.10006	0.99	3.795	3.4	0.2752	3.2	0.96	1625	18	1567	90	1592	53	1.5	1625	18	3
56	3.88	2.97	0.10940	0.63	3.888	3.0	0.2578	3.0	0.98	1789	11	1479	78	1611	48	8.2	1789	11	3
57	2.20	2.45	0.18937	0.63	11.884	2.5	0.4553	2.4	0.97	2737	10	2419	98	2595	46	6.8	2737	10	3
58	3.64	2.28	0.09800	0.66	3.711	2.4	0.2747	2.3	0.96	1586	12	1565	63	1574	37	0.6	1586	12	3
59	3.13	2.17	0.10615	0.62	4.675	2.3	0.3195	2.2	0.96	1734	11	1787	67	1763	37	-1.4	1734	11	3
60	4.81	2.24	0.07944	0.62	2.279	2.3	0.2081	2.2	0.96	1183	12	1219	50	1206	32	-1.1	1183	12	3
62	3.19	2.38	0.10682	0.62	4.611	2.5	0.3132	2.4	0.97	1746	11	1756	73	1751	40	-0.3	1746	11	3
63	4.63	3.92	0.09207	1.52	2.738	4.2	0.2158	3.9	0.93	1469	29	1259	89	1339	61	5.9	1469	29	3
65	3.09	2.20	0.10925	0.70	4.878	2.3	0.3240	2.2	0.95	1787	13	1809	69	1798	38	-0.6	1787	13	3
66	3.12	2.16	0.11348	0.61	5.020	2.3	0.3210	2.2	0.96	1856	11	1795	67	1823	37	1.5	1856	11	3
69	3.23	2.24	0.10942	0.61	4.675	2.3	0.3100	2.2	0.97	1790	11	1741	68	1763	38	1.3	1790	11	3
73	2.44	2.22	0.14355	0.66	8.095	2.3	0.4092	2.2	0.96	2270	11	2211	83	2242	41	1.4	2270	11	3
74	3.34	2.22	0.10302	0.61	4.248	2.3	0.2992	2.2	0.96	1679	11	1687	65	1683	37	-0.2	1679	11	3
77	3.43	2.21	0.10077	0.63	4.054	2.3	0.2919	2.2	0.96	1638	12	1651	64	1645	37	-0.4	1638	12	3
78	3.24	2.32	0.10319	0.62	4.384	2.4	0.3083	2.3	0.97	1682	11	1732	70	1709	39	-1.3	1682	11	3
80	1.83	2.31	0.19517	0.61	14.682	2.4	0.5458	2.3	0.97	2786	10	2808	104	2795	44	-0.5	2786	10	3
81.1	2.21	2.71	0.17169	1.05	10.706	2.9	0.4525	2.7	0.93	2574	18	2406	108	2498	53	3.7	2574	18	3
81.2	1.48	2.29	0.33292	1.33	31.050	2.7	0.6767	2.3	0.86	3631	20	3332	118	3521	51	5.4	3631	20	3
83	1.87	2.22	0.18933	0.63	13.935	2.3	0.5341	2.2	0.96	2736	10	2759	99	2745	43	-0.5	2736	10	3
84	3.85	2.25	0.09377	0.62	3.353	2.3	0.2594	2.2	0.96	1503	12	1487	59	1493	36	0.4	1503	12	3
85	4.14	2.21	0.08758	0.64	2.914	2.3	0.2414	2.2	0.96	1373	12	1394	55	1386	34	-0.6	1373	12	3
87	3.74	2.32	0.10019	0.62	3.695	2.4	0.2676	2.3	0.97	1628	11	1528	63	1570	38	2.7	1628	11	3
89	4.77	2.34	0.08194	0.62	2.369	2.4	0.2098	2.3	0.97	1244	12	1228	52	1233	34	0.5	1244	12	3
90	4.03	2.39	0.08907	0.62	3.050	2.5	0.2484	2.4	0.97	1406	12	1430	61	1420	37	-0.7	1406	12	3
92	1.80	2.31	0.20242	0.61	15.515	2.4	0.5561	2.3	0.97	2846	10	2851	105	2847	45	-0.1	2846	10	3
93	2.08	2.22	0.17502	0.64	11.610	2.3	0.4813	2.2	0.96	2606	11	2533	92	2573	42	1.6	2606	11	3

			Tera-Wasserberg plot			Normal - Wetherill plot						Ages						Discordance	Preferred Ages		
Grain	^{238}U/^{206}Pb	± 1σ %	^{207}Pb/^{206}Pb	± 1σ %	^{207}Pb/^{235}U	± 1σ %	^{206}Pb/^{238}U	± 1σ %	ρ	^{207}Pb/^{206}Pb	± 2σ	^{206}Pb/^{238}U	± 2σ	^{207}Pb/^{235}U	± 2σ	6-38/7-35	Age	± 2σ	Notes
94	4.34	2.27	0.08453	0.67	2.686	2.4	0.2305	2.3	0.96	1305	13	1337	55	1325	34	-1.0	1305	13	3
101	3.47	1.36	0.09587	0.76	3.804	1.6	0.2879	1.4	0.87	1545	14	1631	39	1594	25	-2.4	1545	14	3
104	3.74	1.17	0.09287	0.59	3.426	1.3	0.2677	1.2	0.89	1485	11	1529	32	1510	20	-1.2	1485	11	3
105	1.80	1.03	0.18839	0.57	14.439	1.2	0.5561	1.0	0.88	2728	9	2851	47	2779	22	-2.6	2728	9	3
106	3.68	1.00	0.09356	0.57	3.503	1.2	0.2717	1.0	0.87	1499	11	1549	28	1528	18	-1.4	1499	11	3
108	1.81	0.26	0.18411	0.76	14.031	0.8	0.5530	0.3	0.32	2690	12	2837	12	2752	15	-3.1	2690	12	3
112	3.75	1.21	0.09389	0.56	3.454	1.3	0.2669	1.2	0.91	1506	10	1525	33	1517	21	-0.6	1506	10	3
114	3.66	1.25	0.09494	0.57	3.573	1.4	0.2731	1.3	0.91	1527	11	1556	35	1544	22	-0.8	1527	11	3
116	1.75	1.94	0.19240	0.80	15.130	2.1	0.5706	1.9	0.92	2763	13	2910	90	2823	39	-3.1	2763	13	3
117	4.05	1.18	0.09555	0.65	3.253	1.4	0.2470	1.2	0.88	1539	12	1423	30	1470	21	3.2	1539	12	3
118	3.15	0.79	0.10681	0.57	4.677	1.0	0.3177	0.8	0.81	1746	11	1779	25	1763	16	-0.9	1746	11	3
120	3.42	1.14	0.10049	0.57	4.047	1.3	0.2922	1.1	0.89	1633	11	1653	33	1644	20	-0.5	1633	11	3
121	3.27	1.02	0.10272	0.57	4.327	1.2	0.3057	1.0	0.87	1674	10	1719	31	1699	19	-1.2	1674	10	3
123	1.87	1.15	0.19134	0.61	14.110	1.3	0.5351	1.1	0.88	2754	10	2763	51	2757	24	-0.2	2754	10	3
125	1.83	3.14	0.18434	0.64	13.869	3.2	0.5459	3.1	0.98	2692	11	2808	141	2741	59	-2.5	2692	11	3
126	3.99	1.17	0.08876	0.57	3.067	1.3	0.2507	1.2	0.90	1399	11	1442	30	1424	20	-1.2	1399	11	3
128	3.33	0.54	0.10659	0.57	4.412	0.8	0.3003	0.5	0.68	1742	10	1693	16	1715	13	1.3	1742	10	3
131	1.81	1.22	0.20355	0.58	15.528	1.3	0.5535	1.2	0.90	2855	9	2840	56	2848	25	0.3	2855	9	3
132	2.09	1.16	0.16424	0.57	10.845	1.3	0.4791	1.2	0.90	2500	10	2523	48	2510	24	-0.5	2500	10	3
133	3.14	2.12	0.10730	0.56	4.709	2.2	0.3185	2.1	0.97	1754	10	1782	66	1769	36	-0.8	1754	10	3
134	3.37	0.92	0.10072	0.58	4.114	1.1	0.2963	0.9	0.84	1638	11	1673	27	1657	18	-1.0	1638	11	3
135	3.52	1.28	0.09702	0.58	3.801	1.4	0.2843	1.3	0.91	1568	11	1613	36	1593	22	-1.2	1568	11	3
136	3.60	0.94	0.09576	0.58	3.668	1.1	0.2780	0.9	0.85	1543	11	1581	26	1564	17	-1.1	1543	11	3
139	3.04	0.98	0.10852	0.57	4.918	1.1	0.3288	1.0	0.87	1775	10	1833	31	1805	19	-1.5	1775	10	3
140	3.10	1.00	0.10825	0.57	4.812	1.1	0.3226	1.0	0.87	1770	10	1802	31	1787	19	-0.8	1770	10	3
141	3.33	0.84	0.10138	0.59	4.196	1.0	0.3003	0.8	0.82	1650	11	1693	25	1673	17	-1.2	1650	11	3
142	2.01	1.01	0.17572	0.75	12.048	1.3	0.4975	1.0	0.80	2613	12	2603	43	2608	23	0.2	2613	12	3
143	1.76	0.87	0.22421	0.60	17.538	1.1	0.5676	0.9	0.82	3011	10	2898	40	2965	20	2.3	3011	10	3

			Tera-Wasserberg plot		Normal - Wetherill plot									Ages				Discordance	Preferred Ages		
Grain	^{238}U/^{206}Pb	± 1σ %	^{207}Pb/^{206}Pb	± 1σ %	^{207}Pb/^{235}U	± 1σ %	^{206}Pb/^{238}U	± 1σ %	ρ	^{207}Pb/^{206}Pb	± 2σ	^{206}Pb/^{238}U	± 2σ	^{207}Pb/^{235}U	± 2σ	6-38/7-35	Age	± 2σ	Notes
145	3.16	1.15	0.10147	0.58	4.421	1.3	0.3161	1.1	0.89	1651	11	1771	35	1716	21	-3.2	1651	11	3
146	3.99	1.09	0.08866	0.58	3.061	1.2	0.2505	1.1	0.88	1397	11	1441	28	1423	19	-1.3	1397	11	3
147	1.99	0.82	0.16658	0.58	11.559	1.0	0.5035	0.8	0.81	2524	10	2629	35	2569	19	-2.3	2524	10	3
149	3.31	1.10	0.10198	0.56	4.241	1.2	0.3017	1.1	0.89	1660	10	1700	33	1682	20	-1.1	1660	10	3
150	3.04	0.83	0.11072	0.56	5.013	1.0	0.3285	0.8	0.83	1811	10	1831	26	1822	17	-0.5	1811	10	3

FSC16-49-20B Coarse band in black shale, Holið í Helli

27	104.4	1.3	0.07559	4.92	0.100	5.1	0.0096	1.3	0.26	1084	99	61	2	97	9	36.4	61	2	1
28	110.9	1.4	0.04487	4.04	0.056	4.3	0.0090	1.4	0.33	-63	98	58	2	55	5	-5.0	58	2	1
1	17.4	1.8	0.05423	0.47	0.429	1.9	0.0574	1.8	0.97	380	10	360	13	363	11	0.7	360	13	2
2	17.7	2.5	0.05446	0.46	0.424	2.5	0.0564	2.5	0.98	390	10	354	17	359	15	1.3	354	17	2
3	12.8	1.3	0.05702	0.46	0.614	1.4	0.0781	1.3	0.94	492	10	485	12	486	11	0.2	485	12	2
4	18.0	2.1	0.05394	0.49	0.413	2.2	0.0556	2.1	0.97	368	11	349	14	351	13	0.7	349	14	2
5	17.0	1.9	0.05442	0.44	0.440	1.9	0.0587	1.9	0.97	388	10	368	13	370	12	0.7	368	13	2
6	14.5	1.5	0.05571	0.46	0.531	1.6	0.0691	1.5	0.96	441	10	431	13	432	11	0.3	431	13	2
7	19.9	1.5	0.05326	0.44	0.369	1.6	0.0503	1.5	0.96	340	10	316	9	319	9	0.8	316	9	2
8	13.1	1.4	0.05688	0.46	0.601	1.5	0.0766	1.4	0.95	487	10	476	13	478	11	0.4	476	13	2
9	13.0	1.3	0.05741	0.45	0.607	1.4	0.0768	1.3	0.95	507	10	477	12	482	11	1.1	477	12	2
10	17.8	1.6	0.05455	0.43	0.422	1.7	0.0561	1.6	0.97	394	10	352	11	357	10	1.5	352	11	2
11	17.0	1.7	0.05601	0.45	0.455	1.8	0.0589	1.7	0.97	453	10	369	12	380	11	3.0	369	12	2
12	14.9	1.9	0.05536	0.45	0.513	2.0	0.0672	1.9	0.97	427	10	419	16	420	13	0.2	419	16	2
13	19.0	2.3	0.05315	0.49	0.386	2.4	0.0527	2.3	0.98	335	11	331	15	331	13	0.1	331	15	2
14	18.2	1.7	0.05390	0.45	0.409	1.8	0.0550	1.7	0.97	367	10	345	11	348	10	0.8	345	11	2
15	17.9	2.2	0.05416	0.48	0.417	2.2	0.0558	2.2	0.98	378	11	350	15	354	13	1.0	350	15	2
16	15.8	2.7	0.05476	0.46	0.477	2.8	0.0632	2.7	0.99	403	10	395	21	396	18	0.2	395	21	2
17	17.9	1.4	0.05409	0.43	0.416	1.5	0.0558	1.4	0.95	375	10	350	9	353	9	0.9	350	9	2
18	17.7	1.7	0.05407	0.43	0.421	1.7	0.0564	1.7	0.97	374	10	354	12	357	10	0.7	354	12	2
19	15.6	1.4	0.05518	0.43	0.487	1.4	0.0641	1.4	0.96	420	10	400	11	403	10	0.7	400	11	2
20	15.0	1.5	0.05772	0.50	0.529	1.6	0.0666	1.5	0.95	519	11	415	12	431	11	3.7	415	12	2
21	18.0	2.2	0.05404	0.47	0.413	2.3	0.0555	2.2	0.98	373	10	348	15	351	13	0.9	348	15	2

	Tera-Wasserberg plot				Normal - Wetherill plot						Ages						Discordance	Preferred Ages		
Grain	$^{238}U/^{206}Pb$	± 1σ %	$^{207}Pb/^{206}Pb$	± 1σ %	$^{207}Pb/^{235}U$	± 1σ %	$^{206}Pb/^{238}U$	± 1σ %	ρ	$^{207}Pb/^{206}Pb$	± 2σ	$^{206}Pb/^{238}U$	± 2σ	$^{207}Pb/^{235}U$	± 2σ	6-38/7-35	Age	± 2σ	Notes
22	19.9	1.9	0.05317	0.52	0.368	2.0	0.0502	1.9	0.97	336	12	316	12	318	11	0.7	316	12	2
23	18.9	1.7	0.05357	0.45	0.391	1.8	0.0529	1.7	0.97	353	10	332	11	335	10	0.7	332	11	2
24	14.9	1.8	0.05526	0.45	0.511	1.8	0.0671	1.8	0.97	423	10	419	14	419	13	0.1	419	14	2
25	14.9	2.3	0.05551	0.47	0.515	2.4	0.0673	2.3	0.98	433	11	420	19	422	16	0.4	420	19	2
26	16.0	2.6	0.05472	0.50	0.471	2.7	0.0624	2.6	0.98	401	11	390	20	392	17	0.3	390	20	2
29	18.1	1.3	0.05436	0.47	0.414	1.4	0.0553	1.3	0.94	386	10	347	9	352	8	1.4	347	9	2
30	18.3	1.5	0.05351	0.43	0.403	1.5	0.0547	1.5	0.96	351	10	343	10	344	9	0.2	343	10	2
31	17.4	2.2	0.05439	0.53	0.431	2.2	0.0575	2.2	0.97	387	12	360	15	364	14	1.0	360	15	2
32	12.6	1.4	0.05752	0.62	0.629	1.5	0.0794	1.4	0.92	512	14	492	13	496	12	0.7	492	13	2
33	17.4	1.4	0.05413	0.44	0.429	1.4	0.0576	1.4	0.95	376	10	361	10	363	9	0.5	361	10	2
34	16.3	2.5	0.05491	0.46	0.466	2.5	0.0615	2.5	0.98	409	10	385	19	388	16	0.8	385	19	2
35	15.0	2.1	0.05544	0.44	0.511	2.1	0.0668	2.1	0.98	430	10	417	17	419	15	0.4	417	17	2
36	12.5	1.4	0.05709	0.44	0.629	1.4	0.0799	1.4	0.95	495	10	496	13	495	11	-0.1	496	13	2
37	17.6	1.5	0.05445	0.43	0.425	1.6	0.0567	1.5	0.96	390	10	355	10	360	9	1.2	355	10	2
38	16.8	2.3	0.05458	0.44	0.447	2.3	0.0595	2.3	0.98	395	10	372	16	375	14	0.8	372	16	2
39	15.5	2.7	0.05470	0.46	0.486	2.7	0.0644	2.7	0.99	400	10	403	21	402	18	-0.1	403	21	2
40	17.6	1.5	0.05391	0.45	0.421	1.6	0.0567	1.5	0.96	367	10	355	10	357	9	0.4	355	10	2
41	19.1	2.8	0.05300	0.51	0.382	2.9	0.0523	2.8	0.98	329	12	329	18	329	16	0.0	329	18	2
42	16.4	2.4	0.05476	0.51	0.461	2.4	0.0612	2.4	0.98	402	12	383	18	385	15	0.7	383	18	2
43	16.6	1.8	0.05497	0.43	0.456	1.9	0.0602	1.8	0.97	411	10	377	13	382	12	1.2	377	13	2
44	17.2	2.8	0.05476	0.46	0.438	2.8	0.0580	2.8	0.99	402	10	364	20	369	17	1.4	364	20	2
45	18.1	2.1	0.05436	0.47	0.413	2.2	0.0552	2.1	0.98	386	11	346	14	351	13	1.4	346	14	2
46	14.7	1.4	0.05574	0.46	0.524	1.4	0.0682	1.4	0.95	442	10	425	11	428	10	0.6	425	11	2
47	16.4	2.2	0.05508	0.46	0.463	2.3	0.0610	2.2	0.98	416	10	382	16	386	14	1.2	382	16	2
48	17.3	2.1	0.05465	0.47	0.435	2.1	0.0578	2.1	0.97	398	11	362	14	367	13	1.3	362	14	2

FSC-16-55 Siltstone or tuff, Holið í Helli

8.1	106.11	1.07	0.06016	2.13	0.078	2.4	0.0094	1.1	0.45	609	46	60	1	76	4	20.8	60.5	1.3	1
8.2	105.65	1.07	0.06874	7.12	0.090	7.2	0.0095	1.1	0.15	891	147	61	1	87	12	30.4	60.7	1.3	1
8.3	96.38	1.37	0.06589	3.59	0.094	3.8	0.0104	1.4	0.36	803	75	67	2	91	7	27.2	66.5	1.8	1

	Tera-Wasserberg plot				Normal - Wetherill plot					Ages						Discordance	Preferred Ages		
Grain	^{238}U/^{206}Pb	±1σ %	^{207}Pb/^{206}Pb	±1σ %	^{207}Pb/^{235}U	±1σ %	^{206}Pb/^{238}U	±1σ %	ρ	^{207}Pb/^{206}Pb	±2σ	^{206}Pb/^{238}U	±2σ	^{207}Pb/^{235}U	±2σ	6-38/7-35	Age	±2σ	Notes
8.4	102.89	0.63	0.07912	4.54	0.106	4.6	0.0097	0.6	0.14	1175	90	62	1	102	9	39.0	62.4	0.8	1
1	17.01	1.33	0.05601	1.01	0.454	1.7	0.0588	1.3	0.80	453	22	368	9	380	11	3.1	368.2	9.5	2
2	14.96	1.97	0.05747	1.04	0.530	2.2	0.0669	2.0	0.88	510	23	417	16	431	16	3.3	417.2	15.9	2
3	14.11	0.87	0.05708	1.01	0.558	1.3	0.0709	0.9	0.65	495	22	441	7	450	10	1.9	441.5	7.4	2
4	16.95	3.09	0.05665	1.03	0.461	3.3	0.0590	3.1	0.95	478	23	370	22	385	21	3.9	369.6	22.2	2
5	17.09	1.04	0.05544	1.01	0.447	1.5	0.0585	1.0	0.72	430	23	366	7	375	9	2.3	366.5	7.4	2
6	16.16	0.72	0.05690	1.21	0.485	1.4	0.0619	0.7	0.51	488	27	387	5	402	9	3.6	387.1	5.4	2
10	18.39	1.40	0.05577	1.04	0.418	1.7	0.0544	1.4	0.80	443	23	341	9	355	10	3.7	341.4	9.3	2
12	17.72	0.56	0.05516	1.01	0.429	1.2	0.0564	0.6	0.48	419	23	354	4	362	7	2.4	353.8	3.8	2
13	18.31	0.57	0.05667	1.03	0.426	1.2	0.0546	0.6	0.49	479	23	343	4	361	7	5.0	342.7	3.8	2
14	3.45	2.90	0.12351	1.95	4.931	3.5	0.2897	2.9	0.83	2008	35	1640	83	1808	57	9.3	2007.6	34.5	3

FSC-16-100 Tuff, Reyðibarmur, Hvalba

1	105.86	0.84	0.05139	3.10	0.067	3.2	0.0094	0.8	0.26	258	71	61	1	66	4	7.8	61	1	1
2	110.01	0.89	0.04131	1.49	0.052	1.7	0.0091	0.9	0.51	-269	38	58	1	51	2	-13.9	58	1	1
3	109.82	0.82	0.03679	2.29	0.046	2.4	0.0091	0.8	0.34	-572	62	58	1	46	2	-27.5	58	1	1

SSK76523 Sandstone, well 205/9-1, 3611.76-3611.95 metres

14.1	108.88	1.76	0.07380	3.90	0.093	4.3	0.0092	1.8	0.41	1036	79	59	2	91	7	35.0	58.9	2.1	1
14.2	102.11	1.34	0.14489	5.64	0.196	5.8	0.0098	1.3	0.23	2286	97	63	2	181	19	65.4	62.8	1.7	1
2	23.56	1.10	0.05429	1.12	0.318	1.6	0.0425	1.1	0.70	383	25	268	6	280	8	4.3	268.0	5.8	2
10	12.32	1.50	0.06052	1.34	0.677	2.0	0.0811	1.5	0.75	622	29	503	14	525	16	4.2	502.9	14.5	2
18	10.87	1.43	0.05924	1.05	0.751	1.8	0.0920	1.4	0.81	576	23	567	16	569	15	0.3	567.3	15.5	2
9	1.72	1.75	0.19455	1.06	15.557	2.0	0.5802	1.7	0.85	2781	17	2950	82	2850	38	-3.5	2781.0	17.4	3
15	2.18	1.99	0.19009	1.01	12.009	2.2	0.4584	2.0	0.89	2743	17	2432	80	2605	41	6.6	2743.0	16.7	3
16	2.99	1.24	0.10927	1.02	5.031	1.6	0.3341	1.2	0.77	1787	19	1858	40	1825	27	-1.8	1787.3	18.6	3
17	3.61	1.46	0.09408	1.02	3.588	1.8	0.2767	1.5	0.82	1510	19	1575	41	1547	28	-1.8	1509.7	19.3	3

			Tera-Wasserberg plot							Normal - Wetherill plot				Ages						Discordance	Preferred Ages		
Grain	$^{238}U/^{206}Pb$	±1σ %	$^{207}Pb/^{206}Pb$	± 1σ %	$^{207}Pb/^{235}U$	±1σ %	$^{206}Pb/^{238}U$	±1σ %	ρ	$^{207}Pb/^{206}Pb$	± 2σ	$^{206}Pb/^{238}U$	± 2σ	$^{207}Pb/^{235}U$	± 2σ	6-38/7-35	Age	± 2σ	Notes

SSK76524 Sandstone, well 205/9-1, 3470.5-3470.67 metres

Grain	$^{238}U/^{206}Pb$	±1σ %	$^{207}Pb/^{206}Pb$	± 1σ %	$^{207}Pb/^{235}U$	±1σ %	$^{206}Pb/^{238}U$	±1σ %	ρ	$^{207}Pb/^{206}Pb$	± 2σ	$^{206}Pb/^{238}U$	± 2σ	$^{207}Pb/^{235}U$	± 2σ	6-38/7-35	Age	± 2σ	Notes
1	14.38	1.00	0.05832	1.07	0.559	1.5	0.0696	1.0	0.68	542	23	434	8	451	11	3.9	433.5	8.4	2
4	20.97	1.04	0.05356	1.06	0.352	1.5	0.0477	1.0	0.70	353	24	300	6	306	8	1.9	300.3	6.1	2
7	13.34	1.03	0.05779	1.19	0.597	1.6	0.0750	1.0	0.65	522	26	466	9	476	12	2.0	466.1	9.2	2
9	6.49	1.18	0.07453	1.01	1.582	1.6	0.1540	1.2	0.76	1056	20	923	20	963	19	4.1	923.2	20.3	2
2	2.88	1.08	0.11930	1.00	5.715	1.5	0.3476	1.1	0.73	1946	18	1923	36	1934	25	0.6	1945.8	17.9	3
3	1.63	1.17	0.22408	1.00	18.961	1.5	0.6140	1.2	0.76	3010	16	3086	57	3040	29	-1.5	3010.2	16.1	3
5	1.88	1.09	0.19344	1.00	14.181	1.5	0.5319	1.1	0.73	2772	16	2750	48	2762	28	0.4	2771.6	16.5	3
6	1.73	1.00	0.21427	1.08	17.091	1.5	0.5788	1.0	0.68	2938	17	2944	47	2940	28	-0.1	2938.1	17.5	3
8	2.03	1.38	0.19033	1.03	12.894	1.7	0.4916	1.4	0.80	2745	17	2577	58	2672	32	3.5	2745.0	16.9	3

SSK76525 Sandstone, well 205/01-1, 9635.5 - 9636.2 feet

Grain	$^{238}U/^{206}Pb$	±1σ %	$^{207}Pb/^{206}Pb$	± 1σ %	$^{207}Pb/^{235}U$	±1σ %	$^{206}Pb/^{238}U$	±1σ %	ρ	$^{207}Pb/^{206}Pb$	± 2σ	$^{206}Pb/^{238}U$	± 2σ	$^{207}Pb/^{235}U$	± 2σ	6-38/7-35	Age	± 2σ	Notes
3.1	117.54	2.62	0.11216	10.16	0.132	10.5	0.0085	2.6	0.25	1835	184	55	3	125	24	56.5	54.6	2.8	1
3.2	109.03	1.10	0.11548	5.45	0.146	5.6	0.0092	1.1	0.20	1887	98	59	1	138	14	57.5	58.9	1.3	1
5.1	65.71	5.79	0.05431	3.02	0.114	6.5	0.0152	5.8	0.89	384	68	97	11	110	13	11.1	97.4	11.2	1
1	24.76	0.55	0.05331	1.03	0.297	1.2	0.0404	0.6	0.47	342	23	255	3	264	5	3.3	255.3	2.8	2
2	5.36	0.92	0.07705	1.03	1.983	1.4	0.1867	0.9	0.67	1123	20	1103	19	1110	18	0.6	1103.4	18.7	2
4	21.48	0.57	0.05367	1.03	0.344	1.2	0.0465	0.6	0.48	357	23	293	3	300	6	2.4	293.3	3.2	2
5.3	21.92	3.11	0.05434	1.05	0.342	3.3	0.0456	3.1	0.95	385	23	288	17	298	17	3.6	287.6	17.5	2
6	8.76	0.89	0.06467	1.02	1.018	1.4	0.1142	0.9	0.66	764	21	697	12	713	14	2.2	696.9	11.7	2

SSK76526 Tuff, well 213/26-1, 9472.0 - 9472.10 feet

Grain	$^{238}U/^{206}Pb$	±1σ %	$^{207}Pb/^{206}Pb$	± 1σ %	$^{207}Pb/^{235}U$	±1σ %	$^{206}Pb/^{238}U$	±1σ %	ρ	$^{207}Pb/^{206}Pb$	± 2σ	$^{206}Pb/^{238}U$	± 2σ	$^{207}Pb/^{235}U$	± 2σ	6-38/7-35	Age	± 2σ	Notes
1	4.23	1.75	0.09487	1.19	3.094	2.1	0.2366	1.8	0.83	1525	22	1369	43	1431	32	4.3	1525.4	22.4	3
2	2.90	0.85	0.11524	1.02	5.482	1.3	0.3451	0.9	0.64	1884	18	1911	28	1898	23	-0.7	1883.6	18.4	3
3	2.79	0.79	0.12052	1.01	5.952	1.3	0.3583	0.8	0.62	1964	18	1974	27	1969	22	-0.3	1963.9	18.0	3
5	2.41	1.51	0.17820	1.06	10.199	1.8	0.4153	1.5	0.82	2636	18	2239	57	2453	34	8.7	2636.2	17.6	3

	Tera-Wasserberg plot				Normal - Wetherill plot					Ages						Discordance	Preferred Ages		
Grain	^{238}U/^{206}Pb	±1σ %	^{207}Pb/^{206}Pb	±1σ %	^{207}Pb/^{235}U	±1σ %	^{206}Pb/^{238}U	±1σ %	ρ	^{207}Pb/^{206}Pb	±2σ	^{206}Pb/^{238}U	±2σ	^{207}Pb/^{235}U	±2σ	6-38/7-35	Age	±2σ	Notes
SSK76527 Sandstone, well 204/19-3A, 1936.65-1936.9 metres																			
1	105.3	0.7	0.05591	1.15	0.073	1.3	0.0095	0.7	0.52	449	26	61	1	72	2	15.0	61	1	1
2	95.4	1.2	0.13130	9.07	0.190	9.1	0.0105	1.2	0.13	2115	159	67	2	176	29	61.9	67	2	1
3	89.2	0.8	0.09544	1.16	0.148	1.4	0.0112	0.8	0.55	1537	22	72	1	140	4	48.5	72	1	1
4	99.1	1.4	0.11692	5.43	0.163	5.6	0.0101	1.4	0.25	1910	98	65	2	153	16	57.7	65	2	1
7	102.5	0.6	0.05900	2.53	0.079	2.6	0.0098	0.6	0.22	567	55	63	1	78	4	19.3	63	1	1
8	105.8	0.8	0.06416	2.79	0.084	2.9	0.0094	0.8	0.27	747	59	61	1	81	5	25.6	61	1	1
9	94.4	0.6	0.12633	1.89	0.184	2.0	0.0106	0.6	0.31	2047	33	68	1	172	6	60.5	68	1	1
10	106.8	0.8	0.05821	4.44	0.075	4.5	0.0094	0.8	0.18	538	97	60	1	74	6	18.3	60	1	1
12	73.6	5.0	0.24372	2.33	0.456	5.5	0.0136	5.0	0.91	3144	37	87	9	382	35	77.2	87	9	1
13	98.3	0.7	0.06551	3.64	0.092	3.7	0.0102	0.7	0.19	791	76	65	1	89	6	26.9	65	1	1
15	89.1	1.0	0.18112	1.98	0.280	2.2	0.0112	1.0	0.45	2663	33	72	1	251	10	71.3	72	1	1
16	3.2	1.1	0.10110	0.21	4.374	1.1	0.3140	1.1	0.98	1644	4	1760	34	1707	18	-3.1	1644	4	3
SSK76530 Sandstone, well 204/19-3A, 2036.55-2036.76 metres																			
6	100.5	0.9	0.04672	1.08	0.064	1.4	0.0099	0.9	0.64	35	26	64	1	63	2	-1.2	64	1	1
12	103.7	1.3	0.05062	1.05	0.067	1.6	0.0096	1.3	0.77	224	24	62	2	66	2	6.4	62	2	1
3	21.7	0.9	0.05264	0.49	0.335	1.0	0.0461	0.9	0.88	313	11	291	5	293	5	0.8	291	5	2
8	14.3	1.0	0.05576	0.28	0.538	1.1	0.0701	1.0	0.97	443	6	437	9	437	8	0.2	437	9	2
10	14.1	0.9	0.05721	0.67	0.557	1.2	0.0707	0.9	0.82	499	15	440	8	450	8	2.1	440	8	2
11	13.3	1.0	0.05675	0.51	0.587	1.1	0.0750	1.0	0.90	482	11	466	9	469	8	0.5	466	9	2
13	6.1	0.9	0.07331	0.87	1.648	1.2	0.1631	0.9	0.71	1023	18	974	16	989	15	1.5	974	16	2
1	2.0	0.5	0.19790	0.24	13.398	0.5	0.4913	0.5	0.88	2809	4	2576	19	2708	10	4.9	2809	4	3
2	1.9	0.9	0.18884	0.22	13.881	0.9	0.5334	0.9	0.97	2732	4	2756	39	2742	17	-0.5	2732	4	3
4	1.7	1.4	0.20043	0.27	15.915	1.5	0.5762	1.4	0.98	2830	4	2933	67	2872	27	-2.1	2830	4	3
5	2.1	1.5	0.19371	0.23	13.017	1.5	0.4876	1.5	0.99	2774	4	2560	62	2681	28	4.5	2774	4	3
7	1.8	0.9	0.19454	0.24	14.899	0.9	0.5557	0.9	0.96	2781	4	2849	40	2809	17	-1.4	2781	4	3
9	2.0	0.9	0.18418	0.21	12.756	0.9	0.5025	0.9	0.97	2691	3	2625	38	2662	17	1.4	2691	3	3

			Tera-Wasserberg plot				Normal - Wetherill plot				Ages						Discordance	Preferred Ages		
Grain	^{238}U/^{206}Pb	±1σ %	^{207}Pb/^{206}Pb	±1σ %	^{207}Pb/^{235}U	±1σ %	^{206}Pb/^{238}U	±1σ %	ρ	^{207}Pb/^{206}Pb	±2σ	^{206}Pb/^{238}U	±2σ	^{207}Pb/^{235}U	±2σ	6-38/7-35	Age	±2σ	Notes
SSK76532 Sandstone, well 204/19-3A, 2091.71-2091.83 metres																			
4	96.6	0.5	0.07165	4.99	0.102	5.0	0.0104	0.5	0.09	976	102	66	1	99	9	32.8	66	1	1
8	64.9	0.8	0.05019	0.33	0.107	0.9	0.0154	0.8	0.92	204	8	99	2	103	2	4.1	99	2	1
10	90.4	1.2	0.08645	2.42	0.132	2.7	0.0111	1.2	0.44	1348	47	71	2	126	6	43.6	71	2	1
2	14.0	0.6	0.05700	0.39	0.561	0.7	0.0714	0.6	0.82	492	9	445	5	452	5	1.7	445	5	2
3	21.8	0.5	0.05321	0.41	0.336	0.7	0.0458	0.5	0.78	338	9	289	3	294	3	1.8	289	3	2
7	14.0	1.0	0.05576	0.35	0.550	1.0	0.0716	1.0	0.94	443	8	446	8	445	7	-0.1	446	8	2
11	5.8	1.1	0.07673	1.04	1.809	1.5	0.1711	1.1	0.72	1114	21	1018	20	1049	19	2.9	1018	20	2
13	14.4	1.2	0.05786	0.33	0.554	1.2	0.0695	1.2	0.96	524	7	433	10	448	9	3.3	433	10	2
5	2.0	1.2	0.19176	0.29	13.291	1.2	0.5029	1.2	0.97	2757	5	2626	49	2701	22	2.7	2757	5	3
12	1.9	1.2	0.19272	0.20	14.137	1.2	0.5322	1.2	0.99	2766	3	2751	54	2759	23	0.3	2766	3	3
16	3.4	1.3	0.10118	0.23	4.157	1.3	0.2981	1.3	0.98	1646	4	1682	37	1666	21	-1.0	1646	4	3
17	2.8	0.6	0.11438	0.25	5.665	0.7	0.3594	0.6	0.93	1870	5	1979	21	1926	12	-2.8	1870	5	3
SSK76537 Sandstone, well 213/27-2, 9664.0-9664.7 feet																			
2	251.2	0.9	0.05022	1.22	0.028	1.5	0.0040	0.9	0.60	205	28	26	0	28	1	7.2	26	0	1
5	99.4	1.0	0.12328	7.81	0.171	7.9	0.0101	1.0	0.13	2004	139	65	1	160	23	59.7	65	1	1
6	110.1	0.9	0.04511	5.06	0.056	5.1	0.0091	0.9	0.18	-49	123	58	1	56	6	-4.5	58	1	1
16	105.1	0.6	0.07209	6.33	0.095	6.4	0.0095	0.6	0.10	989	129	61	1	92	11	33.4	61	1	1
4	6.5	0.8	0.07003	0.27	1.491	0.8	0.1545	0.8	0.95	929	5	926	14	927	10	0.1	926	14	2
7	14.3	0.9	0.05557	0.42	0.536	1.0	0.0700	0.9	0.91	435	9	436	7	436	7	-0.1	436	7	2
11	5.1	1.6	0.07694	0.37	2.059	1.6	0.1942	1.6	0.97	1120	7	1144	33	1135	22	-0.8	1144	33	2
12	13.5	0.6	0.05932	1.60	0.604	1.7	0.0739	0.6	0.33	579	35	460	5	480	13	4.2	460	5	2
14	20.5	0.6	0.05401	0.67	0.364	0.9	0.0489	0.6	0.69	371	15	308	4	315	5	2.4	308	4	2
17	14.1	1.2	0.05869	0.83	0.575	1.5	0.0711	1.2	0.83	556	18	443	11	462	11	4.0	443	11	2
18	7.1	0.7	0.06874	0.62	1.328	1.0	0.1402	0.7	0.76	891	13	846	11	858	11	1.4	846	11	2
1	2.4	0.9	0.16526	0.21	9.474	1.0	0.4160	0.9	0.98	2510	3	2242	35	2385	17	6.0	2510	3	3
3	3.5	0.9	0.10058	0.34	3.934	0.9	0.2838	0.9	0.93	1635	6	1610	24	1621	15	0.6	1635	6	3
8	1.8	1.7	0.20420	0.33	15.559	1.8	0.5528	1.7	0.98	2860	5	2837	79	2850	33	0.5	2860	5	3
10	2.0	0.8	0.16892	0.25	11.615	0.9	0.4989	0.8	0.96	2547	4	2609	36	2574	16	-1.4	2547	4	3

			Tera-Wasserberg plot			Normal - Wetherill plot						Ages						Discordance	Preferred Ages		
Grain	$^{238}U/^{206}Pb$	$\pm 1\sigma$ %	$^{207}Pb/^{206}Pb$	$\pm 1\sigma$ %	$^{207}Pb/^{235}U$	$\pm 1\sigma$ %	$^{206}Pb/^{238}U$	$\pm 1\sigma$ %	ρ	$^{207}Pb/^{206}Pb$	$\pm 2\sigma$	$^{206}Pb/^{238}U$	$\pm 2\sigma$	$^{207}Pb/^{235}U$	$\pm 2\sigma$	6-38/7-35	Age	$\pm 2\sigma$	Notes
13	2.0	0.8	0.18194	0.36	12.808	0.8	0.5108	0.8	0.90	2671	6	2660	33	2666	16	0.2	2671	6	3

1. Young grain – $^{206}Pb/^{238}U$ age < 100 Ma (Data reported no matter how discordant)
2. $^{206}Pb/^{238}U$ age 100 – 120 0Ma , < 5% discordant
3. $^{206}Pb/^{238}U$ age age > 1200 Ma, < 10% discordant